Challenging the plant cell cycle

Analysis of key cell cycle regulators in *Arabidopsis thaliana*

Inaugural-Dissertation

zur
Erlangung des Doktorgrades
der Mathematisch-Naturwissenschaftlichen Fakultät
der Universität zu Köln

vorgelegt von

Christina Weinl

aus Reutlingen

Köln 2005

Berichterstatter:	Prof. Dr. Martin Hülskamp
	Prof. Dr. Wolfgang Werr
Prüfungsvorsitzender:	Prof. Dr. Siegfried Roth
Tag der mündlichen Prüfung:	06. Juli 2005

Danke

Mein besonderer Dank gilt Dr. Arp Schnittger für die Überlassung des Themas, die intensive wissenschaftliche Betreuung und die tolle Offenheit gegenüber Fragen und Diskussionen. Bei Prof. Dr. Martin Hülskamp möchte ich mich für die freundliche Aufnahme in seinem Lehrstuhl bedanken und den guten Start in Köln. Für seine Übernahme des Zweitgutachtens möchte ich mich bei Prof. Dr. Wolfgang Werr bedanken.

Großer Dank gebührt dem Team Gärtnerei des MPIZ, v.a. Frank, Andreas und Thomas und den fleißigen Händen von Britta, Heidi und Parisa ohne deren große Hilfe hätte ich niemals die ganze Pflanzenflut bewältigen können. Für die großartige Hilfe bei den diversen Mikroskopen möchte ich mich bei Elmon Schmelzer, Rhiaz Bhat, Marcel Düggelin und Rolf-Dieter Hirtz bedanken. Auch möchte ich mich bei den freundlichen Damen in der Spülküche bedanken die einem den Laboralltag um einiges erleichtert haben.

Herzlichen Dank an das gesamte Team des Lehrstuhls Botanik III für eine tolle Atmosphäre und viel Unterstützung, v. a. an Birgit, Britta, Daniel, Elena, Katja, Martina, Rainer, Steffi, Uli und Viktor.

Was wäre ein Laborleben ohne die lieben Kollegen: von einem anfänglich recht überschaubaren Kreis - ein großer Dank an Martina für die besinnlich heiteren Stunden (unsere Beutezüge und die Öffnung des Ethanol-Kanisters werden mir unvergessen bleiben) hat sich doch ein kleines illustres Grüppchen gebildet. Auch wenn man unterschiedlicher nicht sein kann zeigte sich beim angeregten Mittagsgespräch über die abstrusen Dinge des Lebens eine große Gemeinsamkeit. Bedanken möchte ich mich für das tolle Raumklima bei Arp, Doris, Farshad, Marc, Moritz, Nico, Oliver, Regina, Sebastian, Stefan, Suzanne und Xiaoguo.

Zum Schluß noch ein ganz dickes DANKE SCHÖN für die geneigten Leser dieses Werkes Arp, Daniel, Moritz und Suzanne.

CONTENTS

Zusammenfassung

In der Entwicklung der Pflanze sind Zell-Differenzierung und Zell-Zyklus Kontrolle eng miteinander verknüpft. Eine Klasse von Serin/Threonin Kinasen, die Zyklin-abhängigen Kinasen (CDKs), kontrolliert den Ablauf des Zell-Zyklus. Ein wichtiger Mechanismus um die CDK Aktivität zu regulieren ist die Bindung von CDK-Inhibitoren. Auch in Pflanzen wurden vor kurzem CDK-Inhibitoren entdeckt. Missexpression von CDK-Inhibitoren in *Arabidopsis* führt zu verminderter Endoreplikation und einer Abnahme der Zell-Zahl. Diese Beobachtung ist konsistent mit der postulierten Funktion von CDK-Inhibitoren, den Zell-Zyklus während dem Übergang von der G1- zur S-Phase blockieren zu können. In dieser Arbeit konnte gezeigt werden, dass zumindest der CDK-Inhibitor KRP1 den Eintritt in die Mitose verhindern kann. Der Eintritt in die S-Phase wird nicht blockiert und Endoreplikation findet statt. Die Daten dieser Arbeit weisen darauf hin, dass KRP1 konzentrations-abhängig wirkt. KRP1 spielt eine wichtige Rolle während der Zell-Proliferation, dem Austritt aus dem Zell-Zyklus und dem Umschalten von einem mitotischen- in einen endoreplizierenden Zell-Zyklus-Modus. Endoreplikation wird meist mit einer terminalen Differenzierung assoziiert, interessanterweise wurden endoreplizierte Zellen entdeckt, die wieder in einen mitotischen Zell-Zyklus eintreten konnten. Diese Beobachtung betont die große Flexibilität pflanzlicher Zellen während ihrer Entwicklung. Darüber hinaus konnte in dieser Arbeit gezeigt werden, dass im Gegensatz zu CDK-Inhibitoren aus dem tierischen System, KRP1 sich von Zelle zu Zelle bewegen kann.

CDKs regulieren im tierischen System den Eintritt in die S-Phase durch Aktivierung des E2F-DP Transkriptionsfaktors. Dies geschieht indem CDKs das E2F-DP inhibierende RETINOBLASTOMA PROTEIN phosphorylieren. Mittlerweile sind orthologe Gene für Rb, E2F und DP in *Arabidopsis* isoliert worden. In dieser Arbeit wurde das *RETINOBLASTOMA RELATED1* (*RBR1*) Gen und drei *E2F* Gene (*E2Fa, E2Fb* und *E2Fc*) in endoreplizierenden Trichomen missexprimiert. Die Ergebnisse weisen darauf hin, dass RBR1 ein negativer Regulator der Endoreplikation ist, wohingegen es sich bei E2Fa, E2Fb und E2Fc um positive Regulatoren handelt. Dieses Ergebnis läßt darauf schliessen, dass der RBR-E2F Regulations-Mechanismus in höheren Eukaryoten konserviert ist.

Abstract

Throughout plant development cell differentiation is closely linked with cell cycle control. A class of highly conserved Serine/Threonine kinases, CYCLIN DEPENDENT KINASEs (CDKs) controls progression through the cell cycle. One important mechanism to regulate CDK activity is the binding of CDK inhibitors (CKIs). Recently, CKIs were also identified in plants and in previous studies, *Arabidopsis* plants misexpressing CKIs were found to have reduced endoreplication levels and decreased numbers of cells consistent with a function of CKIs in blocking the G1/S cell-cycle transition. I found that at least one inhibitor from *Arabidopsis*, KRP1, can also block entry into mitosis but allows S-phase progression causing endoreplication. The data presented in this work suggest that KRP1 acts in a concentration-dependent manner and has an important function in cell proliferation as well as in cell-cycle exit and in turning from a mitotic to an endoreplicating cell-cycle mode. Endoreplication is usually associated with terminal differentiation. Strikingly, endoreplicated cells were found to be able to re-enter mitosis emphasizing the high degree of flexibility of plant cells during development. Moreover, it could be shown that in contrast to animal CKIs KRP1 can move between cells.

In animals CDKs regulate entry into S-phase via activation of the E2F-DP transcription factor, by phosphorylating the E2F-DP inhibiting RETINOBLASTOMA protein. Orthologs of Rb, E2F and DP have been identified in the *Arabidopsis* genome. In this work I misexpressed the *RETINOBLASTOMA RELATED1* (*RBR1*) and three genes encoding for *ADENOVIRUS E2 PROMOTOR BINDING FACTOR s* (*E2Fa*, *E2Fb* and *E2Fc*) in endoreplicating trichomes. The obtained data suggest that RBR1 negatively regulates endoreplication, whereas E2Fa, E2Fb and E2Fc act as positive regulators, indicating that the RBR-E2F regulatory pathway is conserved in higher eukaryotes.

Publications

Ectopic D-type cyclin expression induces not only DNA replication but also cell division in Arabidopsis trichomes

Schnittger A, Schöbinger U, Bouyer D, Weinl C, Stierhof YD, Hülskamp M

Proc Natl Acad Sci U S A. 2001, **99**: 6410-6415

For this publication I did some of the *in situ* hybridization experiments and RT-PCR experiments.

Misexpression of the cyclin-dependent kinase inhibitor ICK1/KRP1 in single-celled *Arabidopsis* trichomes reduces endoreduplication and cell size and induces cell death.

Schnittger A, Weinl C, Bouyer D, Schöbinger U, Hülskamp M

Plant Cell 2003, **15**: 303-315

In this work I analyzed the crosses of the *MAP:GFP* and *Talin:GFP* reporter constructs with Pro_{GL2}*:KRP1*^{109} and with Pro_{GL2}*:KRP1* and I did all RT-PCR experiments.

Novel functions of plant cyclin-dependent kinase inhibitors - ICK1/KRP1 can act non-cell-autonomously and inhibit entry into mitosis

Weinl C, Marquardt S, Kuijt SJH, Nowack MK, Jakoby MJ, Hülskamp M, Schnittger A

Plant Cell 2005, **17**:1704-1722

Besides Western-Blot analysis, images of DAPI stained mitotic nuclei in wild-type and Pro_{GL2}*:KRP1*^{109} and the generation of Pro_{GL2}*:GUS:YFP:KRP1*^{109} transgenic plants all data were made by myself.

Abbreviations and gene names

°C	degree Celsius
35S	35S promotor from the *Cauliflower Mosaic virus*
aa	amino acid
AJH1	ARABIDOPSIS JAB1 HOMOLOG 1
APC/C	anaphase-promoting complex/cyclosome
ATP	adenosine triphosphate
bp	base pair
C	DNA content of a haploid genome
CAK	CDK ACTIVATING KINASE
CaMV	*Cauliflower Mosaic Virus*
CCS52	CELL-CYCLE SWITCH 52
CDC6	CELL DIVISION CYCLE DEFECTIVE 6
CDC25	CELL DIVISION CYCLE DEFECTIVE 25
CDK	CYCLIN DEPENDENT KINASE
cDNA	complementary DNA
CDS	coding sequence
CDT1	cdc10-DEPENDENT TRANSCRIPT 1
CFP	cyan fluorescent protein
CKI	cyclin dependent kinase inhibitor
CKS1	CDC KINASE SUBUNIT 1
CLSM	confocal laser scanning microscopy
CPC	CAPRICE
Col	Columbia
COP9	CONSTITUTIVELY PHOTOMORPHOGENIC 9
CPR5	CONSTITUTIVE PATHOGEN RESPONSE 5
CSN	COP9 Signalosome
CSN5	COP9 SIGNALOSOME SUBUNIT 5
CUL1	CULLIN 1
CYC	CYCLIN
DAPI	4’,6’-Diamidino-2-phenylindole
DEL	DP-E2F LIKE
DNA	desoxyribonucleic acid
DP	DIMERIZATION PARTNER
EF1	ELONGATION FACTOR 1
E2F	ADENOVIRUS E2 PROMOTOR BINDING FACTOR
ER	endoplasmatic reticulum
et al.	*et alterni* [Lat.] and others
Fig	Figure
FZR	FIZZY-RELATED
FZY	FIZZY
GFP	green fluorescent protein
GL2	GLABRA2

GL3	GLABRA3
GUS	GLUCURONIDASE
ICK	INTERACTOR/INHIBITOR OF CDKs
kb	kilo bp
kD	kilo Dalton
Ler	Landsberg *erecta*
KRP	KIP RELATED PROTEIN
mRNA	messenger RNA
n	number
N/NLS	nuclear localization signal/sequence
PCR	polymerase chain reaction
PD	plasmodesmata
PI	propidium iodide
PTGS	post transcriptional gene silencing
Rb	RETINOBLASTOMA
RBR1	RETINOBLASTOMA RELATED1
RBX1	RING BOX PROTEIN1
RFP	red fluorescent protein
RNA	ribonucleic acid
RNAi	RNA-interference
rpm	rounds per minute
RUB	RELATED TO UBIQUITIN
RUX	ROUGHEX
RT	room temperature
RT-PCR	reverse transcription PCR
SCF	Skp1; Cdc53 (cullin); F-box protein
SD	standard deviation
SEL	size exclusion limit
SEM	scanning electron microscopy
SIM	SIAMESE
SKP1	S-PHASE KINASE-ASSOCIATED PROTEIN 1
T-DNA	transferred DNA
TIS	trichome initiation site
TMM	TOO MANY MOUTH
TRY	TRIPTYCHON
UTR	untranslated region
WT	wild type
Y-2-H	yeast two hybrid assay
YFP	yellow fluorescent protein
WS-O	Wassilewskaja

All gene and mutant names are written in italics. WT-genes are written in capital letters. Proteins are written in non-italic letters.

The who is who of the plant cell cycle genes

CDKs

CDKA;1 = cdc2a (At3g48750)
CDKB1;1 = cdc2b (At3g54180)

inhibitors of CDKs

KRP1 = ICK1 (At2g23430)
KRP2 = ICK2 (At3g50630)
KRP3 = ICK6 (At5g48820)
KRP4 = ICK7 (At2g32710)
KRP5 (At3g24810)
KRP6 = ICK4 = ACK1 (At3g19150)
KRP7 = ICK5 (At1g49620)

E2Fs

E2Fa = E2F3 (At2g36010)
E2Fb = E2F1 (At5g22220)
E2Fc = E2F2 (At1g47870)

DP-E2F-like

DEL1 = E2Fe = E2L3 = ELP2 (At3g48160)
DEL2 = E2Fd = E2L1 = ELP3 (At5g14960)
DEL3 = E2Ff = E2L2 = ELP1 (At3g01330)

RING box

RBX1a = Rbx1;1 (At5g20570)
RBX1b = Rbx1;2 (At3g42830)

COP9 signalosome subunits

CSN5A = AJH1 (At1g22920)
CSN5B = AJH2 (At1g71320)

The abbreviations used in this work are written in bold.

Figure index

Table index

INTRODUCTION

General features of cell cycle control

During development of higher eukaryotes many different cell types are produced all of which can substantially differ in their cell-cycle program, e. g. mitotic or endoreplication cycle. Also the presence and length of the distinct cell-cycle phases or the proliferation activity can vary between different cell types (Fig1) (Jakoby and Schnittger, 2004).

The prototype of a cell cycle is a mitotic cell cycle consisting of four phases, the synthesis-phase (S-phase) during which DNA is replicated, the mitosis-phase (M-phase), in which sister chromatids are separated and two gap phases, G1 and G2, which separate S- and M-phase. The transition from G1 to S-phase and the transition from G2 to M-phase are controlled by check points, wich are tightly regulated (Fig1). At the G1/S transition multiple extrinsic and intrinsic signals are integrated, e.g. in animals the nutrition status of a cell. Also hormones can regulate the cell cycle, as shown for the plant hormone cytokinin, which activates cell division in *Arabidopsis* (Wang et al., 1998; Riou-Khamlichi et al., 1999). At the G2/M check point it is necessary to ensure that the complete genome has been replicated during S-phase in order to avoid chromosomal aberrations.

Common cell-cycle variants in both animals and plants are endocycles, in which cells replicate their DNA without undergoing a subsequent mitosis leading to polyploid cells (Fig1) (Edgar and Orr-Weaver, 2001). Endoreplication has been implicated in cell differentiation and cell growth, for instance in the development of *Drosophila melanogaster* nurse cells, *Medicago truncatula* nodule cells, or *Arabidopsis thaliana* leaf hairs (trichomes) (Kondorosi et al., 2000; Edgar and Orr-

Weaver, 2001; Schnittger and Hulskamp, 2002; Sugimoto-Shirasu and Roberts, 2003; Kondorosi and Kondorosi, 2004). The cellular need for endoreplication is still not fully understood. It has been suggested that endoreplication might be essential for an enhanced metabolic capacity, e.g. observed in plant endosperm tissue, or that higher ploidy levels might buffer mutations (Kowles and Phillips, 1985). Not much is known about how plant cells switch form a mitotic to an endoreplication cycle during their differentiation and how they manage to regulate starting another round of DNA replication while at the same time inhibiting mitosis. Also nothing is known about how cells enter, progress and terminate an endoreplication cycle in plants.

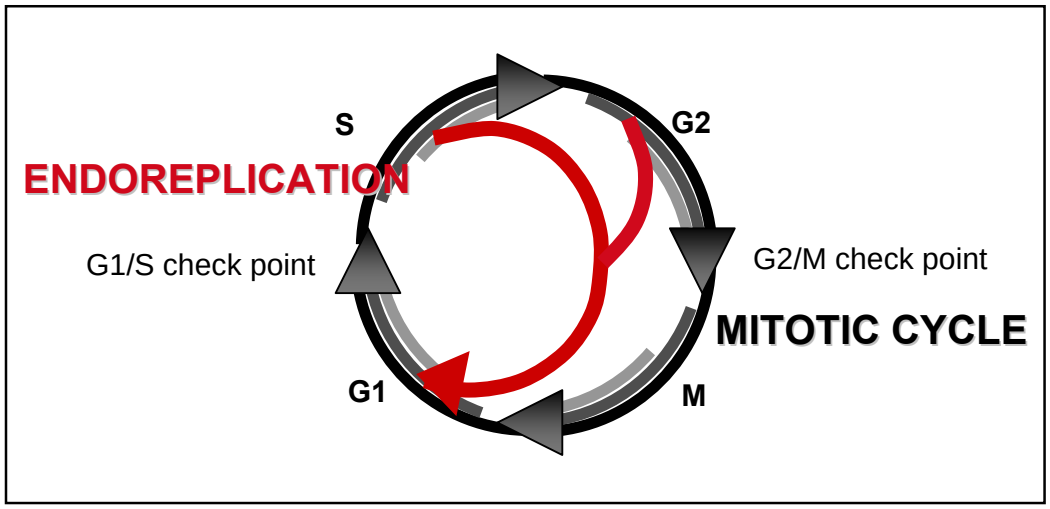

Figure 1 Different cell cycle modes
Simplified model of different cell cycle modes. The length of the individual phases (S, G2, M and G1) and the entry into an endoreplication cycle can vary.

Regulation of cyclin dependent kinases

Intrinsic and extrinsic cues are integrated at a central convergence point of eukaryotic cell-cycle control, which is represented by a group of Serine/Threonine kinases, CYCLIN DEPENDENT KINASEs (CDKs). To ensure a correct progression through

the cell cycle these CDKs need to be tightly regulated. CDKs of higher eukaryotes are regulated at a transcriptional but most importantly at a post-translational level, i.e. phosphorylation and dephosphorylation, subcellular localization and the binding of positive, e.g. cyclins, and negative, e.g. CDK inhibitors, regulators.

Four classes of CDKs have been described in *Arabidopsis*. The most prominent member is the A-type *CDKA;1*, that contains the PSTAIRE sequence which is conserved throughout eukaryotes. CDKA;1 has been shown to be constitutively expressed throughout the cell cycle, whereas expression of the plant-specific B-type *CDKB1;1*, which contains the variant PPTALRE motif, is upregulated at the G2/M transition (Menges and Murray, 2002). In maize overexpression of dominant-negative *CDKA;1* inhibited endoreplication (Leiva-Neto et al., 2004) and completely abolished cell cycle progression in tobacco protoplasts arresting cells in G1 and G2 (Hemerly et al., 1995). Whereas cells were blocked in G2, in *Arabidopsis* plants misexpressing a dominant-negative *CDKB1;1* (Boudolf et al., 2004). Taken together these data suggest that CDKA;1 is involved in the regulation of G1/S and G2/M transition, whereas B-type CDKs play only a role at G2/M transition.

In yeast and animals it has been shown that phosphorylation and dephosphorylation of specific CDK residues are essential for a fully active CDK/cyclin complex. WEE1 kinase phosphorylates CDKs at residues Thr14 and Tyr15, thereby inhibiting ATP fixation and substrate binding of the CDK (Fig2). In order to activate the CDK/cyclin complex the phosphogroups at position 14 and 15 have to be removed by the CDC25 phosphatase (Fig2). Additionally, CDKs need to be phosphorylated at Thr160 by CDK activating kinases. In the *Arabidopsis* genome orthologs have been identified for most of the components involved in the phosphorylation and dephosphorylation of CDKs (Vandepoele et al., 2002). Recently

a *CDC25*-like gene has been identified in *Arabidopsis* .The protein has been shown to stimulate kinase activity of *Arabidopsis* CDKs *in vitro* (Landrieu et al., 2004b; Landrieu et al., 2004a). The in vivo role of this CDC25-like protein, however, remains to be determined.

Also the spatial and temporal localization of the CDKs is important. In the study of Weingartner et al. the CDKA;2 from *Medicago sativa* was fused to GFP and its subcellular localization was followed in tobacco suspension culture (2001). The authors showed that during interphase CDKA;2 is localized in the nucleus and the cytoplasm. During mitosis CDKA;2 associates with mitotic structures like preprophase band, metaphase spindles and phragmoplast.

A prerequisite for an active CDK is the binding of a cyclin partner. A principal control mechanism is the abundance of cyclins, which involves transcriptional and post-translational regulation. To date, 49 putative cyclins have been identified in the *Arabidopsis* genome and are grouped into ten classes (Wang et al., 2004). The class of A-type cyclins is important for the G1/S and G2/M control; B-type cyclins play a key role at the G2/M transition and during mitosis; D-type cyclins are involved in the regulation of G1/S and G2/M transition (Riou-Khamlichi et al., 1999; Riou-Khamlichi et al., 2000; Schnittger et al., 2002b). The recently isolated H-type cyclin is part of the CDK-activating kinase (CDKD) (Fig2) (Shimotohno et al., 2004).

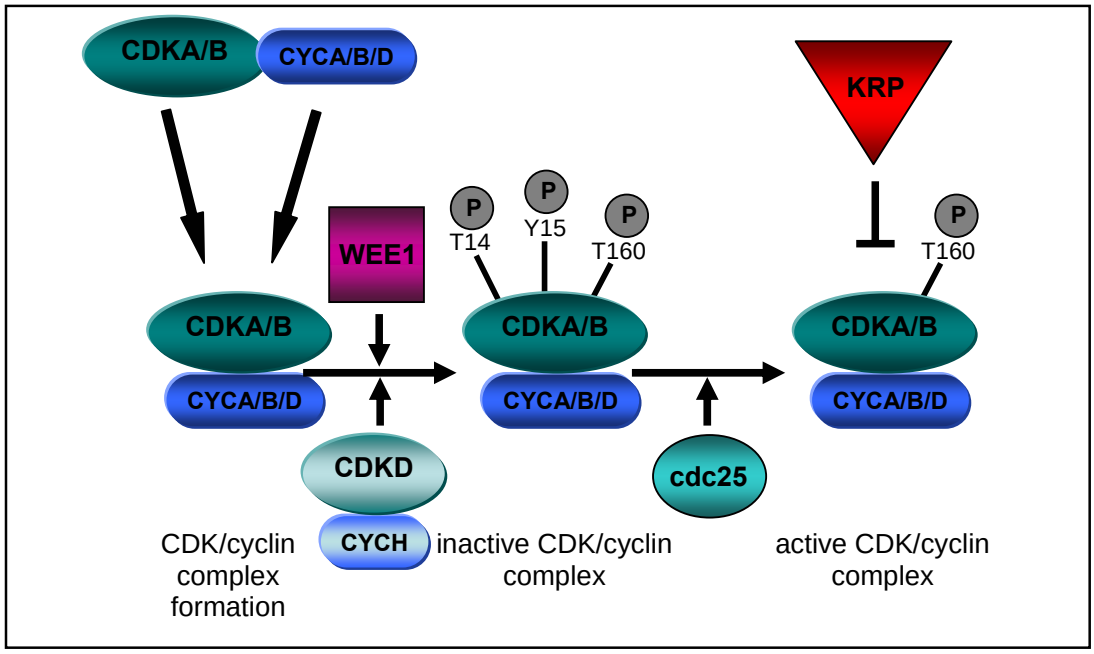

Figure 2 CDK-regulation in *Arabidopsis*
Simplified model of the different regulatory steps during CDK activation

Moreover, the CDC KINASE SUBUNIT (CKS) which has been identified in fission yeast by its ability to rescue certain temperature sensitive CDK mutants, has shown to bind to the CDK/cyclin complex (Hayles et al., 1986). In *Xenopus*, binding of CKS to the CDK/cyclin complex stimulates the ability of this complex to be dephosphorylated or phosphorylated by cdc25 or WEE1, respectively (Patra et al., 1999). Only little information is available about the function of plant CKSs. Two genes encoding for *CKS1* and *CKS2* have been identified in *Arabidopsis* and overexpression of *CKS1* has shown to inhibit cell cycle progression, but did not affect endoreplication (De Veylder et al., 2001a).

Another important regulatory mechanism of CDK activity is the binding of CDK inhibitors, which stochiometrically bind to cyclins and CDKs and inhibit the kinase activity (Fig2).

CDK inhibitors

In animals, two classes of CDK inhibitors (CKIs) have been identified, the INK4 class and the CIP/KIP family. The ankyrin containing INK4 class comprises p15, p16, p18, and p19, which inhibit CDK4 but can also bind to CDK6. Members of the CIP/KIP family ($p21^{Cip1}$, $p27^{Kip1}$ and $p57^{Kip2}$) block cyclin D-, E-, and A-dependent kinases, but predominantly inhibit CDK2 activity (Pavletich, 1999; Sherr and Roberts, 1999). Besides a negative role in CDK regulation, CKIs have also been found to help assemble and stabilize a CDK4-cyclin D complex (Sherr and Roberts, 1999). It is not clear, however, whether these CDK/cyclinD-CKI complexes are active or not (Olashaw et al., 2004).

Several mechanisms control the abundance of CKIs either on a transcriptional or a post-translational level. Recently, it has been reported in mouse that E2F1 binds to the $p27^{Kip1}$ promotor thereby activating its expression and that depletion of E2F1 causes a reduction of the $p27^{Kip1}$ expression level (Wang et al., 2005). Activated CDK2/cyclinE phosphorylates $p27^{Kip1}$ on Threonin residue 187 (Sheaff et al., 1997; Vlach et al., 1997; Montagnoli et al., 1999). This phosphorylated form of $p27^{Kip1}$ is recognized by the nuclear localized E3 ligase SCF^{Skp2}, and subsequently becomes ubiquitinated and degraded by the 26S proteasome during S- and G2-phase (Pagano et al., 1995; Carrano et al., 1999; Sutterluty et al., 1999; Tsvetkov et al., 1999). In addition, Kamura and colleagues have reported the existence of a Skp2 independent pathway for $p27^{Kip1}$ degradation at G1-phase by the cytoplasmic Kip1 ubiquitination-promoting complex (KPC) (Kamura et al., 2004).

The subcellular localization of the CDK inhibitor $p27^{Kip1}$ has been shown to play an important role for its action and regulation. $p27^{Kip1}$ exerts its inhibitory function in the nucleus whereas $p27^{Kip1}$ becomes degraded in the cytoplasm (Tomoda

et al., 1999; Connor et al., 2003). Upon phosphorylation at the Serine residue (S10) by the nuclear human kinase interacting stathmin (hKIS) $p27^{Kip1}$ is translocated from the nucleus to the cytoplasm (Boehm et al., 2002). To retain $p27^{Kip1}$ in the cytoplasm Akt-mediated phosphorylation at Threonine 157 is necessary during G1, thereby the association of p27 with importin α is inhibited preventing re-entry into the nucleus (Shin et al., 2005). The mammalian COP9 signalosome subunit 5 (CSN5) but not $p27^{Kip1}$ contains a nuclear export signal (NES). CSN5 can bind to $p27^{Kip1}$ and functions as an adaptor between $p27^{Kip1}$ and the exportin CRM1 to induce $p27^{Kip1}$ nuclear export and its subsequent degradation (Tomoda et al., 1999; Tomoda et al., 2002).

Putative CKIs have also been found in plants (Wang et al., 1998; De Veylder et al., 2001b; Jasinski et al., 2002). In *Arabidopsis*, seven genes were identified, which display homologies to the animal $p27^{Kip1}$, and thus were named *KIP RELATED PROTEINS* (*KRP*s) or *INHIBITORs/INTERACTORs OF CDK* (*ICK*s) (Wang et al., 1998; De Veylder et al., 2001b). The homology to $p27^{Kip1}$ protein, however, is restricted to about 30 amino acids in the C-terminus. Information about plant CKIs is still very limited. In yeast two hybrid interaction assays it has been shown that KRP1 could bind to CDKA;1 and CYCLIN D3;1. Moreover, it has been demonstrated that KRP1 can inhibit the histone phosphorylation activity of CDKA;1 *in vitro* (Wang et al., 1997; Wang et al., 1998). In several misexpression studies it has been found that KRPs can block endoreplication and reduce cell numbers leading to dwarf plants, when ubiquitously expressed (Wang et al., 2000; De Veylder et al., 2001b; Zhou et al., 2002; Schnittger et al., 2003). All these results are consistent with the presumed function of KRPs as inhibitors of CDKs at the G1/S transition. However, analysis of the transcript profile of *KRP1* in synchronized cell cultures suggested an additional

role for KRP1 during G2/M transition, as expression levels are elevated during late G2-phase (Menges and Murray, 2002). To date not much is known about the regulation of plant CKIs, neither on the transcriptional level nor the post-translational level, such as localization and degradation.

Controlling the abundance of cell cycle regulators by protein degradation

Regulated protein degradation plays a crucial role in cell cycle progression. One mechanism for proteolysis in eukaryotes is the ubiquitin-proteasome pathway. First, a thiolester bond is formed between ubiquitin and an ubiquitin-activating enzyme (E1). Second, ubiquitin is transferred to a Cystein residue within an ubiquitin-conjugating enzyme (E2). Third, the E2 interacts with an ubiquitin-protein ligase (E3) and transfers ubiquitin to E3-bound substrates. Finally, proteins with polyubiquitin chains are recognized and degraded by the 26S proteasome, a complex consisting of a 20S core and two 19S regulatory particles (Ciechanover, 1998).

The most important E3 enzymes involved in cell cycle regulation are the Anaphase Promoting Complex/Cyclosome (APC/C) and the Skp1-cullin F-box (SCF) complex; both complexes contain a RING-finger protein as the catalytical core. In animals, the most prominent targets of the APC/C are the B-type cyclins, which become rapidly degraded at the onset of anaphase. The SCF consists of four subunits: a cullin, a S-phase kinase-associated protein1 (Skp1), a RING finger protein (RBX1) and a F-box protein. The F-box protein confers the substrate specificity for the SCF targets. One well-known example is the SCF^{Skp2} which is required for $p27^{Kip1}$ ubiquitination (Carrano et al., 1999; Sutterluty et al., 1999; Tsvetkov et al., 1999). The APC/C is conserved in plants, but at present little is known about its substrates and regulation. Several SCF E3 enzymes have been described in *Arabidopsis* and more

than 700 genes encoding for F-box proteins have been identified (Gagne et al., 2002; Hellmann and Estelle, 2002).

Another component involved in protein degradation is the COP9 signalosome (CSN). The CSN is a multi-protein complex, which was first discovered through loss-of-function mutations that repressed photomorphogenesis in *Arabidopsis* (Wei et al., 1994; Chamovitz et al., 1996). It consists of eight subunits (CSN1-8), all of which are related to proteins of the 19S regulatory particle of the proteasome. Mutations in six of the eight CSN subunits destabilize the entire complex. Moreover, it has been shown that the turnover of LONG HYPOCOTYL 5 (HY5) is inhibited in *csn* mutants and that in these mutants elevated amounts of ubiquitinated proteins accumulate (Osterlund et al., 2000; Peng et al., 2001a, b; Holm et al., 2002). Moreover the mammalian COP9 signalosome subunit 5 (CSN5) has shown to be involved in the nuclear export of $p27^{Kip1}$ (Tomoda et al., 1999; Tomoda et al., 2002).

The CSN interacts with the cullin and the RBX1 subunits of SCF E3s, suggesting a role of CSN in mediating SCF function (Schwechheimer and Deng, 2001). Rubylation (i.e. attachment of RELATED TO UBIQUITIN (RUB) to certain proteins) of the SCF subunit cullin, has shown to be an important regulatory step for of the SCF activation, by facilitating substrate polyubiquitination and E2 recruitment (Wu et al., 2000; Kawakami et al., 2001). The *Arabidopsis* CSN5A has shown to derubylate CUL1, thereby providing evidence for a positive role of the CSN in the regulation of *Arabidopsis* SCF through RUB deconjugation (Gusmaroli et al., 2004).

Targets of CDK action: regulation of G1/S transition via the RB-E2F pathway

In mammals activated CDK/cyclin complexes phosphorylate the retinoblastoma (RB) tumor suppressor protein (Weinberg, 1995). In its non-phosphorylated form RB binds

to the heterodimeric E2F-DP transcription factor (adenovirus E2 promotor binding factor; dimerization partner), thereby masking its transcriptional activation domain. Upon phosphorylation the RB protein dissociates from the E2F-DP heterodimer thereby allowing the transcription factor to activate genes required for S-phase entry. The mechanism that regulates G1/S transition appears to be conserved between animals and plants since close homologs exist in both systems.

In the *Arabidopsis* genome three genes encoding for E2F transcription factors (E2Fa, E2Fb and E2Fc) have been identified. E2Fs have also been isolated from carrot, rice, tobacco and wheat (Ramirez-Parra et al., 1999; Sekine et al., 1999); (Albani et al., 2000; de Jager et al., 2001; Kosugi and Ohashi, 2002b). Plant E2Fs share common domains and motifs similar to their animal homologs, such as a DNA binding motif, a hetero-dimerization domain, a retinoblastoma binding motif and a transcriptional activation domain, this tranactivation domain is lacking in E2Fc. Together with their DP dimerization partners E2Fs regulate the transcription of multiple genes via binding to specific E2F consensus sites in their promotor region. 5765 *Arabidopsis* genes have been found that contain potential E2F-sites in their promotors. E2F regulated genes include genes required for DNA replication such as CDC6 and DNA polymerase α (Ramirez-Parra et al., 2003).

The family of *Arabidopsis* E2F transcription factors can be divided into two classes. E2Fa and E2Fb act together with the appropriate dimerization partner as transcriptional activators whereas E2Fc, which lacks the transcriptional activation domain, might act as a repressor competing for the same E2F-sites (Fig3). This has been reported at least for the transcriptional regulation of *CDC6,* a subunit of the origin recognition complex (ORC) which has been shown to be upregulated in plants overepxressing *E2Fa* together with *DPa* whereas overexpression of *E2Fc* results in a

decrease of *CDC6* expression (De Veylder et al., 2002; del Pozo et al., 2002). Moreover, *Arabidopsis* and tobacco plants misexpressing *E2Fa* and *DPa* together show ectopic cell divisions and excessive endoreplication (De Veylder et al., 2002; Kosugi and Ohashi, 2003).

In the *Arabidopsis* genome, two genes have been identified encoding for DP proteins (DPa and DPb) (Magyar et al., 2000). Not much is known about DPs function *in planta*. So far no mutants have been described. The only insights into DP function came from the misexpression of *DPa*, that only led to morphological changes if overexpressed together with *E2Fa* (De Veylder et al., 2002).

The three *Arabidopsis DP-E2F-like* genes (*DEL*s) might also act as repressors. In contrast to the heterodimeric E2F-DP transcription factor which can only bind to DNA as a dimer, DELs can bind to the same promotor-E2F sites as monomers, because they contain two DNA binding domains. Like for E2Fc, DEL proteins lack the transcriptional activation domain suggesting that DELs act as competitors of E2Fa/b-DPa/b (Fig3) (Kosugi and Ohashi, 2002a). DEL proteins appear to be involved in the regulation of endoreplication since enhanced ploidy levels have been reported for the *del1* mutant whereas overexpression results in a down-regulation of the expression of E2F target genes and a reduction of endoreplication (Vlieghe et al., 2005).

Recently, a gametophytic lethal *rbr1* mutant has been isolated. Loss of function of *RBR1* results in an overproliferation of gametophytic and endosperm nuclei (Ebel et al., 2004). Ectopic expression of *RBR1* under control of promotors active in the shoot- or root-meristem results in cell cycle arrest, whereas the misexpression of RBR1-RNAi constructs under control of these promotors leads to ectopic cell divisions (Wilhelm Gruissem, personal communication). Similar

observations were made by suppression of *RBR1* from *Nicotiana benthamiana* via virus induced gene silencing (Park et al., 2005).

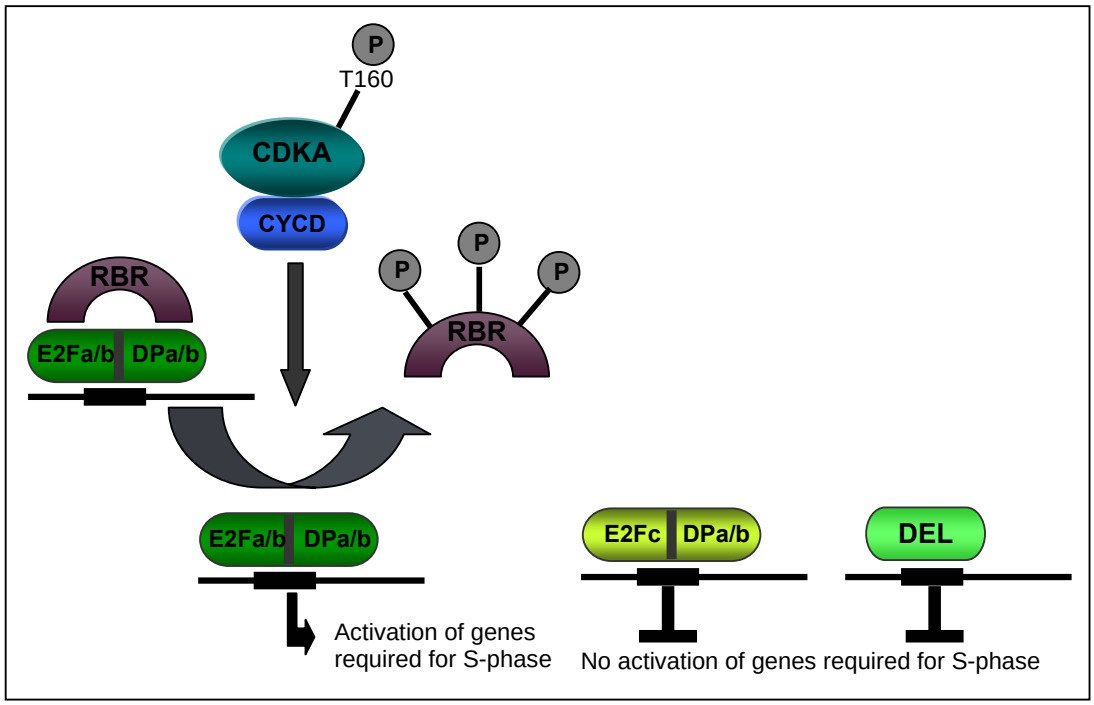

Figure 3 The RBR-E2F pathway in *Arabidopsis*
Simplified model about the regulation of the transcription of genes required for S-phase by the RBR-E2F pathway in *Arabidopsis*.

Model systems to study the function of cell cycle regulators

Since many mutants in cell cycle regulators are either embryonic or gametophytic lethal, e.g. *rbr1*, or display no alteration from wild type plants due to backup systems and redundancies, e.g. B-type cyclins (Farshad Roodbarkelari, personal communication) the analysis of plant cell cycle regulators has strongly relied on the use of misexpression experiments. For this purpose mostly the ubiquitously active 35S promotor (Pro_{35S}) from the *Cauliflower Mosaic Virus* (*CaMV*) has been applied. The positive aspect is that a wide range of different cell types can be analyzed for their reaction to the overexpression of the respective cell cycle regulator. However, ectopic expression of cell cycle regulators can cause severe effects on plant growth.

For examples plants misexpressing *Pro_{35S}:E2Fa* together with *Pro_{35S}:DPa* are tremendously retarded in growth (De Veylder et al., 2002) and overexpression of the N-terminally truncated *$KRP1^{109}$* under control of *Pro_{35S}* was lethal (Zhou et al., 2003). In these lines, it is difficult to distinguish whether the observed phenotype is caused by the misexpression of the cell cycle regulator directly, or whether this phenotype refelects the misregulation of multiple genes challenged by the misexpression, or whether it is an indirect effect, e.g. in *Pro_{35S}:KRP1* misexpressing plants also root development is severely affected.

Misexpression in specific cells, such as *Arabidopsis* leaf hairs (trichomes), have been proven to be suitable to study the function of cell cycle regulators in a developmental context, also largely avoiding general growth and fertility problems (Schnittger et al., 2002b; Schnittger et al., 2002a; Schnittger et al., 2003). Trichomes are single-celled leaf hairs, which are initiated with a controlled distance to each other in the basal part of young and developing leaves. Archetypical for many differentiating cells, incipient trichomes exit the mitotic program and switch to an endoreplication mode. Concurrent with outgrowth and initiation of branches, trichomes undergo approximately four rounds of endoreplication leading mature three-branched trichomes with a DNA content of approximately 32C (Marks, 1997; Hulskamp et al., 1999).

To specifically study the role of cell cycle regulators in an endoreplicating context various promotors can be used, such as *CAPRICE*, *GLABRA2* or *TRIPTYCHON* promotor. These three genes play important roles in trichome development and are expressed from very early stages until late stages of trichome development (Fig4C,D,E; Fig10A,F) (Szymanski et al., 1998; Schellmann et al., 2002). Besides its expression in trichomes *GLABRA2* is expressed in alternating

epidermal files of the hypocotyls of developing embryos, from late-heart stage until bent-cotyledon stage (Fig4A,B) (Costa and Dolan, 2003). Thus expression of cell cycle regulators under control of the *GLABRA2* promotor provided a tool to analyze their function in a mitotic and an endoreplicating context.

To analyze the function of cell cycle regulators in dividing epidermal cells during post-embryonic development, the promotor of the *TOO MANY MOUTH* gene (*TMM*) has been used. TMM is involved in the control of stomata distribution and has been found to randomize the plane and alter the number of asymmetric divisions in stomata neighboring cells (Geisler et al., 2000). *TMM* is expressed during early leaf development in cells of the stomatal lineage. Expression could be detected in meristemoids, guard mother cells and some of their neighboring cells, but also in guard cells (Fig4F,G;Fig17A,B) (Nadeau and Sack, 2002a).

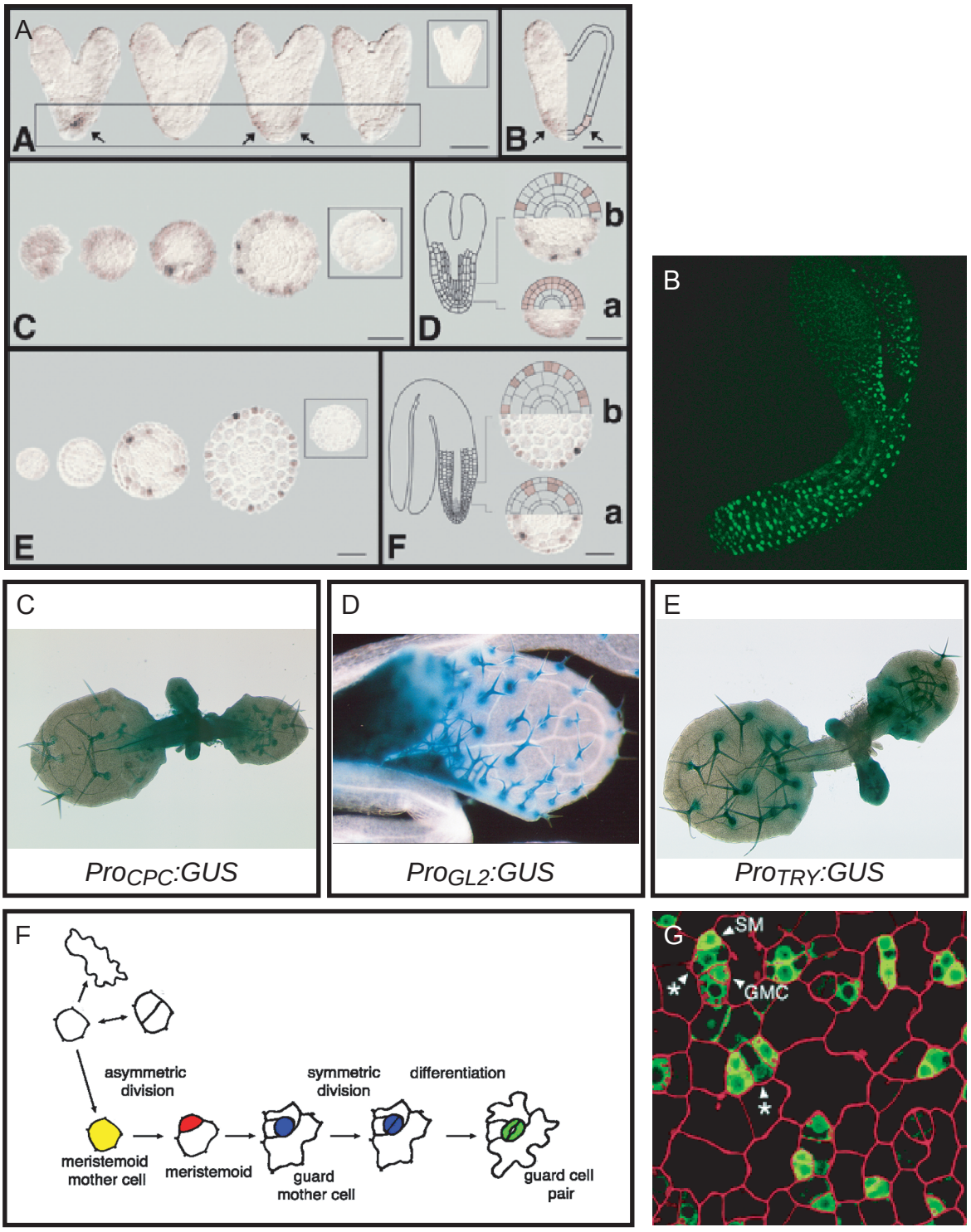

Figure 4 Model cells to study cell cycle regulation in *Arabidopsis*
(A) and **(B)** Expression of *GLABRA2* (*GL2*) during embryo development is shown in (A) by *in situ* hybridization experiments; picture taken from (Costa and Dolan, 2003) and in (B) by laser scanning microscopy of a bent cotyledon stage embryo expressing *Pro$_{GL2}$:nls:GFP:GUS*.
(C) Expression pattern of *CAPRICE* (*CPC*) in rosette leaves revealed by Promotor:GUS analysis
(D) Expression pattern of *GLABRA2* in rosette leaves revealed by Promotor:GUS analysis
(E) Expression pattern of *TRIPTYCHON* (*TRY*) in rosette leaves revealed by Promotor:GUS analysis
(F) Schematic drawing of guard cell development; picture taken from (Nadeau and Sack, 2002b)
(G) Confocal scanning micrograph of leaf epidermal cell from plants expressing *Pro$_{TMM}$:TMM:GFP*; to visualize cell walls the leaf was stained with propidium iodide; picture taken from (Nadeau and Sack, 2002a). GMC: guard mother cell, SM: satellite merisetemoid

Aim of this work

In this work I wanted to study the regulation of endoreplication in the context of cell differentiation in *Arabidopsis thaliana*. The analysis focused on two groups of key-regulators of the cell cycle. First, the CDK inhibitors (KRPs), which block the activity of CYCLIN DEPENDENT KINASEs. Second, the components of the RBR-E2F pathway, which are downstream targets of CDKs, involved in the regulation of entry into S-phase. To analyze their function cell type specific misexpression experiments in dividing or endoreplicating cells were performed.

RESULTS

1. Studying KRP function: loss of function approach

1.1. Isolation of a *krp1* mutant

One approach to learn more about the function of KRPs is to isolate mutants and analyze their phenotypes. Therefore I performed a PCR-based screen for T-DNA insertions in the *KRP1* (At2g23430) and the *KRP4* (At2g32710) gene in the Koncz T-DNA line collection, which contains more than 80000 individual *Arabidopsis* insertion-lines (Rios et al., 2002).

Whereas for *KRP4* no insertion line could be found, for *KRP1* one insertion line was found in Pool #36537. Sequencing of the PCR product obtained with the screening primer S1 and the left border primer T1 revealed that the T-DNA is inserted in the second intron, 387 bp downstream from the start codon (Fig5A). So far all PCR attempts, using the primer combinations S2+T2, S2+T4 and S2+T6, to proof that the complete 7 kb T-DNA was inserted in the *KRP1* gene failed to reveal the insertion of the right border. However, plants were resistant to hygromycin and the *HYGROMYCIN PHOSPHOTRANSFERASE* (HPH) which confers resistance is located approximately 2 kb from the right border. Also no PCR products could be amplified with the S2 primer and any left border primer (T1, T3 and T5). To test whether the insertion resulted in a knock-out, a knock-down or knock-in of *KRP1*-function semiquantitative RT-PCR analyses were performed. No transcript could be detected in the homozygous mutant with a primer combination spanning the complete coding sequence of *KRP1* (R1+R2) (Fig5B upper panel). However, using the primers R3 and R2, which anneal downstream of the T-DNA insertion, transcript could be

obtained (Fig5B lower panel). This could be because the T-DNA contains promotor-like elements, which then result in a transcription of the *KRP1* C-terminal domain. Even though the transcript level is reduced in the mutant compared to wild type it cannot be ruled out that this mRNA becomes translated and that this peptide interferes for example with the CDK/cyclin complex, especially because it contains the cyclin- and CDK-interacting domains (see Fig7).

1.2. The *krp1* mutant

Analysis of the phenotype of the homozygous *krp1* T-DNA insertion plants revealed no obvious morphological alterations in comparison to wild type. Promotor-reporter analysis (Lieven de Veylder personal communication) and *in situ* hybridization of *KRP1* mRNA suggested that *KRP1* is expressed in endoreplicating trichome cells (Ormenese et al., 2004). Therefore I measured the trichome DNA content, which revealed a subtle enhancement of endoreplication in the homozygous *krp1* mutant. The median of the relative fluorescence of DAPI stained wild-type trichome nuclei was set as 32C (Fig5C). Three independent measurements of trichome DNA levels in the homozygous *krp1* mutant revealed an elevated DNA content, 37.2C, 40.1C and 44.1C respectively, in comparison to wild type (Fig5C). This finding suggests that KRP1 might be involved in the termination of endocycles in trichomes.

Figure 5 The *krp1* mutant
(A) Schematic drawing of the *KRP1* gene showing the T-DNA insertion in the second intron. Grey boxes represent the four exons, S1, S2 and T1 are the screening primers used for the identification of the insertion line. Also the primers used for the RT-PCR are shown (R1, R2 and R3).
(B) Semi-quantitative RT-PCR showing the relative expression strength of wild-type and the *krp1* mutant. The used *KRP1* primers are indicated on the left side. For the control, primers which amplify the *ELONGATION FACTOR 1* (*EF1*) were used. Samples were taken after 30 or 40 cycles as indicated at the top of the figure.
(C) Distribution of trichome cell DNA contents are given in relative fluorescence units (RFUs). The median RFU of wild-type was set as 32C so that 2 RFUs represent approximately 2C. The sample size (n), the mean (m) +/- standard deviation and the median (md) are given.

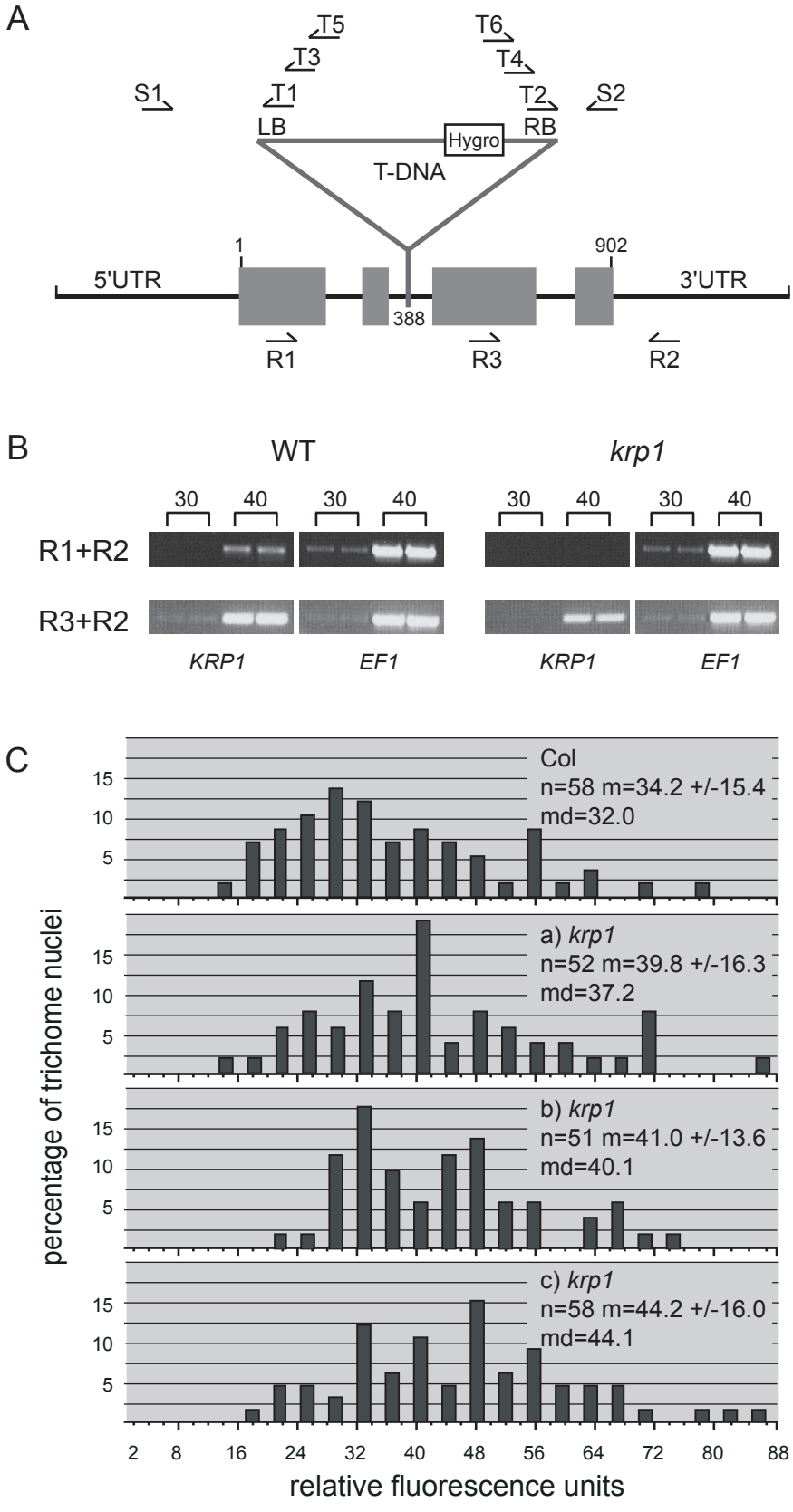

Figure 5 The *krp1* mutant

1.3. RNAi approach

At the time the mutant was characterized no further insertion lines for *KRP1* were available from other T-DNA collections to support the observed trichome phenotype. Therefore I tried to knock-out KRP-function using a RNA interference approach by which introduction of double-stranded RNA should lead to a post-transcriptional silencing of the respective gene. In several attempts I tried to knock out KRP1 in trichomes. For that purpose I expressed double-stranded RNA of either the full-length *KRP1* gene or the N-terminal domain of *KRP1*, which shows only low homology with the other members of the KRP family, by using the *GLABRA2* promotor *(*Pro_{GL2}). However analysis of seedlings in the T1 generation revealed a wild-type phenotype with respect to trichome morphology, leaf size and all over plant morphology (Tab1). Additionally, I expressed double-stranded RNA of full-length *KRP4*, its N-terminal domain and a 141 bp fragment, which shows a high homology to *KRP1*, in trichomes. Primary transformants did not display any morphological changes. Also the expression of double-stranded RNA of a short fragment of exon 3 from *KRP1* or of two fragments of exon 4 from *KRP7*, which has shown to be expressed in endoreplicating and dividing cells (Ormenese et al., 2004), under control of the ubiquitously active *CaMV35S* promotor (Pro_{35S}) did not result in a detectable phenotype in seedlings (Tab1).

In summary these results indicate that either the RNAi approach did not sufficiently reduce transcript levels of *KRPs*, or that the individual members of the KRP family act in a highly redundant manner, so that only in plants with a loss of function for more than one *KRP* gene a phenotype can be detected. The latter scenario is supported by the observation that even double and triple mutant combinations of

krp2 with other *krp* mutants did not display any morphological alterations in comparison to wild type (Lieven de Veylder, personal communication).

TABLE 1
RNAi CONSTRUCTS TO KNOCK OUT *KRPS*

line	template	position sense primer	position antisense primer	Trichome or seedling* phenotype
Pro$_{GL2}$:fl-KRP1-RNAi	*KRP1*	Exon 1	Exon 4	WT
Pro$_{GL2}$:N-KRP1-RNAi	*KRP1*	Exon 1	Exon 3	WT
Pro$_{35S}$:Exon3-KRP1-RNAi	*KRP1*	Exon 3	Exon 3	WT
Pro$_{GL2}$:fl-KRP4-RNAi	*KRP4*	Exon 1	Exon 3	WT
Pro$_{GL2}$:N-KRP4-RNAi	*KRP4*	Exon 1	Exon 1	WT
Pro$_{GL2}$:cons-KRP4-RNAi	*KRP4*	Exon 2	Exon 3	WT
Pro$_{35S}$:Exon4a-KRP7-RNAi	*KRP7*	Exon 4	Exon 4	WT*
Pro$_{35S}$:Exon4b-KRP7-RNAi	*KRP7*	Exon 4	Exon 4	WT*

2. Studying KRP function: gain of function approach

2.1. Misexpression of *Arabidopsis KRP1* and *KRP4* in trichomes

As described previously by Schnittger et al. the misexpression of *KRP1* or the N-terminal truncated *KRP1*^{109} in trichomes under control of the *GLABRA2* promotor results in smaller trichomes with reduced number of branches in comparison to wild type (Fig6A;B;E) (2003). In addition trichomes misexpressing *KRP1* underwent cell death (Fig6G). DAPI stainings (see Fig6C,F for DAPI stained trichome nuclei) and DNA measurements revealed that endoreplication levels were reduced.

To test whether KRPs display similar functions in endorpelicating cells, I misexpressed another member of the KRP family, KRP4, which has not been characterized so far. The trichomes of the *Pro$_{GL2}$:KRP4* transgenic plants also had fewer branches, the cell size was reduced and they showed the cell death phenotype as seen for *Pro$_{GL2}$:KRP1* expressing plants (Fig6D). Taken together these data indicate that both *KRP1* and *KRP4* have similar effects, when misexpressed in trichomes.

Figure 6 Misexpression of *KRP1* and *KRP4* in trichomes
(A) to **(C)** Landsberg *erecta* wildtype In (A) an overview of a two week old seedling with mostly three-branched trichomes is given. (B) Scanning electron micrograph and (C) light micrograph of DAPI-stained mature trichomes with its neighboring cells, arrowheads point at trichome and trichome-neighboring cell nuclei.
(D) Overview of a two week old *Pro$_{GL2}$:KRP4* misexpressing seedling with two- and unbranched trichomes
(E) to **(G)** *Pro$_{GL2}$:KRP1*^{109} misexpressing line. (E) and (G) Scanning electron micrographs showing in (E) a small and two-branched and in (G) a dead trichome. Note the enormously increased trichome-neighboring cells. (F) Light micrograph of DAPI-stained trichome with its neighboring cells, arrowheads point at trichome and the large trichome-neighboring cell nuclei.
(H) and **(I)** Scanning electron micrograph of (H) *glabra3* and (I) *cpr5* mutant trichomes, which have fewer branches, but normal sized trichome-neighboring cells
(J) and **(K)** Confocal laser scanning micrographs of enhancer trap line #254. (J) Showing the youngest state when GFP is detectable in the trichome-neighboring cells (indicated by arrowheads) and (K) a close up of line #254 showing GFP fluorescence in a mature trichome and its neighboring cells.
(L) Confocal laser scanning micrograph of *Pro$_{GL2}$:KRP1*^{109} crossed in enhancer trap line #254, showing GFP expression in the enlarged trichome-neighboring cells.
Scale bar in all panels 100µm.

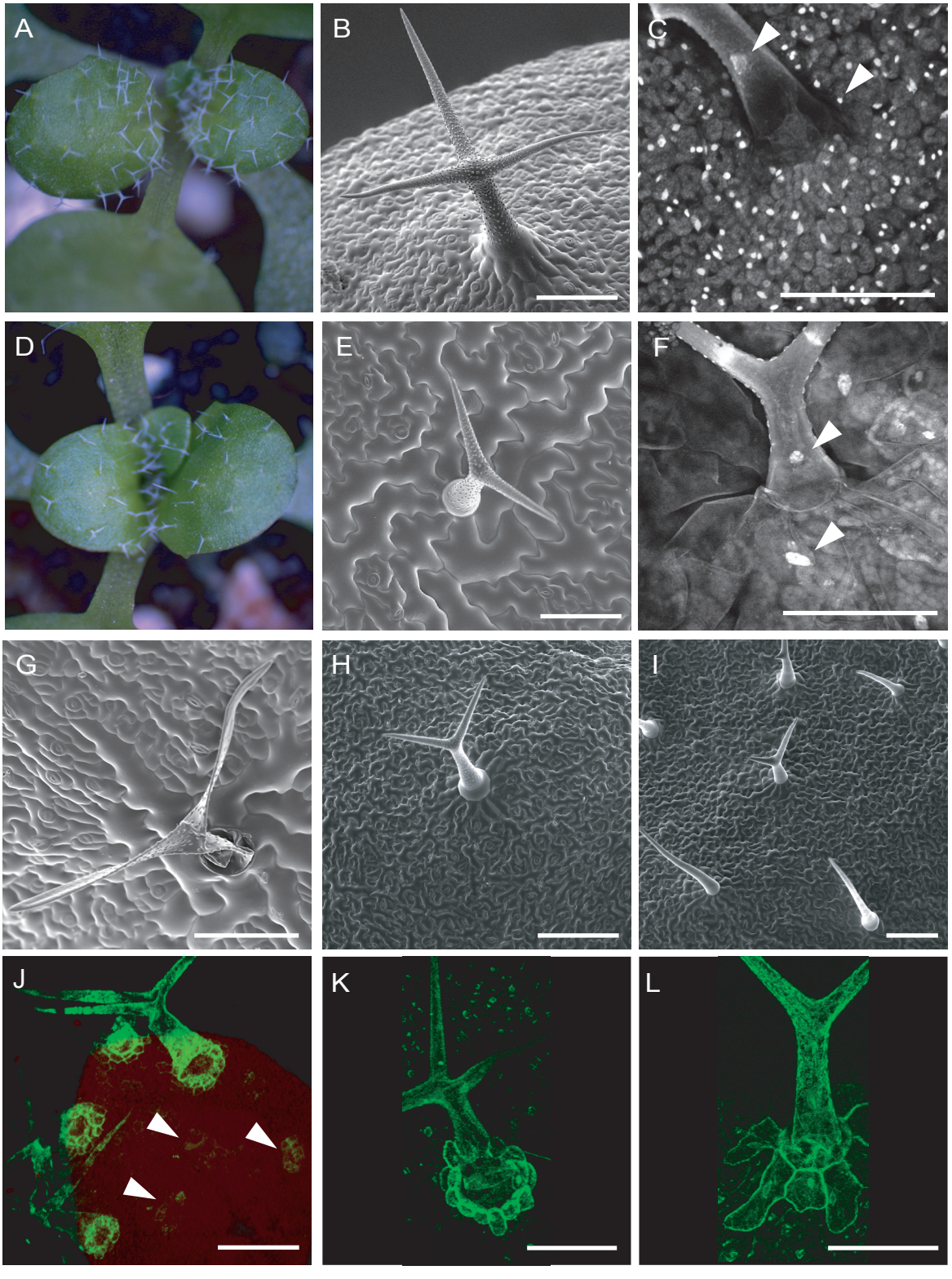

Figure 6 Misexpression of *KRP1* and *KRP4* in trichomes

2.2. Domain analysis of the KRP1 protein

Wang et al.,1998 examined in a yeast two hybrid assay KRP1 interactions with CDKA;1 and CYCLIN D3;1. Creating deletion constructs the authors could identify distinct functional domains within the *KRP1* gene. The CDK and the D-type cyclin interacting domain are harbored in the C-terminus because a deletion after amino acid (aa) 152 resulted in a loss of interaction with CDK and cyclin. In this assay also an inhibitory domain could be identified, deletion of the first 108 aa lead to a strong enhancement of CDK and cyclin interaction (Fig7). In the work of Schnittger et al. 2003 those two truncated versions of *KRP1* (*KRP1*^{152} and *KRP1*^{109}) were misexpressed in trichomes and reflected the yeast data. *Pro*$_{GL2}$*:KRP1*^{152} misexpressing trichomes looked like wild-type, whereas the misexpression of *Pro*$_{GL2}$*:KRP1*^{109} caused a much stronger phenotype than the full-length *KRP1* (Fig7). Similar results have been reported by Zhou et al., 2003 for the overexpression of *KRP1*^{162} and *KRP1*^{176} under control of the 35S promotor, which had a wild type appearance, while overexpression of *KRP1*^{109} resulted in dwarf plants, which eventually died. Also in their study the KRP1 phenotype was enhanced in transgenic lines misexpressing the truncated *KRP1*^{109}. All these data pointed towards an important regulatory role of the first 108 aa. To test whether this N-terminal domain might be necessary for KRP1 stability or whether it plays a role in the subcellular localization of the protein I generated misexpressing lines containing either the *Pro*$_{GL2}$*:YFP:KRP1*^{108} or the *Pro*$_{GL2}$*:KRP1*^{108}*:YFP* construct. Analysis of these transgenic lines revealed a wild type phenotype based on their trichome morphology, as expected as CDK- and cyclin-interacting domains are missing. (For a detailed description of the localization, see below.)

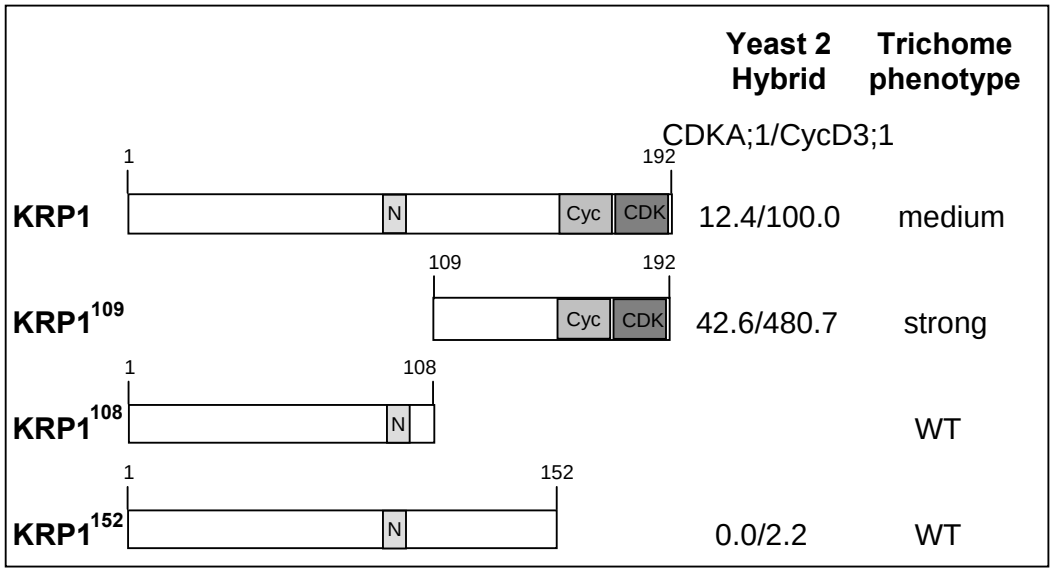

Figure 7 The KRP1 domains
Schematic drawing of the KRP1 domains in order to give an overview of the full-length KRP1 and the three truncated versions KRP1^{109}, KRP1^{108} and KRP1^{152}. Moreover the interaction strength of the constructs with CDKA;1 and cyclin D3;1 is given. These results were obtained from β-galactosidase activity assays of yeast two hybrid experiments performed by Wang et al., 1998. KRP1^{108} was not analyzed in the yeast two hybrid assay. The *in planta* data of KRP1, KRP1^{109} and KRP1^{152} were obtained by Schnittger et al., 2003 representing the trichome misexpression phenotypes.
Cyc: cyclin interacting domain; CDK: CDK interacting domain; N: putative nuclear localization sequence

2.3. Trichome-neighboring cells in *Pro$_{GL2}$:KRP1* misexpressing plants are enlarged and have an increased DNA content

Analyzing the cells surrounding a trichome on old rosette leaves of plants expressing the *Pro$_{GL2}$:KRP1^{109}* construct I made an unexpected observation: the trichome-neighboring cells were strongly enlarged (Fig6B,E). Whereas wild-type trichome-neighboring cells reached in average a total surface-cell-area of ca. 1200µm², on comparable leaves of *Pro$_{GL2}$:KRP1^{109}* plants trichome-neighboring cells encompassed a more than 10 time larger total surface area of approximately 13500µm² (Tab2). Examining transgenic plants carrying the full length *KRP1* misexpression construct, which showed a weaker trichome phenotype, I observed an enlargement of the trichome-neighboring cells to an average of 4800µm² (Tab2).

Since cell size is often correlated with the degree of cellular polyploidization, I measured the DNA content by quantifying the fluorescence of DAPI-stained nuclei (Fig6C,F; Fig8). I detected a strongly increased DNA content in the trichome-neighboring cells in the *KRP1*-misexpressing plants, a mean of 17.4C versus 6.4C in wild type (Fig8). An even stronger increase in DNA levels was measured in plants expressing the truncated $KRP1^{109}$ construct with an average of 29.5C, and occasionally, extremely enlarged nuclei with up to 80C were found (Fig8).

The observed cell enlargement and increase in nuclear size of the trichome-neighboring cells in the *KRP1*-misexpression plants are reminiscent of a trichome developmental program. Trichome patterning is thought to involve a mutual inhibition mechanism, by which all epidermal cells compete with each other in order to adopt trichome cell fate (Larkin et al., 2003). Hence, the hypothesis was raised that due to a compromised and eventually dead trichome as a result of *KRP1* misexpression, the lateral inhibition is released and the trichome-neighboring cells start to develop into trichomes. Analysis of an early trichome reporter (*Pro_{GL2}:nls:GFP:GUS*), however, revealed no expression in cells surrounding the *KRP1*-misexpressing trichomes, indicating that an initiated trichome developmental program is not responsible for the observed phenotype (Fig10A,K).

To further investigate whether the enlargement of the trichome-neighboring cells could be a response to a compromised trichome-differentiation program, the cells surrounding a trichome in *glabra 3* (*gl3*) and *constitutive pathogen response 5* (*cpr5*) mutant plants were analyzed. Trichomes in both mutants have reduced endoreplication levels, are smaller than wild-type trichomes, and develop mostly only two branches (Hulskamp et al., 1994; Kirik et al., 2001). In addition, similar to trichomes on *Pro_{GL2}:KRP1* expressing plants *cpr5* mutant trichomes have been

reported to die. However, neither the trichome-neighboring cells in the *gl3* nor in the *cpr5* mutant displayed any significant difference to wild-type trichome-neighboring cells with respect to cell size and DNA content (Fig6H,I; Fig8; Tab2).

Taken together, these data suggest that trichome-neighboring cell enlargement and increase in DNA content is due to *KRP1* misexpression in trichomes, and is not a general feature of altered trichome development.

TABLE 2
Total surface area of trichome-neighboring cells

line	total surface area [1]		Σ cells
L*er*	1208+/-493	(1114)	40
gl3	1422+/-789	(1159)	38
cpr5	1103+/-761	(790)	54
Pro$_{GL2}$:KRP1	4755+/-2120	(4908)	55
Pro$_{GL2}$:KRP1^{109}	13459+/-6295	(13180)	45
Pro$_{GL2}$:YFP:KRP1	1101+/-425	(1154)	46
Pro$_{GL2}$:KRP1^{109}:YFP	2495+/-1253	(2007)	86
Pro$_{GL2}$:GUS:YFP:KRP1^{109}	717+/-346	(587)	54
Enhancer trap line #254	675+/-241	(639)	51
Pro$_{UAS}$:YFP:KRP1^{109} in #254	738+/-392	(658)	47

[1] Total surface area of trichome-neighboring cells on rosette leaves was measured from at least five different plants per line, average plus/minus standard deviation and median in parenthesis are given in μm^2.

Figure 8 Analysis of the DNA content of trichome-neighboring cells
Distributions of the DNA content of trichome-neighbouring cells are given in relative fluorescence units (RFUs). RFUs are calibrated with the fluorescence of guard cell nuclei of the analyzed leaves so that 2 RFUs represent approximately 2C. The sample size (n), the mean (m) +/- standard deviation and the median (md) are given.

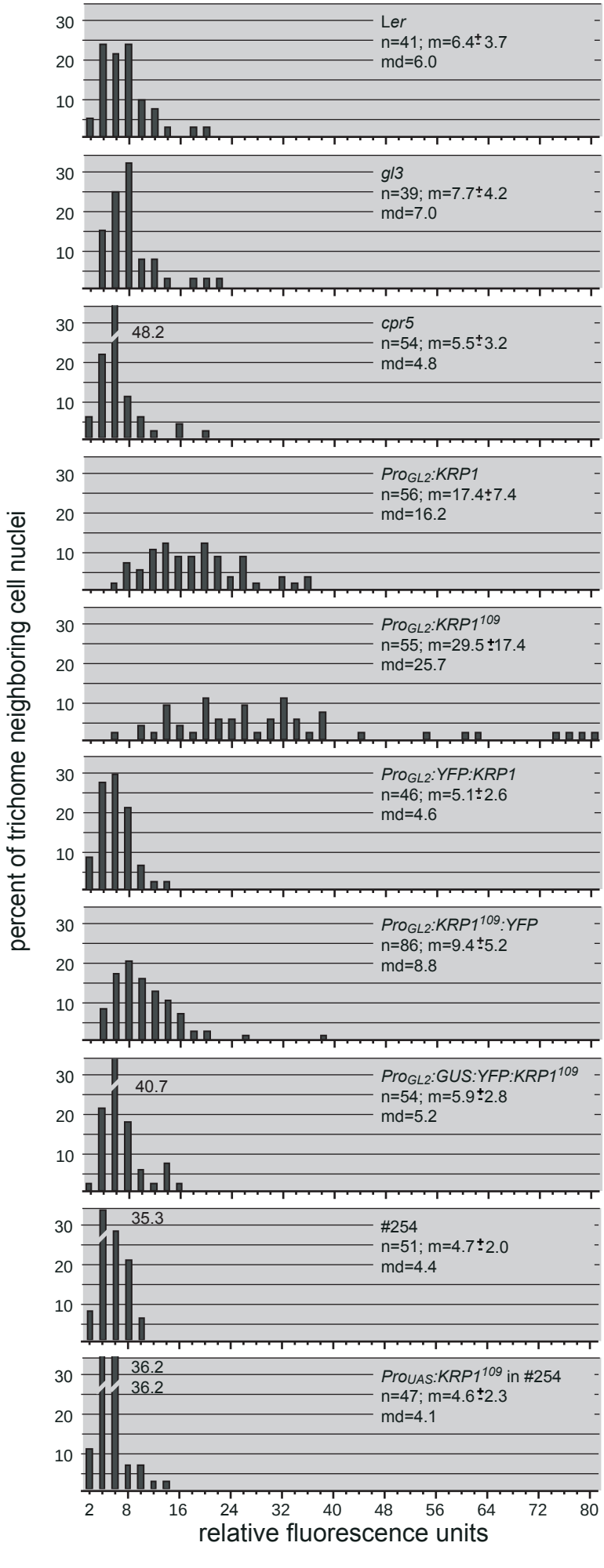
percent of trichome neighboring cell nuclei
relative fluorescence units
Ler
n=41; m=6.4±3.7
md=6.0
gl3
n=39; m=7.7±4.2
md=7.0
cpr5
n=54; m=5.5±3.2
md=4.8
48.2
Pro GL2:KRP1
n=56; m=17.4±7.4
md=16.2
Pro GL2:KRP1 109
n=55; m=29.5±17.4
md=25.7
Pro GL2:YFP:KRP1
n=46; m=5.1±2.6
md=4.6
Pro GL2:KRP1 109:YFP
n=86; m=9.4±5.2
md=8.8
Pro GL2:GUS:YFP:KRP1 109
n=54; m=5.9±2.8
md=5.2
40.7
#254
n=51; m=4.7±2.0
md=4.4
35.3
Pro UAS:KRP1 109 in #254
n=47; m=4.6±2.3
md=4.1
36.2
36.2
0
10
20
30
2
8
16
24
32
40
48
56
64
72
80

2.4. Intercellular localization of KRP1

Based on the conclusion that the phenotype of trichome-neighboring cells is specific for *KRP1*-misexpression, two different scenarios were reasoned by which KRP1 could influence the cells surrounding a trichome. First, KRP1 might act indirectly and its expression in trichomes would induce a non-cell-autonomous response. Alternatively, given that plant cells are symplastically connected by plasmodesmata (Ding et al., 2003; Oparka, 2004), KRP1 itself might move into the neighboring cells.

In order to test the localization and mobility of KRP1, the yellow fluorescent protein (YFP) was fused to KRP1 and KRP1^{109} and misexpression lines using the *GL2* promotor were generated. Homozygous lines were created and based on mRNA expression strength comparable lines were chosen as reference lines for further investigations (Fig9A). All data provided in the following was obtained from the same reference line. As a control, transgenic plants expressing a cell-autonomous version of the green fluorescent protein (*GFP*) with a localization signal for the endoplasmatic reticulum (*Pro$_{GL2}$:GFP5ER*), and plants expressing an untagged YFP protein (*Pro$_{GL2}$:YFP*) were created (Siemering et al., 1996; Haseloff et al., 1997; Crawford and Zambryski, 2000).

Plants expressing the fusion proteins were first analyzed with respect to their trichome phenotype, in order to compare their phenotypical strength with that of unfused KRPs. Plants carrying an N-terminal YFP fusion to KRP1 (*Pro$_{GL2}$:YFP:KRP1*) displayed smaller and under-branched trichomes, which eventually died, resembling the *KRP1*-misexpression phenotype (Tab2). The expression of *KRP1* with a C-terminal fusion (*Pro$_{GL2}$:KRP1:YFP*) did not result in a phenotype and transgenic plants were not further analyzed. For *KRP1^{109}*, plants misexpressing both N- and C-terminal fusion proteins with YFP resembled the

phenotype of *Pro$_{GL2}$:KRP1^{109}* plants (Tab2). Similarly to the expression of the unfused KRP1, I recognized that expression of fusion proteins containing the N-terminally truncated *KRP1^{109}* resulted in a stronger trichome phenotype than the expression of fusion protein with the *KRP1* full length version (Tab2). Thus, although fusions in the C-terminus to the full length KRP1 seemed to interfere with protein action, concluding that a fusion with YFP in the other three constructs did not result in an altered KRP1 protein activity as judged by their trichome phenotypes.

In order to determine whether the fusion proteins were expressed as complete proteins western blot experiments of the generated transgenic plants were performed and the blots were probed with antibodies raised against GFP, which also recognizes YFP. The protein work was done with the help of Sebastian Marquardt. For plants expressing *Pro$_{GL2}$:YFP* a strong band could be detected at the expected size of 27 kD. The majority of the *KRP1^{109}* fusion proteins can be detected at the predicted size of 37 kD (Fig9B). For the full-length version no band could be detected, although on RNA level the construct appeared even to be slightly stronger expressed than the truncated version (Fig9A,B). Previously it has been shown that a negative regulatory signal resides in the N-terminus of the KRP1 protein (Schnittger et al., 2003; Zhou et al., 2003). The limitation in detection of the full-length CDK inhibitor argues that this domain might regulate the stability of KRP1 protein. Consistently, Zhou et al. recently reported that a N-terminally truncated version was present in much higher abundance than the full-length inhibitor (2003).

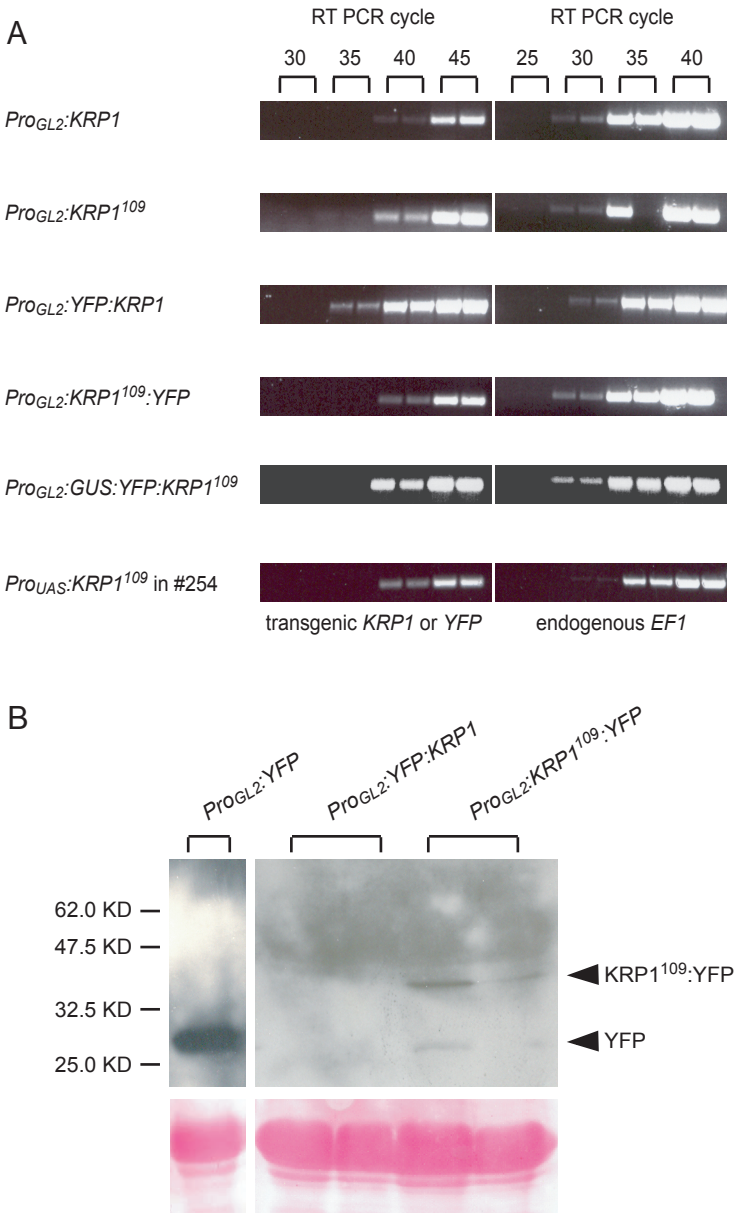

Figure 9 Analysis of expression levels

(A) Semi-quantitative RT-PCR showing the relative expression strength of the transgenic constructs *Pro$_{GL2}$:KRP1*, *Pro$_{GL2}$:KRP1^{109}*, *Pro$_{GL2}$:YFP:KRP1*, *Pro$_{GL2}$:KRP1^{109}:YFP*, *Pro$_{GL2}$:GUS:YFP:KRP1^{109}* and *Pro$_{UAS}$:KRP1^{109}* in enhancer trap line #254. The expression strength was compared with the endogenous expression of *translation elongation factor 1* (*EF1*). The numbers at top indicate the number of RT-PCR cycles. *Pro$_{GL2}$:YFP:KRP1* and *p$_{UAS}$:KRP1^{109}* appeared to be slightly stronger expressed than the other transgenes.

(B) Western Blot analysis of *Pro$_{GL2}$:YFP, Pro$_{GL2}$:YFP:KRP1*, and *Pro$_{GL2}$:KRP1^{109}:YFP* misexpressing plants with an antibody against GFP/YFP. As a loading control Ponceau staining of the membrane after protein transfer is shown in the lower panel. From extracts of *Pro$_{GL2}$:YFP* plants a band of approximately 27 kD was detected matching the calculated size of YFP. No bands could be detected for YFP:KRP1. For KRP1^{109}:YFP a band was detected at the expected fusion protein size of approximately 37 kD, in addition, a faint band appeared at about 27 kD resembling most likely a degradation product.

Next, the cellular localization of the fusion proteins was analyzed by Confocal-Laser-Scanning-Microscopy. As controls I first analyzed the expression of two *GL2* reporter lines in a wild-type background and in plants expressing Pro_{GL2}*: KRP1*^{109}. In wild-type, both GFP5ER and a nls:GFP:GUS fusion protein expressed from the *GL2* promotor were only detected in trichomes and trichome precursor cells (Fig10A,F). In the F1 generation of the cross of the Pro_{GL2}*:nls:GFP:GUS* reporter line with the reference line expressing Pro_{GL2}*:KRP1*^{109} the GFP signal was still restricted to trichomes and trichome precursor cells indicating that trichome-specific expression of *KRP1*^{109} did not alter the expression domain of the *GL2* promotor (Fig10K).

In contrast to the trichome-specific localization of the two *GL2* promotor reporter lines, the KRP1 fusion proteins could also be detected in cells around trichomes. In young leaves, KRP1 fusion protein could be detected in many epidermal cells (Fig10B,C,D). In older leaves, the full length KRP1 and the KRP1^{108} fused to YFP were predominantly found in one to two concentric rings around a trichome (Fig10G,H). The truncated version KRP1^{109} was detectable in three to four rings with decreasing intensity (Fig10I). Also, I could detect a weak YFP signal in the nuclei of mesophyll cells demonstrating that movement of KRP1 fused to YFP is not restricted to epidermal cells but reflects rather a general feature of KRP1:YFP fusion proteins (Fig10N, arrowhead). Based on these localization patterns it is conceivable that the unfused KRP1 when expressed in trichomes will also enter the neighboring cells.

A morphological analysis of the trichome-neighboring cells revealed, however, that only plants expressing the N-terminally truncated KRP1^{109} fused to YFP displayed a significant increase in trichome-neighboring cell size and DNA content with about 2500µm² and 9.4C (Tab2, Fig8). Thus, in contrast to trichomes, the alterations of the trichome-neighboring cells were correlated with the protein size

of the misexpressed KRP1 protein, i.e. smaller proteins caused a more severe phenotype: KRP1^{109} (10kD) > KRP1 (22kD) > KRP1^{109}:YFP (37kD) > YFP:KRP1 (49kD).

To address the dynamics of the movement of KRP1 and to test whether larger fusion proteins were less abundant in trichome-neighboring cells than smaller KRP1 versions, the fluorescence intensities of KRP1:YFP fusions were compared with that of free YFP. As previously reported, the YFP-related GFP is able to diffuse up to 16 cells wide in microprojectile bombardment experiments in *Arabidopsis* (Itaya et al., 2000). Consistently, in the generated transgenic plants expressing YFP without any localization signals from the *GL2* promotor (*Pro$_{GL2}$:YFP*) YFP could be detected in trichomes and in neighboring cells (Fig11A,B). Determination of the fluorescence intensity of trichome-neighboring-cell nuclei in comparison to trichome nuclei revealed for KRP1^{109}:YFP (37 kD) a similar ratio of approximately 0.5 as for YFP (27 kD) whereas for the larger KRP1 fusion (49 kD) a lower ratio of approximately 0.2 was obtained (Fig11C). This is consistent with a reduced movement and therefore a lower concentration of increasingly larger fusion proteins in trichome-neighboring cells.

However, it could not be excluded that the different KRP1 protein versions have different molecular properties in trichome-neighboring cells versus trichomes, e.g. protein stability and/or nuclear import rate, which could influence the ratio of fluorescence intensities independent of protein size. To test more directly for a protein-size dependent movement, transgenic plants were created expressing another KRP fusion protein, in which the GUS protein was combined with YFP:KRP1^{109}; the size of this fusion protein is approximately 105 kD (kindly provided by Moritz Nowack). Expression of *GUS:YFP:KRP1^{109}* from the *GL2* promotor caused a

significant reduction in trichome branch number similarly to the other KRP1 protein versions demonstrating the functionality of this fusion protein (Tab3). CLSM revealed that *GUS:YFP:KRP1*^{109} was restricted to trichomes (Fig10E,J;O) and no increase in trichome-neighboring cell size nor DNA content was observed (Fig8,Tab2).

Taken together, it can be concluded that KRP1 can act non-cell-autonomously, and that the phenotype of the trichome-neighboring cells in the KRP1 misexpression lines is due to a direct action of the CDK inhibitor in the neighboring cells.

TABLE 3
Trichome branch number

line	number of branches in percent per leaf [1]				Σ trichomes
	1	2	3	4	
L*er*	0.0+/-0.0	0.2+/-0.9	**99.6+/-1.2**	0.2+/-0.8	477
Pro$_{GL2}$:KRP1	13.7+/-11.1	**65.3+/-14.4**	21.0+/-14.9	0.0+/-0.0	428
Pro$_{GL2}$:KRP1^{109}	19.5+/-15.3	**71.1+/-15.1**	9.4+/-12.9	0.0+/-0.0	150
Pro$_{GL2}$:YFP:KRP1	13.0+/-4.9	**58.7+/-10.2**	28.3+/-9.4	0.0+/-0.0	488
Pro$_{GL2}$:KRP1$^{109:}$*YFP*	14.8+/-8.0	**65.4+/-7.2**	19.8+/-7.1	0.0+/-0.0	338
Pro$_{GL2}$:GUS:YFP:KRP1^{109}	21.2+/-6.2	**59.2+/-6.0**	19.6+/-3.9	0.0+/-0.0	335

[1] All trichomes on rosette leaf number 3 and 4 were counted from at least 10 plants per line, the average plus/minus standard deviation is given, the branch number with the highest percentage is shown in bold.

Figure 10 Localization of KRP1, KRP1^{108} and KRP1^{109} in endoreplicating trichome cells

(A) to **(O)** Confocal-laser-scanning micrographs of **(A)** to **(E)** young rosette leaves, **(F)** to **(J)** old rosette leaves and **(L)** to **(O)** shows a close up of a trichome and its neighboring cells.
(A) and **(F)** Show the expression of the *GLABRA2* promotor in *Pro$_{GL2}$:GFP5ER* transgenic lines, which is only detectable in trichomes and trichome precursor cells.
(B), **(G)** and **(L)** Localization and distribution of YFP:KRP1 fusion protein in *Pro$_{GL2}$:YFP:KRP1* misexpressing plants. In young leaves, the nuclei of almost all epidermal cells show a YFP:KRP1 signal. In old leaves, the YFP:KRP1 signal is detected in the nuclei of trichomes and in the nuclei of trichome-neighboring cells in concentric rings. Trichomes are indicated by arrowheads. The nuclear localization in the trichome and its neighboring cells is shown in a close up (L)..
(C), **(H)** and **(M)** Localization and distribution of YFP:KRP1^{108} fusion protein in *Pro$_{GL2}$:YFP:KRP1^{108}* misexpressing plants. While the nuclear signal is evenly distributed in the basal part of young leaves (C) it becomes restricted to the trichome (indicated by arrowheads) and its neighbouring cells at the tip and in old leaves (H). Nuclear localization in the trichome and its neighboring cells, note that the nuclei are not evenly stained, there are patches with brighter signals (M).
(D), **(I)** and **(N)** Localization and distribution of KRP1^{109}:YFP fusion protein in *Pro$_{GL2}$:KRP1^{109}:YFP*misexpressing plants. The distribution of the fusion protein of the truncated KRP1^{109} has an even greater range than YFP:KRP1 with two to three concentric rings of cells around a trichome (I). KRP1^{109}:YFP is found in the trichomes in the nucleus and cytoplasm (N) whereas the trichome-neighboring cells show a nuclear localization. Note that KRP1^{109}:YFP could also be found in nuclei of mesophyll cells, indicated by an arrowhead.
(E), **(J)** and **(O)** Localization and distribution of GUS:YFP:KRP1^{109} fusion protein in *Pro$_{GL2}$:GUS:YFP:KRP1^{109}* misexpressing plants. GUS:YFP:KRP1^{109} can only be detected in trichome precursor cells and trichomes but not in surrounding cells.
(K) Analysis of the marker line *Pro$_{GL2}$:nls:GFP:GUS* crossed in *Pro$_{GL2}$:KRP1^{109}*. The GFP signal is only detectable in the trichomes (indicated by arrowheads) and not in the surrounding cells.
Scale bar in (A) to (K) 50µm; (L) to (O) 10µm.

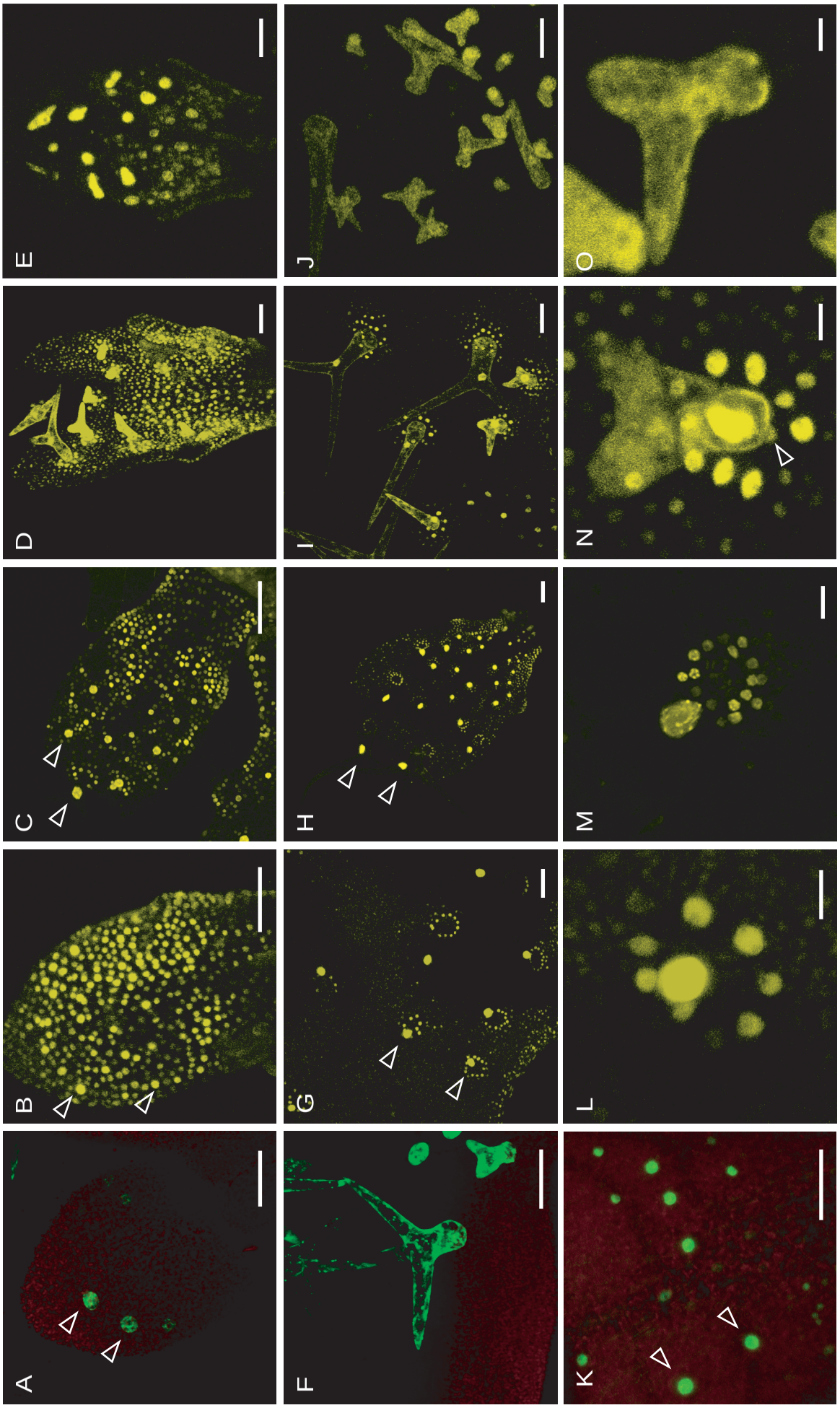

Figure 10 Localization of KRP1 in endoreplicating trichome cells

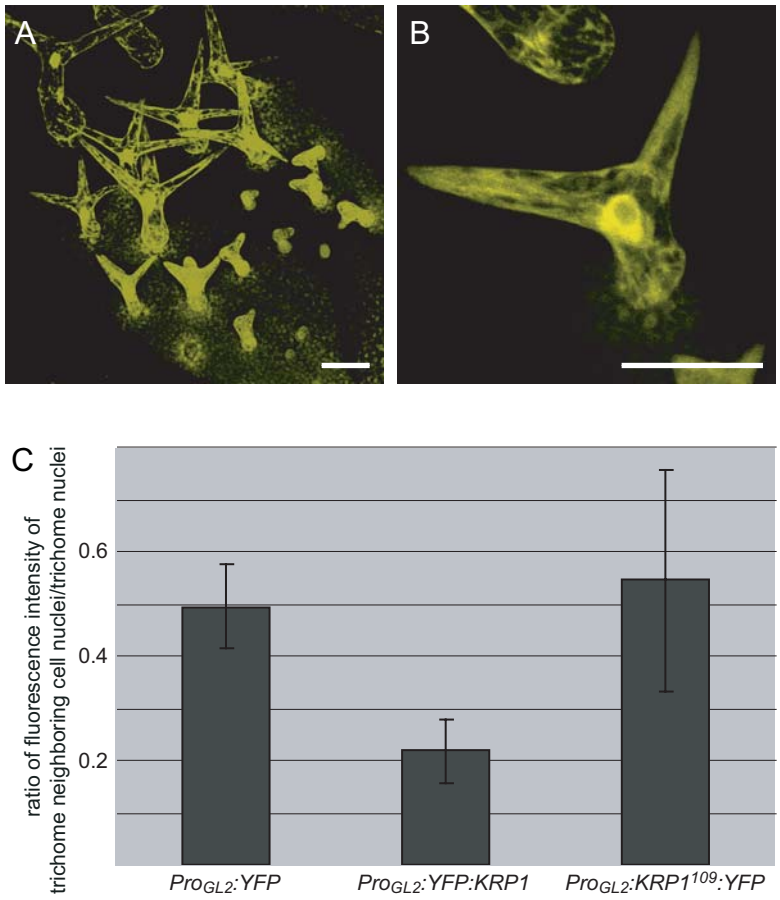

Figure 11 Analysis of KRP1 movement

(A) and **(B)** Confocal-laser-scanning micrograph of a (A) young and (B) old rosette leaves of *Pro$_{GL2}$:YFP* expressing plants. Note that the YFP signal can be observed in the nucleus and the cytoplasm of trichomes and their surrounding cells of young and old leaves.

(C) Analysis of KRP1 movement in *Pro$_{GL2}$:YFP:KRP1* and *Pro$_{GL2}$:KRP1^{109}:YFP* misexpressing plants in comparison to plants expressing *ProGL2:YFP* as a control. The ratio of the average YFP intensity of trichome-neighboring cell nuclei to the average YFP intensity of the young trichome nucleus was determined. Whereas the smaller KRP1^{109}:YFP fusion protein appears to move similarly as YFP, the fusion-protein of the full length KRP1 to YFP is found at lower levels in the nuclei of trichome-neighboring cells in comparison to trichome nuclei.

Scale bar in (A) and (B) 50µm.

2.5. Intracellular localization of KRP1

In animals the intracellular localization of the CKI $p27^{Kip1}$ is strictly regulated and appears to be inherently connected with protein abundance and activity (Sherr and Roberts, 1999; Slingerland and Pagano, 2000). The general notion is that $p27^{Kip1}$ exerts its inhibitory function in the nucleus and becomes degraded in the cytoplasm (Tomoda et al., 1999; Connor et al., 2003). The regulatory elements which mediate $p27^{Kip1}$ localization are not conserved in plant CKIs and therefore, I was interested in the intracellular localization of KRP1.

Whereas YFP expressed from the *GL2* promotor could be detected in the nucleus and the cytoplasm, *KRP1* and $KRP1^{108}$ fused with YFP exhibited a nuclear localization (Fig10B,C,G,H; Fig11A,B). While this work was in progress a similar intracellular localization of KRP1 was reported by analyzing GFP fusions with KRP1 (Zhou et al., 2003). Consistent with the report by Zhou and colleagues I found that YFP fusions with the truncated $KRP1^{109}$ localized to the nucleus and the cytoplasm in trichomes (Fig10D,I,N); a cytoplasmic localization was even more prominent for the GUS:YFP:$KRP1^{109}$ fusion protein (Fig10E,J,O). In the trichome-neighboring cells, however, both N- and C-terminal YFP fusions with $KRP1^{109}$ could only be detected in the nucleus (Fig10N). On the one hand this could indicate different cell-type dependent dynamics of the intracellular localization of KRP1. On the other hand it is very well possible that a cytoplasmic fraction of $KRP1^{109}$:YFP was below the detection limit since already in the much brighter stained trichomes the cytoplasmic fluorescence was weak (compare also Fig11C for a reduction of fluorescence intensities in trichome-neighboring cells).

Two explanations might account for the different intracellular localization patterns of KRP1, $KRP1^{108}$ and $KRP1^{109}$: First, the N-terminal 108 amino acids might

contain a strong degradation signal but degradation takes place in the cytoplasm leaving only a nuclear fluorescence for YFP:KRP1 and YFP:KRP1^{108}. Second, KRP1^{108} might contain a nuclear localization signal (NLS). This latter scenario is supported by the recent identification of a putative NLS in the first 108 aa. Exchanges of two basic aa in this NLS with Ala residues resulted in transient expression experiments in a cytoplasmic localization of YFP:KRP1 (Marc Jakoby, personal communication). However, at the moment it is still unclear, what the nature of the inhibitory signal in the N-terminus of KRP1 is.

Closer inspection of the N- and C-terminal YFP fusions with KRP1^{108} revealed, that the fluorescence was unevenly distributed in the nucleus in comparison to the nuclear YFP signal of KRP1 and KRP1^{109} (Fig 10L,M,N; Fig12A,B). These images had similarities to a typical DAPI stained nucleus, in which the chromocenters show a much brighter fluorescence compared to the rest of the nucleus (Fig6C,F). An overlay of the YFP and the DAPI image showed an exact match of the bright stained regions indicating that the N-terminal domain of *KRP1* is chromatin associated (Fig12B,C,D).

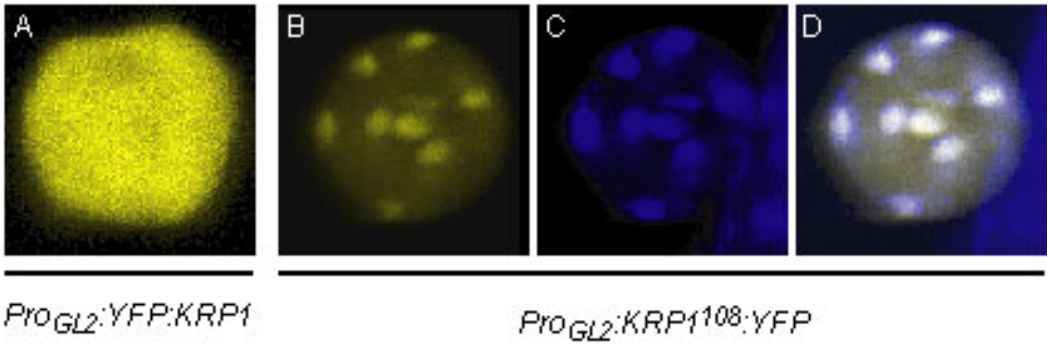

Figure 12 Nuclear localization of YFP:KRP1 and YFP:KRP1^{108}
(A) Confocal laser scanning micrograph of a trichome nucleus of *Pro$_{GL2}$:YFP:KRP1* transgenic line
(B) to **(D)** Confocal laser scanning micrographs of trichome nucleus of *Pro$_{GL2}$:YFP:KRP1^{108}* misexpressing plants. In (B) the YFP signal is shown, (C) shows the DAPI image of the same nucleus as in (B); (D) represents the overlay of (B) and (C).

2.6. Premature endoreplication does not interfere with the adaptation of cell specific marker gene expression

In wild-type, the cells directly neighboring a trichome develop into morphologically distinct cells, called socket or support cells. Socket cells are rectangular versus the typically lobed pavement cells and are oriented in their longitudinal axis towards the trichome (Fig6B). In addition, the expression of a few genes and enhancer trap lines has been found to discriminate socket cells from epidermal pavement cells (Molhoj et al., 2001; Vroemen et al., 2003).

Since the trichome-neighboring cells in the *KRP1*-misexpressing plants were greatly enlarged and developed lobes (Fig6E), I asked whether these cells still have socket-cell fate. The analysis of two *GAL4* enhancer trap lines from the Scott Poethig collection (http://enhancertraps.bio.upenn.edu/) marking trichome-socket cells, #232 and #254, crossed into the reference line for Pro_{GL2}:$KRP1^{109}$ revealed expression in the cells surrounding a trichome (Fig6J,K,L note also the increase in cell size and the enlarged neighboring-cell nuclei in line #254 expressing Pro_{GL2}:$KRP1^{109}$). In addition, most of the cells surrounding a trichome were still polarized towards the trichome (Fig6E). Taken together, these data suggested that the trichome-neighboring cells in *KRP1*-misexpressing plants have developed, at least to some degree, into socket cells.

Entry into an endoreplication cycle has been found to be associated with cell differentiation and the adoption of the special cell morphology occurring after cell-fate specification (Nagl, 1976; Sugimoto-Shirasu and Roberts, 2003). The data presented in this work, however, implied that trichome-neighboring cells in the *KRP1*-misexpressing plants become specified as socket cells independent and after the onset of an endoreplication program. To explore this hypothesis, the cell division activity

around incipient wild-type and *KRP1*-misexpressing trichomes was analyzed more closely. Figure 13 shows that in cells adjacent to young and growing wild-type trichomes newly formed cell walls can be found indicating a recent cell division (Fig13A,B,C). In contrast, around young trichomes of *KRP1*-misexpressing plants the neighboring cells had already started to enlarge (Fig13D,E,F). Consistent with this, I found in DAPI staining that nuclei of trichome-neighboring cells in *KRP1*-misexpressing plants had already started to endoreplicate in contrast to wild-type leaves (Fig13G,H).

As judged by their morphology, the dividing cells around an incipient trichome on wild-type plants have not acquired a specific fate (Fig13A,B). Also, from previous studies it is known that trichomes and trichome-socket cells are not of clonal origin suggesting that socket cells become recruited by trichomes at some later stage of trichome development (Larkin et al., 1996). Consistent with this, the expression of the two socket-cell markers used above only starts when the trichome is already three-branched and expanded (Fig6J). Further evidence from the *glabra 2* (*gl2*) mutant supports an instruction of socket cells at a time point late during trichome development. In *gl2* mutants two classes of trichomes can be found, one class of expanding and even branching trichomes surrounded by socket cells, the other class displays aborted trichomes, which had started to grow out but failed to expand and become arrested as young bulges (Fig21A,B) (Koornneef, 1990; Rerie et al., 1994). In this latter class stomata can be found to develop in direct contact with trichomes suggesting that socket cells have not yet been specified. Finally, in the *KRP1*-misexpressing plants the socket-cell marker became also expressed at later stages of trichome development (data not shown).

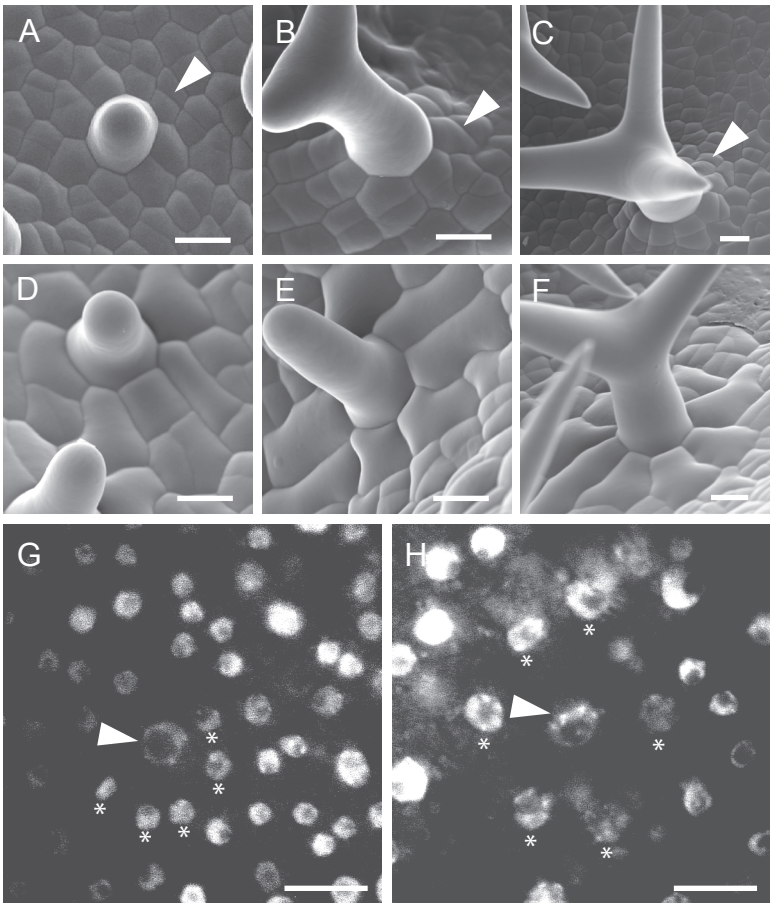

Figure 13 Analysis of cell division activity in trichome-neighboring cells

(A) to **(C)** Scanning electron micrographs showing the development of trichome-neighboring cells in wild type. Wild-type trichome-neighboring cells divide until the centrally located trichome develops its third branch. Examples for newly formed cell walls are marked by arrowheads.

(D) to **(F)** Scanning electron micrographs showing the development of trichome neighboring cells in in Pro_{GL2}:$KRP1^{109}$ plants. In Pro_{GL2}:$KRP1^{109}$ trichome-neighboring cells enlarge and do not divide.

(G) Light micrograph of DAPI-stained wild type trichome with their neighboring cells

(H) Light micrograph of DAPI-stained Pro_{GL2}:$KRP1^{109}$ trichome at an early stage of trichome development,corresponding to (A) and (D). Corresponding to the cell enlargement and the absence of cell division, trichome-neighboring cells in Pro_{GL2}:$KRP1^{109}$ plants start to endoreplicate as seen by the increased nuclear sizes of the trichome-neighboring cells in comparison to wild type. Arrowheads point to the trichome nuclei and the nuclei of the trichome-neighboring cells are marked by asterisks.

Scale bar in all panels 10µm.

Taken together, these findings suggest that in the KRP1-misexpressing plants endoreplication has started in the trichome-neighboring cells before these cells have been specified as socket cells and thus, it can becconcluded that plant cells can be specified independent of an endoreplication program.

2.7. The induction of endocycles by KRP1 depends on the cell-cycle mode and the developmental state

To test whether KRP1 is generally a positive regulator of endoreplication in trichome-neighboring cells and its expression is always sufficient to promote endoreplication, *KRP1* was misexpressed at late stages of socket-cell development. For that $KRP1^{109}$ was cloned behind an *UAS* regulatory element and introduced into the *GAL4* driver line #254 from the Scott Poethig collection by transformation (compare Fig6J) (http://enhancertraps.bio.upenn.edu/). Examining plants expressing Pro_{UAS}:$KRP1^{109}$ in the *GAL4* line #254 for a socket-cell phenotype revealed neither an alteration in cell size nor in DNA content in comparison to line #254 itself or in wild-type plants (Fig8; Tab2;Fig9A). This observation together with the finding that the trichome-neighboring cells will undergo a few cell division rounds when the *GL2* promotor is already highly active (compare Fig10A and Fig13A,B,C), indicated that the induction of endocycles by KRP1 depends on the developmental state and/or the cell-cycle mode of the cells. This is also supported by the observation that in all transgenic lines generated expressing the various KRP1 constructs in trichomes never any indication for an increase of endoreplication levels in trichomes by KRP1 has been observed.

To test further whether induction of endocycles by KRP1 depends on the cell-cycle mode of the cells, the effect of *KRP1* misexpression in other proliferating cells was analyzed. For that I made use of the observation that *GL2* is also expressed

during embryo development starting at heart stage and persisting till bent-cotyledon stage (Fig4A,B) (Lin and Schiefelbein, 2001; Costa and Dolan, 2003). Figure 14A and B show a torpedo stage embryo with the typical expression pattern of the *GL2* promotor in roughly every second cell file in the embryonic epidermis. Expression of *KRP1* under the *GL2* promotor did not alter this expression pattern as revealed by the analysis of the *GL2* promotor reporter line Pro_{GL2}*:nls:GFP:GUS* crossed into plants expressing Pro_{GL2}*: KRP1*^{109} (Fig14C,D). Similar to leaves it was found that KRP1-YFP fusion proteins could be detected in almost all epidermal cells and also weaker in subepidermal cells demonstrating that the movement of KRP1 is not restricted to leaf cells (Fig14E,F).

Next, I attempted to determine the DNA content of epidermal cells in embryos of plants misexpressing *KRP1*. However, measurements of fluorescence intensities were compromised due to a small cell size and therefore a close vicinity of nuclei giving rise to high background fluorescence. Therefore, DNA levels were approximated by nuclear sizes. For that plants carrying a Pro_{GL2}*:nls:GFP:GUS* construct were analyzed and the nuclear sizes of *pGL2*-postive cells in this line was compared with Pro_{GL2}*: KRP1*^{109} plants (Fig14A,B,C,D). Nuclei in the *KRP1*^{109}-misexpressing embryos were larger than in wild type supporting the hypothesis that KRP1 induced endoreplication in mitotic cells. A quantification of nuclear sizes using the DNA stain propidium iodide revealed approximately an area of 12µm² in Pro_{GL2}*: KRP1*^{109} embryos whereas in wild-type embryos the nuclei of epidermal cells spanned an average area of approximately 8µm² (Fig14E). Taking together these findings suggest that misexpression of *KRP1* in dividing cells can induce endorpelication, but the induction depends on the developmental state of the cell.

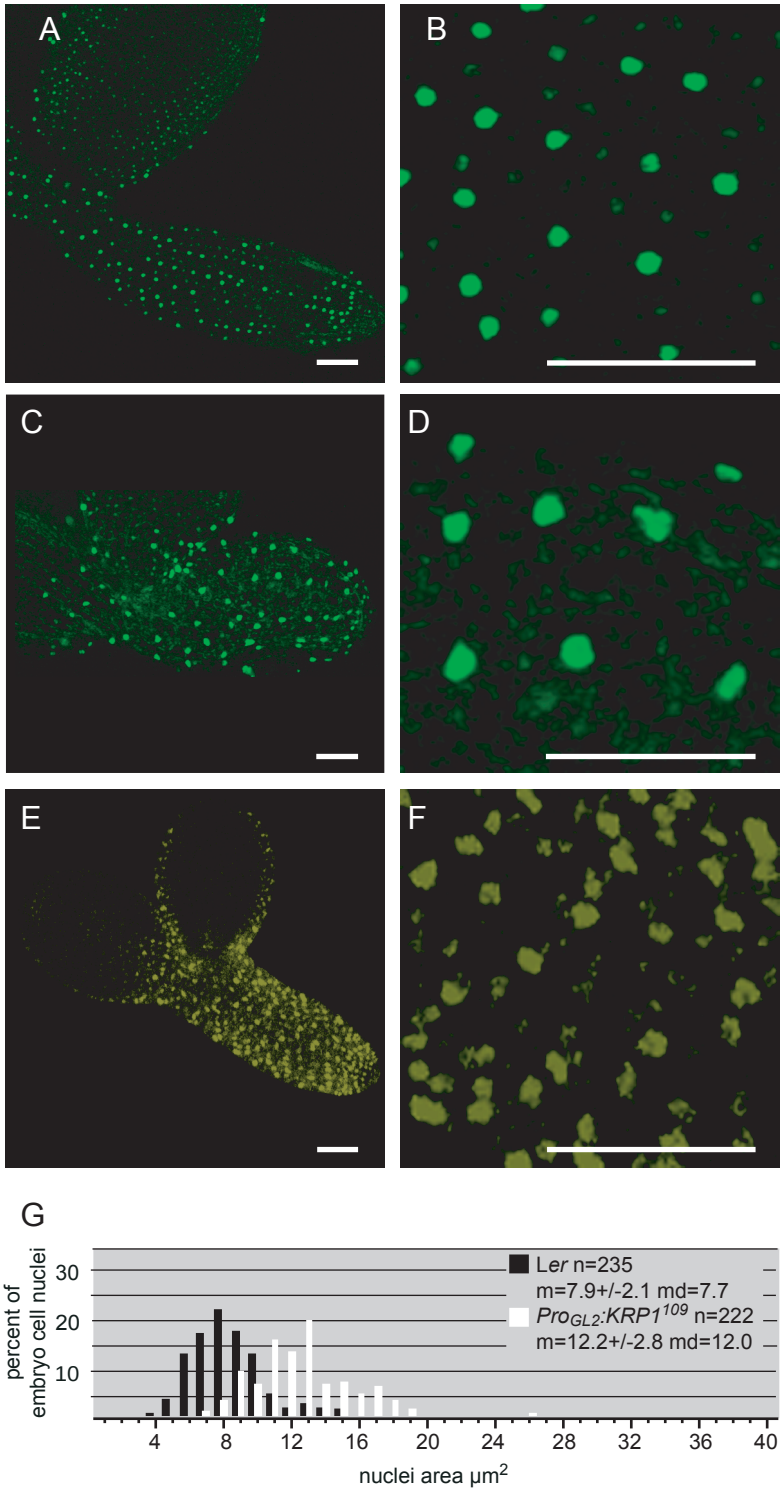

Figure 14 Analysis of *KRP1*^{109} misexpression in embryonic epidermal cells

2.8. Misexpression of *KRP1* in dividing epidermal cells of rosette leaves

Because of the experimental limitation of embryonic epidermis, I sought for another promotor active in dividing cells, yet not active in all mitotic cells in order to interfere as little as possible with plant fertility and viability. For this purpose the promotor of the *TOO MANY MOUTHS* gene (Pro_{TMM}) was used (Nadeau and Sack, 2002a). *TMM* is expressed during early leaf development in cells of the stomatal lineage and some adjacent cells (Fig4G; Fig17A,B); many of these cells will undergo at least one more cell division during leaf development.

To assess whether endoreplication levels were increased, transgenic plants misexpressing from the *TMM* promotor the N-terminally truncated KRP1 version fused to YFP were generated. Transgenic plants displayed a strong leaf phenotype with an increased degree of serration and a reduction of leaf size in comparison to wild type (Fig16A,B,D,E). Moreover the number of epidermal cells was reduced, but these cells were greatly enlarged compared to wild type (Fig16C,E). Rough analysis of the primary transformants misexpressing Pro_{TMM}*:YFP:KRP1* revealed a less severe phenotype than that of $KRP1^{109}$. Again misexpression of the N-terminal domain ($KRP1^{108}$) did not lead to any morphological alterations.

Figure 14 Analysis of $KRP1^{109}$ misexpression in embryonic epidermal cells
(A) and **(B)** Confocal-laser-scanning micrographs of Pro_{GL2}*:nls:GFP:GUS* reporter line in wild-type torpedo stage embryo. In (B) a close up of hypocotyl epidermal cells is shown.
(C) and **(D)** Confocal-laser-scanning micrographs of Pro_{GL2}*:nls:GFP:GUS* reporter line in Pro_{GL2}*:*$KRP1^{109}$ torpedo stage embryo. In (D) a close up of hypocotyl epidermal cells is shown.
(E) and **(F)** Confocal laser-scanning micrographs of a Pro_{GL2}*:*$KRP1^{109}$*:YFP* embryo. The YFP signal can be detected in all cell files of the hypocotyl. (F) Close up of hypocotyl epidermal nuclei.
(G) Analysis of the area of propidium iodide stained hypocotyl nuclei of embryos of the same age for wild type (black) and Pro_{GL2}*:*$KRP1^{109}$ (white) showing an enlargement of nuclear sizes in Pro_{GL2}*:*$KRP1^{109}$ expressing plants. The sample size (n), the mean (m) +/- standard deviation and the median (md) are given.
Scale bar in (A) to (F) 50µm.

The degree of polyploidization in 10, 15, and 20 days old seedlings was studied by fluorescence activated cell sorting (FACS) of cells of the first and second rosette leaf, stained with propidium iodide (Fig15A-F). At all time points, I found a quantitative as well as a qualitative shift towards higher replication levels in comparison to wild-type plants. In leaves of 10 days old Pro_{TMM}*:YFP:KRP1*^{109} seedlings elevated levels for 4C and 8C nuclei as well as a new, although small 16C peak were present (Fig15A,B). In 15 days old seedlings the 16C peak was increased and a new 32C peak appeared (Fig15C,D). And in 20 days old seedlings a greater 16C peak and a pronounced 32C peak were detected (Fig15E,F). Taken together, these data showed that KRP1 can block cell divisions and induce endoreplication in mitotic cells.

A detailed morphological analysis at the cellular level revealed that the number of stomata was drastically reduced in the strong Pro_{TMM}*:YFP:KRP1*^{109} transgenic plants in comparison to wild type, suggesting that cell division might be blocked at early stages and cells do not develop into normal guard cells (Fig16G,H). Besides the decrease of stomata number also the morphology and the spatial pattern of the guard cells were disturbed in *KRP1*^{109} misexpressing plants. Some of the guard cells were enlarged and had a "swollen" apperarance (Fig16J see arrowheads). In some cases the guard cells started to form lobes similar to differentiated pavement cells (Fig16K). Frequently, I observed that stacks of four guard cells are formed, instead of the typical pair of guard cells forming the pore (Fig16L). From these phenotypes one can conclude first, that misexpression of *KRP1*^{109} in dividing epidermal cells interfered with cell divisions resulting in fewer cells in comparison to wild type. Second, endorpelication was enhanced and finally, the development of stomata is severely impaired.

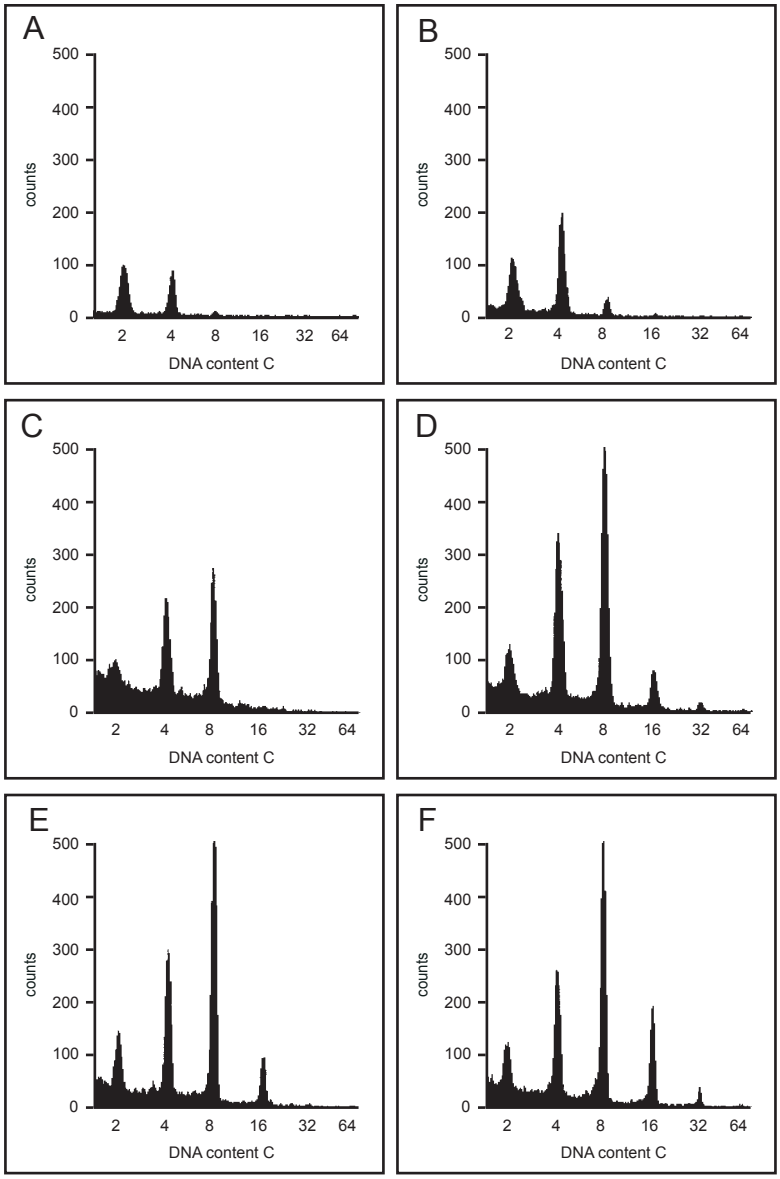

Figure 15 FACS-Analysis of *KRP1*^{109} misexpressed in leaf epidermal cells
(A), **(C)** and **(E)** Fluorescence activated cell sorting analysis (FACS) of the first and second rosette leaf from wild-type plants. (A) 10-day, (C) 15-day and (E) 20-day old seedlings.
(B), **(D)** and **(F)** FACS analysis of the first and second rosette leaf from *Pro*$_{TMM}$*:YFP:KRP1*^{109} transgenic plants. (B) 10-day, (D) 15-day and (F) 20-day old seedlings. In the transgenic line a quantitative and a qualitative shift towards more replicated nuclei compared to wild-type is visible at all time points.

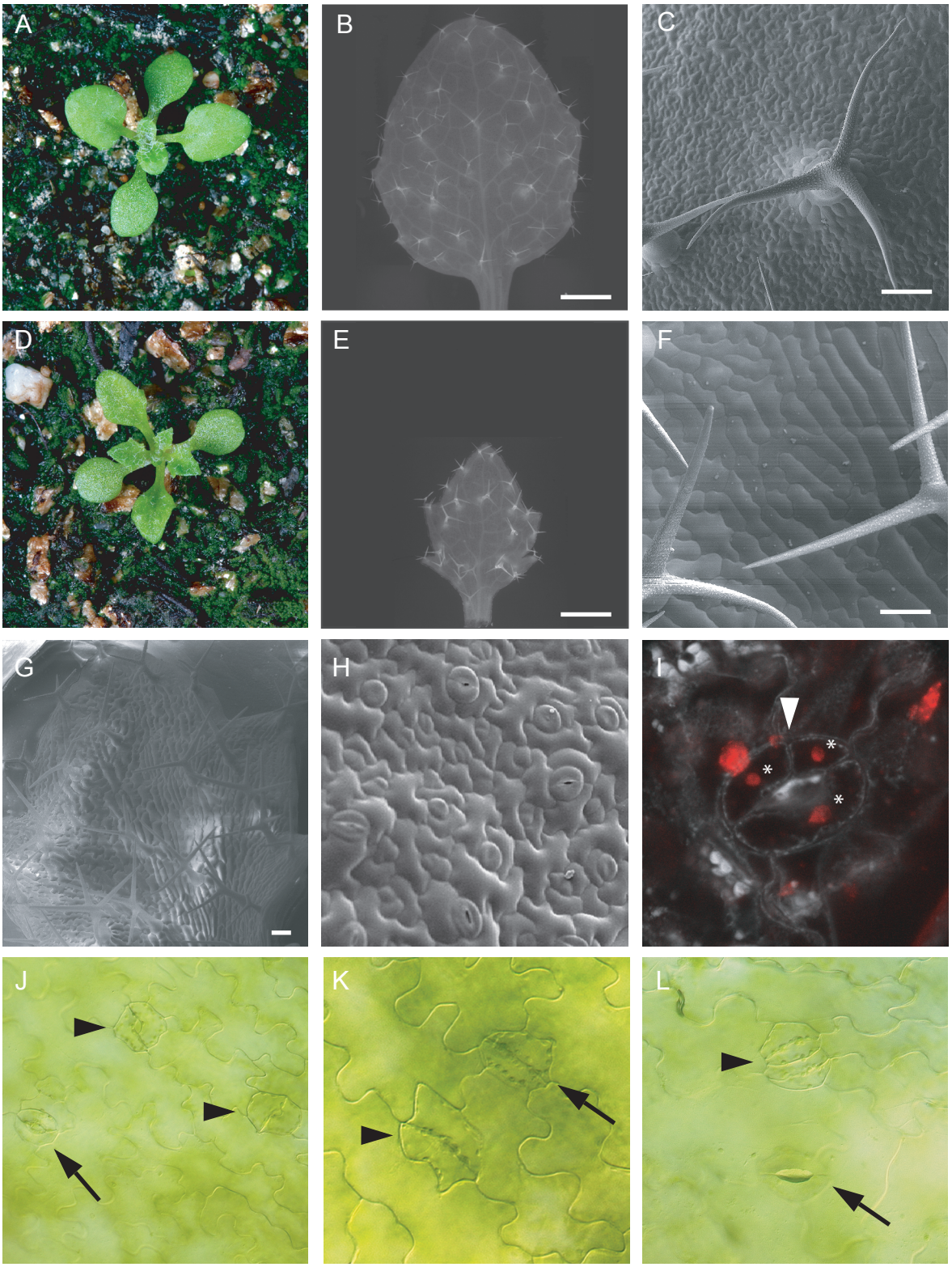

Figure 16 Analysis of *KRP1*^{109} misexpression in *TMM*-positive cells

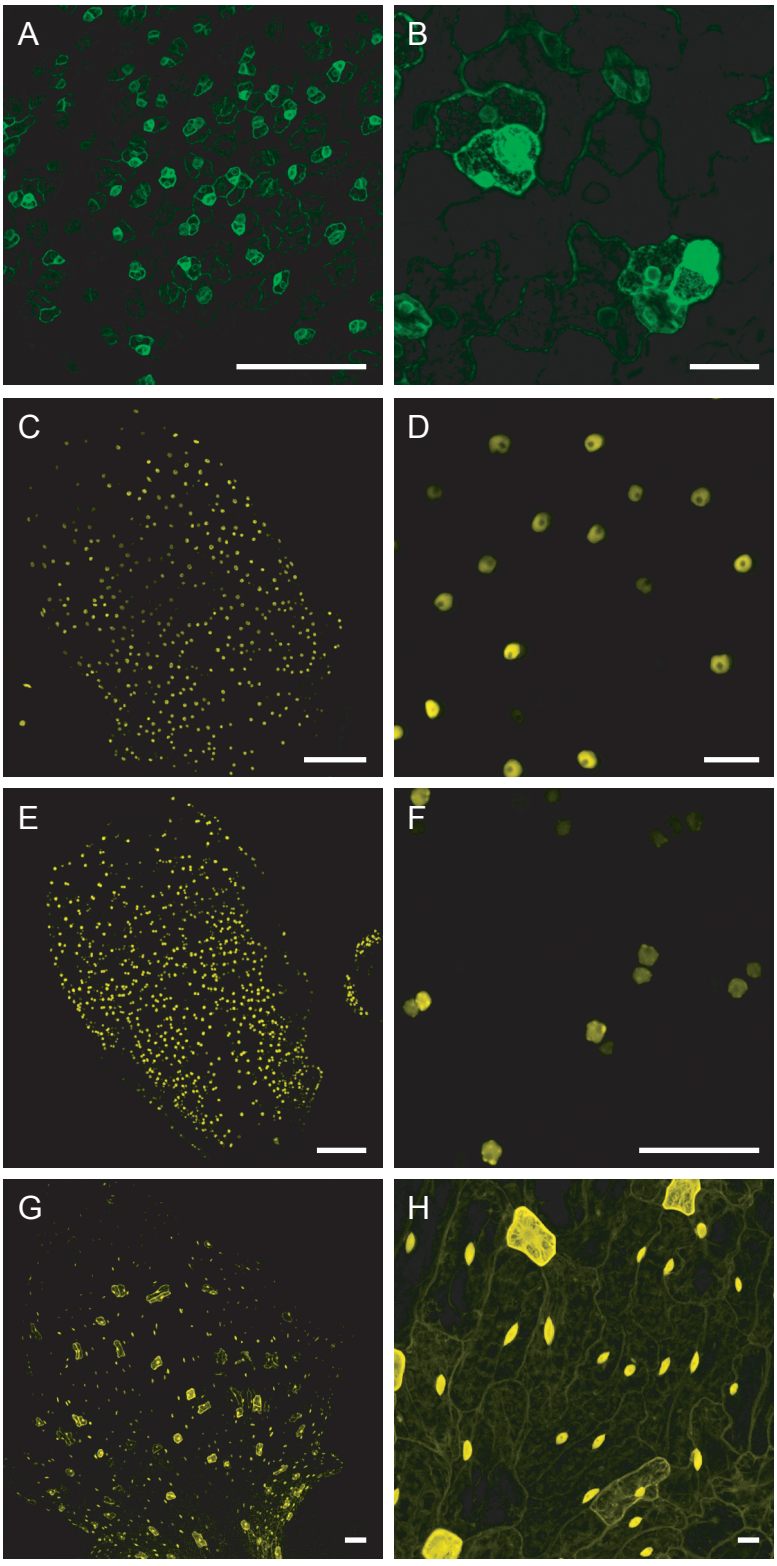

Figure 17 Localization of KRP1, KRP1^{108} and KRP1^{109} in dividing leaf epidermal cells

Concerning the subcellular localization of KRP1, KRP1^{108} and KRP1^{109} in *TMM* expressing cells the same pattern was observed as in endoreplicating trichomes. The YFP signals for KRP1 and KRP1^{108} were only detectable in the nuclei and again KRP1^{108} nuclei showed spotted patches with a very bright fluorescence (Fig17C,D,E,F). KRP1^{109} was found in the nucleus and the cytoplasm (Fig17G,H). Interestingly a few cells accumulated very high amounts of the YFP:KRP1^{109} protein in the cytoplasm. Whether this is due to the activity of the *TMM* promotor needs to be resolved by further experiments, e.g. crossing of the *Pro$_{TMM}$:YFP:KRP1^{109}* transgenic plants with the plants expressing the *Pro$_{TMM}$:GFPER* reporter.

Figure 16 Analysis of *KRP1^{109}* misexpression in *TMM*-positive cells
(A) to **(C)** show images of wild-type plants ecotype Columbia. In (A) an overview of two week old seedling is shown. (B) Light micrograph and (C) Scanning electron micrograph of rosette leaves.
(D) to **(G)** *Pro$_{TMM}$:YFP:KRP1^{109}* misexpressing plants. In (D) an overview of two week old seedling is shown. (E) Light micrograph, (F) and (G) scanning electron micrographs of rosette leaves. Note the strong reduction in cell number, the enormous increase in cell size of all pavement cells and the reduction of stomata number in (G).
(H) A scanning electron micrograph of a mature wild-type rosette leaf giving an impression of typical stomata size and shape.
(I) Confocal scanning micrograph of a DAPI-stained stoma from *Pro$_{TMM}$:YFP:KRP1^{109}* transgenic line consisting of three cells forming the pore. The cell wall in the divided guard cell is marked by an arrowhead, asterisk mark the three nuclei of the stoma.
(J) to **(L)** Light micrographs of *Pro$_{TMM}$:YFP:KRP1^{109}* misexpressing plants. In (J) enlarged stomata are marked by arrowheads in contrast to a "normal" stoma marked by an arrow. (K) Misshaped stoma with lobed cell walls is marked by an arrowhead, the "normal" by an arrow. (L) Shows a stack of guard cells similar to the *flp* mutant marked by an arrowhead.
Scale bar in (B) and (E) 1mm; (C) and (F) 100µm.

Figure 17 Localization of KRP1 in dividing leaf epidermal cells
(A) and **(B)** Confocal laser scanning micrographs of rosette leaves from *Pro$_{TMM}$:GFP5ER* transgenic plants.
(C) and **(D)** Confocal laser scanning micrographs of rosette leaves from *Pro$_{TMM}$:YFP:KRP1* transgenic plants.
(E) and **(F)** Confocal laser scanning micrographs of rosette leaves from *Pro$_{TMM}$:YFP:KRP1^{108}* transgenic plants.
(G) and **(H)** Confocal laser scanning micrographs of rosette leaves from *Pro$_{TMM}$:YFP:KRP1^{109}* transgenic plants.
In the left panel an overview is given, whereas close up is shown in pictures of the right panel. Scale bar in (A), (C), (E), (G) 80 µm and in (B), (D), (F), (H) 20 µm.

2.9. Mode of KRP1-induced endoreplication

From animals it is known that a conversion of a mitotic cycle into an endocycle can be initiated from different phases of a mitotic cell cycle discriminating different endocycles. For instance, in the first endocycles of Drosophila nurse cells a new G1 phase is initiated shortly after S-phase, whereas mammalian megakaryocytes progress through a G2 phase and switch to a G1 phase with the beginning of mitosis (Edgar and Orr-Weaver, 2001).

In order to determine how KRP1-induced endocycles proceeded, a promotor reporter line for a mitotic cyclin (*Pro$_{CYCB1;2}$:DB:GUS*) was used, which marks cells in a late G2- till M-phase of a cell-division cycle (Schnittger et al., 2002a). Next, the number of *Pro$_{CYCB1;2}$:DB:GUS*-positive socket cells surrounding outgrowing but not yet maturated trichomes were compared in a wild-type background and in plants misexpressing *KRP1^{109}* from the *GL2* promotor. It was found that wild-type as well as *Pro$_{GL2}$: KRP1^{109}* plants displayed approximately the same proportion of stained cells adjacent to a trichome, 31 versus 35 percent (Tab4). Thus, endoreplicating trichome-neighboring cells in KRP1 misexpressing plants still entered a G2 phase.

I found that in the KRP1 induced endocycles the Anaphase Promoting Complex/Cyclosome (APC/C) was active. This became evident since the GUS reporter utilized was fused to the N-terminal 149 amino acids of CYCLIN B1;1 including the destruction box (DB) (Schnittger et al., 2002a). Such a marker becomes degraded in late mitosis with the onset of APC/C activity, which degrades mitotic substrates as cyclins and securin and promotes by that exit from mitosis (Colon-Carmona et al., 1999). Trichome-neighboring cells in KRP1 misexpressing plants, however, did not display a continuous staining of the DB:GUS marker indicating a cyclic degradation of the marker.

TABLE 4
***Pro*$_{CYCB1;2}$*:DB:GUS* in socket cells of young trichomes**

line	percentage of young trichomes with at least one GUS-positive socket cell [1]	n	Σ trichomes
Pro$_{CYCB1;2}$*:DB:GUS* in L*er*	31.3+/-4.2	4	400
Pro$_{CYCB1;2}$*:DB:GUS* in *Pro*$_{GL2}$*:KRP1*^{109}	34.5+/-2.9	4	400

[1] Socket cells of young trichomes (stage 2 to stage 5 according to Szymanski et al. 1998) were analyzed; average plus/minus standard deviation per 100 counted trichomes.

2.10. Expression of *KRP1* in the *siamese* mutant

The observation that KRP1 could only induce endoreplication in cells with a mitotic cell-cycle program and not in endoreplicating cells as trichomes or trichome-neighboring cells suggested that KRP1 acts by blocking a mitotic activity while allowing S-phase entry rather than by actively promoting S-phase entry. This is also supported by the cyclic expression of a late G2 reporter.

It is not clear, however, why KRP1 misexpression only in trichomes and not in proliferating cells appeared to interfere with S-phase entry. To test whether other developmental cues might be responsible for a differential response of trichome-neighboring cells versus trichomes with respect to S-phase entry I made use of the *siamese* (*sim*) mutant. In *sim* mutant plants trichomes undergo mitosis leading to clustered and multicellular trichomes with strongly reduced endoreplication levels; yet these multicellular trichomes display characteristics of typical trichomes with branch formation and papillae on the outer surface (Fig18A) (Walker et al., 2000).

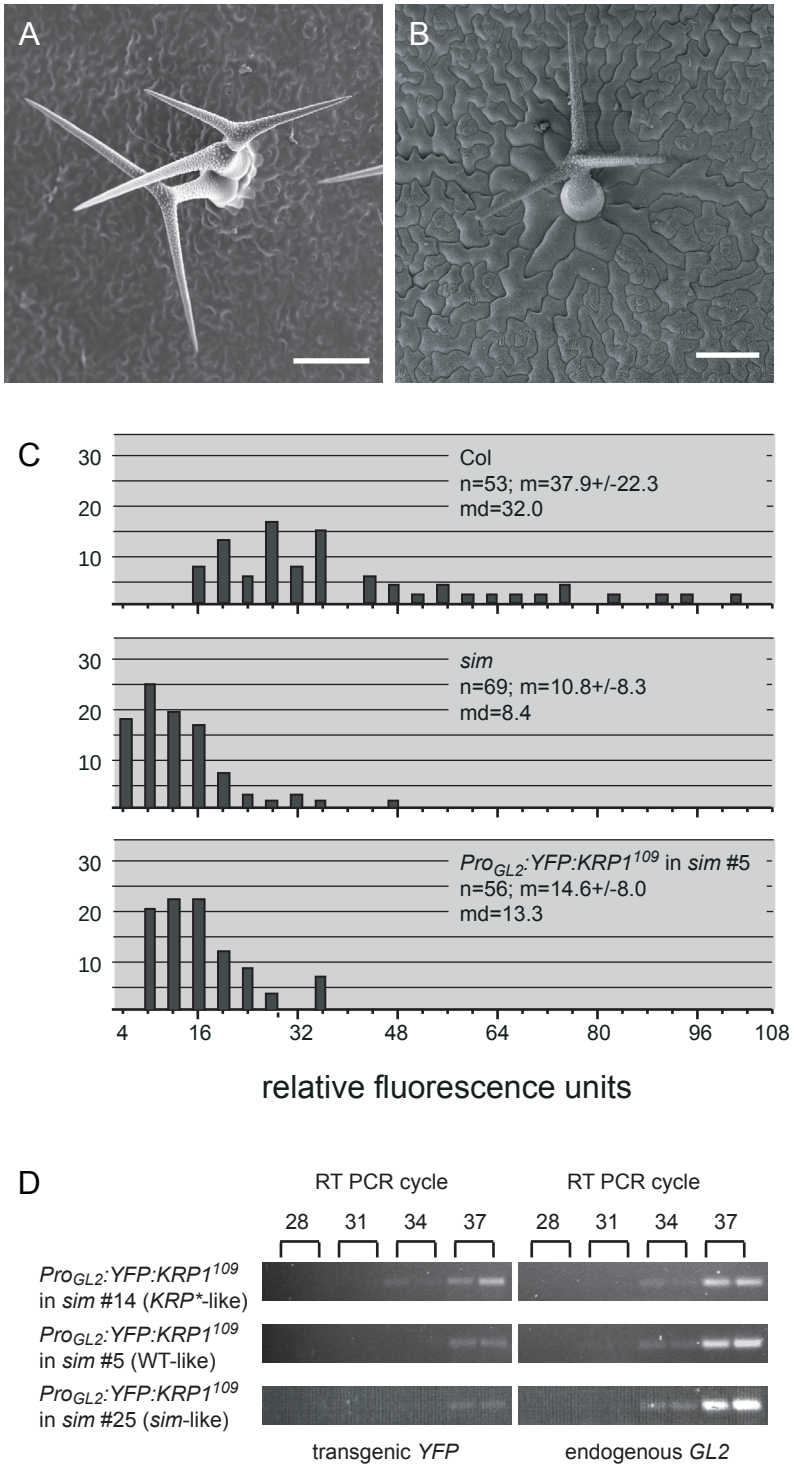

Figure 18 Misexpression of *KRP1^109^* in *siamese*

Pro$_{GL2}$:YFP:KRP1 and *Pro$_{GL2}$:YFP:KRP1^{109}* were introduced into *sim* mutant plants and analysis of the 14 and 28 generated transgenic plants showed the following three phenotypical classes: 7% (for *Pro$_{GL2}$:YFP:KRP1*) and 43% (for *Pro$_{GL2}$:YFP:KRP1^{109}*) of the plants displayed a *KRP1* misexpression like phenotype, i.e. small trichomes with fewer branches, which eventually died. 64%/40% contained almost wild-type like trichomes with none or only few clusters (Fig18B), and 29%/18% developed *sim*-like clustered and multicellular trichomes. Similar results were also obtained by crossing the untagged *KRP1* and *KRP1^{109}* misexpression lines into *sim* plants as well as by introduction the untagged version by plant transformation into *sim* plants (data not shown).

Next, the DNA content of wild-type like *sim* mutant plants expressing *Pro$_{GL2}$:YFP:KRP1^{109}* was measured. Although nuclei of these trichomes did not fully reach wild-type replication levels both a quantitative and a qualitative increase in endoreplication levels were found.

Figure 18 Misexpression of *KRP1^{109}* in *siamese*
(A) Scanning-electron micrographs of a mature multicellular *siamese* mutant trichome.
(B) Scanning-electron micrographs of a mature unicellular wild-type like trichome in *siamese* mutants misexpressing *Pro$_{GL2}$:KRP1^{109}* (as seen in line *Pro$_{GL2}$:YFP:KRP1^{109}* in *sim* #5), note that trichome-neighboring cells are enlarged.
(C) Analysis of trichome DNA content of Col wild type, *sim* and *Pro$_{GL2}$:YFP:KRP1^{109}* in *sim* line #5. Distributions of trichome DNA contents are given in relative fluorescence units (RFUs). The median value of Col trichomes was set as 32 C. From this value the respective C values of the trichome nuclei were calculated. The sample size (n), the mean (m) +/- standard deviation and the median (md) are given.
(D) Semi-quantitative RT-PCR showing the relative expression strength of *YFP:KRP1^{109}* in three independent lines misexpressing *Pro$_{GL2}$:YFP:KRP1^{109}* in *siamese* mutant background. These lines resemble either a *KRP*-like, a WT-like or a *sim*-like phenotype. The expression strength was compared with the endogenous expression of *GLABRA2* (*GL2*). The numbers at top indicate the RT-PCR cycle number. Line #14 showed the strongest, line #5 an intermediate and #25 the weakest transgene expression which correlates with their phenotypes.
Scale bar in (A) and (B) 100µm.

In *sim* mutants roughly 20 percent of the individual nuclei have a DNA content of 4C or less and the average DNA content of all nuclei is approximately 8C. In contrast, all of the trichome nuclei on plants expressing Pro_{GL2}*:YFP:KRP1*^{109} in the *sim* mutant background had a DNA content of more than 4C and the overall average DNA content was approximately 13C (Fig18C, line #15). These data showed that *KRP1* expression can at least partially rescue the *sim* mutant phenotype. Thus, also in a trichome environment *KRP1* expression can induce endoreplication suggesting that the difference between trichomes and trichome-neighboring cells is more directly associated with the execution of a mitotic program than with other developmental differences.

Furthermore, the spectrum of phenotypes obtained by expressing *KRP1* in *sim* mutant plants suggested that KRP1 could act in a concentration dependent manner. Semi-quantitative RT-PCR of representative plants from the different phenotypical classes revealed that weak *sim*-like and wild-type like phenotypes were correlated with low expression strength of the *KRP1* construct whereas a *KRP1*-like phenotype was associated with higher expression levels of the construct (Fig18D).

Thus, this data suggests that KRP1 supplies a mitosis-suppressing function which is compatible with an endoreplication program at a low concentration whereas at higher levels of expression KPP1 blocks cell-cycle progression completely.

2.11. Endoreplicated trichome socket cells re-enter mitosis

Along with maturation and differentiation most of *Arabidopsis* leaf cells switch to an endoreplication cycle (Melaragno et al., 1993) (compare also Fig15A,C,E). Correspondingly, cell-divisions become progressively restricted to the basal part of the leaf and finally stop completely (Donnelly et al., 1999).

Surprisingly in very old leaves of Pro_{GL2}:$KRP1^{109}$ plants the $Pro_{CYCB1;2}$:*DB:GUS* reporter was expressed again in trichome-socket cells, indicating that these cells again entered a G2-phase (Fig19A). A comparison with wild-type plants carrying the $Pro_{CYCB1;2}$:*DB:GUS* transgene confirmed that in comparable stages on wild-type leaves cell divisions have ceased with the exception of a few meristemoid cells at the leaf base. I determined the ratio of GUS-positive trichome-neighboring cells to total number of trichomes and obtained for leaves of Pro_{GL2}:$KRP1^{109}$ plants with a few meristemoid cells in a G2-phase a ratio of about 0.024 and on somewhat older leaves without any other detectable cells in a G2 phase a ratio of about 0.006 (Tab5). Analysis of these mature socket cells in an SEM revealed new cell walls in very large cells (Fig19B). This finding was supported by the observation of cell divisions in differentiated guard cells in Pro_{TMM}:*YFP:*$KRP1^{109}$ misexpressing plants resulting in a stoma composed of three cells(Fig16I).

Intriguingly, at the time when the $Pro_{CYCB1;2}$ marker is turned on again the majority of the trichomes on Pro_{GL2}:$KRP1^{109}$ plants are dead, in addition this is about the time when the activity of the *GL2* promotor ceases (Szymanski et al., 1998). This correlation suggested that only after the withdrawal from the KRP1 regime trichome-neighboring cells entered mitosis.

The general notion is that cells, which have started an endoreplication program, are terminally differentiated and cannot re-enter mitosis (Nagl, 1976; Melaragno et al., 1993; Edgar and Orr-Weaver, 2001). However, at the time when neighboring cells resumed cell division all of them appeared to have undergone substantial endoreplication suggesting that endoreplicated cells were able to re-enter mitosis. To find further support for this possibility DAPI-stained leaves were examined with the help of Suzanne Kuijt for the appearance of mitotic figures

(Fig19C-F). Figure 19 D and F shows two representative mitotic figures, most likely a metaphase (D) and a late anaphase or telophase (F) of trichome-neighboring cells in *KRP1*-misexpressing plants. The comparison with similar mitotic stages of wild-type root meristem cells or young leaf cells, which are not polyploid (Fig19C,E), revealed that mitotic figures obtained from *KRP1*-misexpressing plants contained more DNA than dividing cells in wild type (Fig19D,F). This demonstrates that endoreplicated trichome-neighboring cells underwent mitosis.

As judged by the number of cell walls I identified in the SEM many neighboring cells re-entered mitosis (Fig19B). DAPI staining revealed that the most common nuclear type was an interphase nucleus indicating that cell divisions did not result in abnormal mitoses or mitotic arrest but rather that mitosis of an endoreplicated cell proceeded without aberrations. Thus, it can be concluded that plant cells maintain the ability after going through endoreplication cycles to divide again, demonstrating a high degree of flexibility in plant development.

TABLE 5
***Pro*$_{CYCB1;2}$*:DB:GUS* in socket cells of mature trichomes**

line	stage [1]	GUS positive socket cells per total trichome number per leaf [2]	Σ leaves	Σ trichomes
Pro$_{CYCB1;2}$*:DB:GUS* in L*er*	GUS+	0.000+/-0.000	9	326
Pro$_{CYCB1;2}$*:DB:GUS* in L*er*	GUS-	0.000+/-0.000	15	304
Pro$_{CYCB1;2}$*:DB:GUS* in *Pro*$_{GL2}$*:KRP1*^{109}	GUS+	0.024+/-0.035	16	508
Pro$_{CYCB1;2}$*:DB:GUS* in *Pro*$_{GL2}$*:KRP1*^{109}	GUS-	0.006+/-0.031	52	868

[1] stage GUS+: GUS staining in other epidermal cells besides socket cells
stage GUS-: GUS staining only in socket cells

[2] Mature trichomes (stage 6 according to Szymanski et al., 1998) were analyzed; average plus/minus standard deviation.

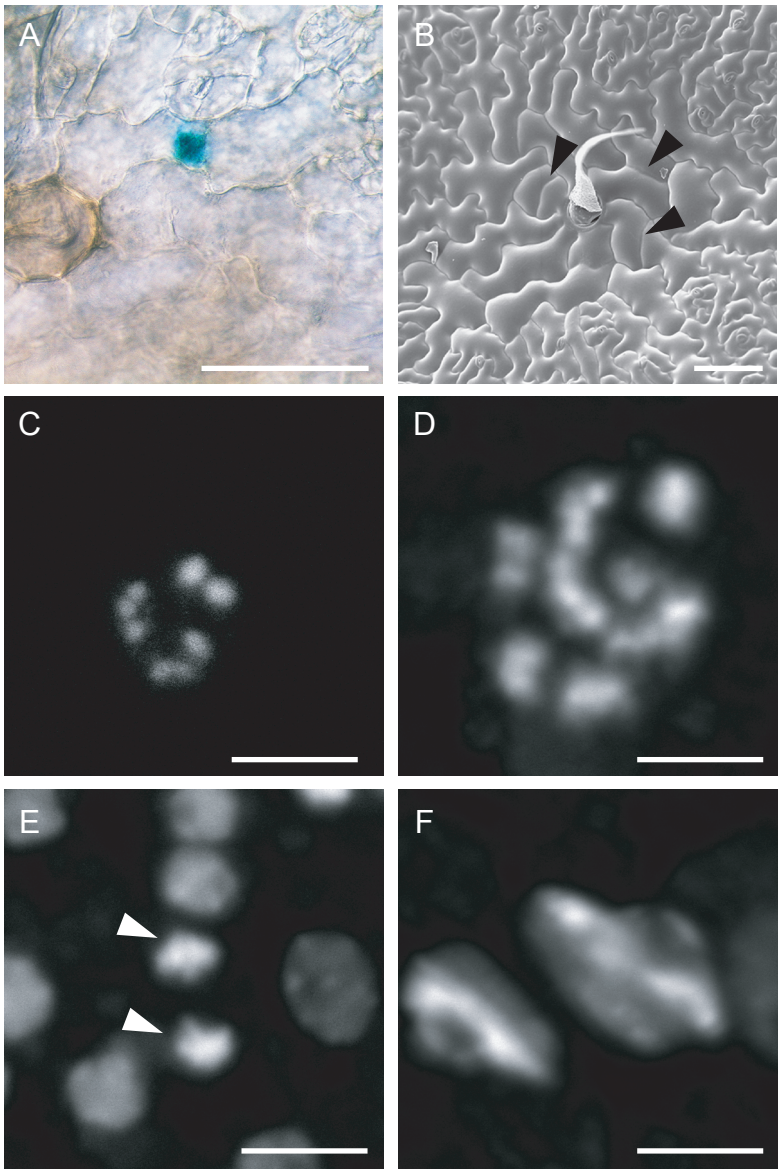

Figure 19 Analysis of late cell divisions in endoreplicated trichome-neighboring cells
(A) Light micrograph of a whole-mount GUS-staining of the reporter line *Pro$_{CYCB1;2}$:DB:GUS* in *Pro$_{GL2}$:KRP1^{109}* showing GUS activity in one trichome-neighboring cell of an old rosette leaf, in which no other cell divisions are detectable.
(B) Scanning-electron micrograph of trichome-neighboring cells surrounding a dead trichome of an old rosette leaf of *Pro$_{GL2}$:KRP1^{109}*-expressing plants. Arrowheads mark a straight wall indicative for a newly formed wall in enlarged trichome-neighboring cells.
(C) and **(E)** Confocal-laser-scanning micrographs of wild-type non-endoreplicated nuclei at different mitotic stages. (C) shows a metaphase nucleus with condensed chromosomes from a root meristem cell. (E) reflects a late anaphase/early telophase nucleus (marked by arrowheads) from a young leaf epidermal cell.
(D) and **(F)** show mitotic figures in endoreplicated nuclei of trichome-neighboring cells in *Pro$_{GL2}$:KRP1^{109}* expressing plants. Note the increased DNA content compared to wild-type. Condensed chromosomes most likely reflecting a (D) metaphase, (F) a late anaphase/early telophase.
Scale bar in (A) and (B) 100µm; (C) to (F) 5µm.

3. Interactors of KRP1 and KRP1^{109}

3.1. A-type cyclin dependent kinase CDKA;1

One of the best known *Arabidopsis* KRP1 interacting protein is the A-type cyclin-dependent kinase CDKA;1. In several yeast two hybrid assays a strong protein-protein interaction of KRP1 and CDKA;1 has been shown (Wang et al., 1998; De Veylder et al., 2001b). Moreover Wang and colleagues were able to show in a histone1 kinase assay that overexpression of *KRP1* interferes with CDKA;1 activity (Wang et al., 2000). The first hints for an interaction of KRP1 with CDKA;1 *in planta* came from Schnittger et al. 2003. In their work they could completely rescue the trichome phenotype of Pro_{GL2}*:KRP1*^{109} expressing plants by crossing these plants with transgenic lines misexpressing *CDKA;1* under control of the *GLABRA2* promotor. Misexpression of Pro_{GL2}*:CDKA;1* alone did not result in any morphological changes. The trichomes in the progeny of the cross Pro_{GL2}*:KRP1*^{109} with Pro_{GL2}*:CDKA;1* had wild type morphology.

To study whether the interaction with CDKA;1 causes changes in the subcellular localization of KRP1, transgenic plants containing either the Pro_{GL2}*:YFP:KRP1* or the Pro_{GL2}*:KRP1*^{109}*:YFP* construct were crossed with plants misexpressing Pro_{GL2}*:CDKA;1*. Also plants expressing the dominant active variant of CDKA;1, Pro_{GL2}*:CDKA;1-AF*, were used for crossings. In the *CDKA;1-AF* variant the two inhibitory phosphorylation sites Tyr14 and Thr15 were mutated to Phe and Ala respectively, thus preventing the inhibitory phosphorylation (Hemerly et al., 1995). Misexpression of *CDKA;1-AF* under control of the *GL2* promotor did not result in a phenotype (Arp Schnittger personal communication). By crossing of Pro_{GL2}*:CDKA;1-AF* or Pro_{GL2}*:CDKA;1* with Pro_{GL2}*:KRP1*^{109}*:YFP* the KRP1

trichome phenotype could be rescued. Because homozygous *Pro$_{GL2}$:KRP1^{109}:YFP* expressing plants showed only a very weak enlargement of the socket cells rescue was difficult to judge and (Tab2) therefore this aspect has not been taken into account for further analysis.

Concerning the localization of YFP:KRP1 in *Pro$_{GL2}$:CDKA;1* misexpressing plants, YFP signal was still detected in the cytoplasm and the nucleus (Tab6). In F1 plants of the cross of the two CDK variants with *Pro$_{GL2}$:YFP:KRP1* the YFP signal could only be detected in the nucleus corroborating that the interaction of KRP1 or KRP1^{109} with CDKA;1 does not alter the subcellular localization of KRP protein. Interestingly, phenotypical analysis of the F1 generation of the crosses of YFP:KRP1 with both CDK variants revealed no rescue, i.e. the trichomes were smaller and had fewer branches as compared to wild type trichomes (Tab6). I observed this phenotype in the progeny of all crosses, using *Pro$_{GL2}$:YFP:KRP1* expressing plants either as the male or the female crossing partner. Taken together, these findings show that KRP1^{109} interacts with CDKA;1 and CDKA;1-AF *in planta*. It needs to be further analyzed why in plants expressing *YFP:KRP1* KRP1 interaction with both CDK variants is hindered. The *Pro$_{GL2}$:YFP:KRP1* construct seemed to be functional as the trichomes in this line looked like *Pro$_{GL2}$:KRP1* misexpressing trichomes (Tab3). However, CDKA;1 and CDKA;1-AF do not interfere with the subcellular localization of KRP1 and KRP1^{109}.

3.2. B-type cyclin dependent kinase CDKB1;1

As mentioned in the previous chapter misexpression of *KRP1* can block cell division. Therefore the interaction of KRP1 with the mitotic CDKB1;1 was studied. Misexpression of the dominant-negative *CDKB1;1* resulted in a block in G2-phase in

Arabidopsis (Boudolf et al., 2004). So far no interactions have been found for CDKB1;1 with KRPs based on yeast two hybrid assays (De Veylder et al., 2001b); (Zhou et al., 2002). Also *in planta* crosses of Pro_{GL2}*:KRP1*^{109} with Pro_{GL2}*:CDKB1;1* showed that truncated KRP1 does not interact with CDKB1;1 (Schnittger et al., 2003).

In this work, I crossed Pro_{GL2}*:YFP:KRP1* and Pro_{GL2}*:KRP1*^{109}*:YFP* misexpressing plants with Pro_{GL2}*:CDKB1;1* expressing plants and analyzed the phenotype in their progeny. In addition, the subcellular localization of KRP1 and KRP1^{109} in the CDKB1;1 overexpressing background was analyzed. The F1 generation of all crosses revealed the KRP phenotype (small trichomes with fewer branches) and the subcellular localization of KRP1and KRP1^{109} remained unchanged (Tab6). These data corroborate that there is no genetic interaction between the two KRP1 versions and the mitotic CDKB1;1.

TABLE 6
Interactors of KRP1 and KRP1^{109}

male		Pro_{GL2}*:YFP:KRP1*	Pro_{GL2}*:KRP1*^{109}*:YFP*	Pro_{GL2}*:nls:GFP:GUS*
female				
Pro_{GL2}*:CDKA;1*	**p**	KRP	WT	WT
	l	nucleus	nucleus+cytoplasm	NA
Pro_{GL2}*:CDKA;1-AF*	**p**	KRP	WT	WT
	l	nucleus	nucleus+cytoplasm	NA
Pro_{GL2}*:CDKB1;1*	**p**	KRP	KRP	WT
	l	nucleus	nucleus+cytoplasm	NA
Pro_{GL2}*:CYCD3;1*	**p**	WT	WT	weak *CYCD3;1*
	l	nucleus	nucleus+cytoplasm	NA
Pro_{GL2}*:CKS1*	**p**	KRP	WT	WT
	l	nucleus	nucleus+cytoplasm	NA
Pro_{GL2}*:nls:GFP:GUS*	**p**	KRP	KRP	
	l	NA	NA	

p: trichome phenotype; l: localization; NA: not analyzed

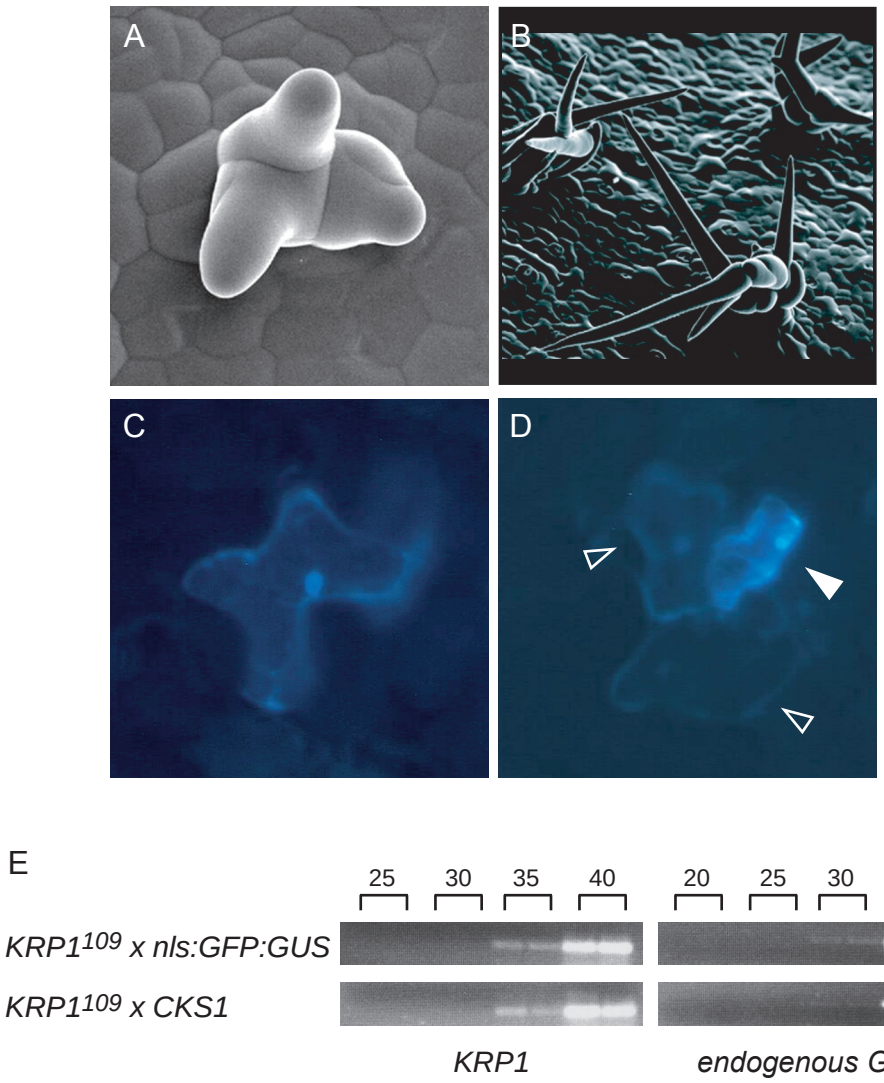

Figure 20 Interactors of KRP1

(A) and **(B)** Scanning electron micrographs of plants misexpressing *Pro$_{GL2}$:CYCD3;1*. (A) shows a young developing multicellular trichome, (B) shows mature trichomes (pictures were taken from Schnittger et al., 2002).

(C) and **(D)** UV excited micrographs of Arabidopsis leaves expressing transiently *Pro$_{35S}$:CFP:CKS1* after particle gold bombardment. CFP:CKS1 can be detected in the nucleus and the cytoplasm. In (D) the closed arrowhead indicates the cell, which was hit by the gold particle, whereas open arrowheads indicate the neighboring cells, which show a weaker CFP signal, suggesting CKS1 movement or diffusion.

(E) Semiquantitative RT-PCR showing the expression of *KRP1^{109}* and as control *GL2*. RNA was isolated from F1 seedlings obtained from crossings of Pro$_{GL2}$:KRP1^{109} with either *Pro$_{GL2}$:nls:GFP:GUS* (upper panel) or with *Pro$_{GL2}$:CKS1* (lower panel). The numbers at top indicate the RT-PCR cycle number.

3.3. D-type cyclin CYCLIN D3;1

Besides the C-terminal CDK interacting domain (Fig7) also a cyclin interacting domain has been identified in yeast two hybrid experiments using various KRP1 deletion constructs (Wang et al., 1998). The authors could show a strong interaction of KRP1 and KRP1^{109} with the D-type cyclin CYCD3;1. The first evidence for a genetic interaction *in planta* has been described by Schnittger et al. (2003). In their study they made use of the trichome *CYCD3;1* misexpression line (*Pro$_{GL2}$:CYCD3;1*), in which the wild-type single, unicellular trichome is transformed into clusters of multicellular trichomes (Fig20A,B) (Schnittger et al., 2002b). The progeny of the crosses of *Pro$_{GL2}$:KRP1^{109}* with *Pro$_{GL2}$:CYCD3;1* misexpressing lines had mostly three-branched, unicellular trichomes and the cluster frequency was like in wild-type. This means that overexpression of both components could completely rescue the KRP1- and the CYCD3;1 trichome phenotypes, emphasizing that KRP1^{109} and CYCD3;1 interact. Additional information came from the work of Zhou et al., who could partially rescue the growth retardation of *Pro$_{35S}$:KRP1* expressing plants by overexpressing CYCD3;1 under control of the *CaMV35S* promotor (2003). In this work a complete rescue was also observed in crosses of plants expressing the YFP fused to KRP1 or KRP1^{109} with the *Pro$_{GL2}$:CYCD3;1* plants. To rule out that the observed phenotypes are not caused by co-suppression the F1 generation of *Pro$_{GL2}$:CYCD3;1* crossed to *Pro$_{GL2}$:nls:GFP:GUS* was analyzed. The trichomes were multicellular and were initiated in clusters, but the phenotype was milder than in homozygous *Pro$_{GL2}$:CYCD3;1* expressing plants (Tab6). With respect to the subcellular localization of KRP1 and KRP1^{109} no alterations have been observed in the crosses with *Pro$_{GL2}$:CYCD3;1*. Taking these data together, the previously reported

interaction between KRP1 and KRP1^{109} with CYCD3;1 could be confirmed, also with YFP translational fusions of KRPs.

3.4. CDC KINASE SUBUNIT CKS1

Like in yeast and animals the *Arabidopsis* CDC KINASE SUBUNIT 1 has been identified as an interactor of CDKA;1 in a yeast two hybrid screen. Besides this interaction CKS1 was also found to interact with B-type CDKs, such as CDKB1;1, CDKB1;2 and CDKB2;1 (De Veylder et al., 1997). So far not much is known about further proteins interacting with CKS1 *in planta*. In the mammalian system it was shown that CKS1 binds to the F-box protein Skp2 which is part of the SCF^{Skp2} ubiquitin ligase involved in the ubiquitination of the CDK inhibitor p27^{Kip1} (Carrano et al., 1999; Sutterluty et al., 1999; Tsvetkov et al., 1999). Furthermore CKS1 is required for the ubiquitination of phosphorylated p27^{Kip1} and stabilization of Skp2 and CKS1 results in increased proteolysis of p27^{Kip1} (Ganoth et al., 2001; Spruck et al., 2001; Bashir et al., 2004).

In this work a possible interaction between the *Arabidopsis* CDK inhibitor KRP1 and CKS1 was analyzed. *In situ* hybridization experiments revealed that *CKS1* and *KRP1* are expressed in partially overlapping domains. While *CKS1* is expressed in mitotic and endoreplicating cells, *KRP1* can only be detected in endoreplicating cells (Jacqmard et al., 1999; Ormenese et al., 2004). To test if KRP1 and CKS1 show the same subcellular localization I made N-terminal fusions of CFP or YFP to CKS1 and expressed them under control of the *CaMV35S* promotor (*Pro$_{35S}$:CFP:CKS1*, *Pro$_{35S}$:YFP:CKS1*). With the help of Marc Jakoby and Doris Falkenhahn the subcellular localization of *Pro$_{35S}$:CFP:CKS1* was analyzed by particle bombardment of *Arabidopsis* leaves. The CFP:CKS1 fusion protein could be detected in the nucleus

and the cytoplasm. Interestingly, the CFP signal was also observed in the cells adjacent to the hit cell indicating that CKS1 might move from cell to cell (Fig20C,D).

To gain insights in the function of *CKS1 in planta*, this gene was misexpressed in endoreplicating trichomes (*Pro$_{GL2}$:CKS1*). However, transgenic plants containing this construct did not display a phenotype (Arp Schnittger personal communication). As mentioned above the mammalian CKS1 seems to be involved in the degradation of the KRP ortholog p27^{Kip1}. Thus I crossed *Pro$_{GL2}$:KRP1*, *Pro$_{GL2}$:KRP1^{109}*, *Pro$_{GL2}$:YFP:KRP1* and *Pro$_{GL2}$:KRP1^{109}:YFP* transgenic plants with the *Pro$_{GL2}$:CKS1* misexpressing plants and analyzed the trichome phenotype and the subcellular localization of KRP1 and KRP1^{109} in the F1 generation. As in the parental generation, YFP:KRP1 could only be detected in the nucleus and KRP1^{109}:YFP was localized in the nucleus and the cytoplasm (table 6). In the cross of *Pro$_{GL2}$:YFP:KRP1* with *Pro$_{GL2}$:CKS1* misexpressing plants trichomes were small and had fewer branches, comparable to the *Pro$_{GL2}$:KRP1* phenotype. In all other crosses the KRP1 trichome phenotype was completely rescued by the misexpression of *CKS1* (table 6). To ensure that the observed rescue was not due to co-suppression semiquantitative RT-PCR was performed with primers for *KRP1* and for *GL2* as control. RNA was isolated from young seedlings of the F1 generation of the cross *Pro$_{GL2}$:KRP1^{109}*x*Pro$_{GL2}$:CKS1* and the cross *Pro$_{GL2}$:KRP1^{109}*x*Pro$_{GL2}$:nls:GFP:GUS*. In both crosses *KRP1^{109}* is expressed at similar levels (Fig20E), indicating that the observed phenotype was due to the genetic interaction between KRP1 and CKS1 *in planta*. Interestingly, work from the lab of Geert de Jaeger provided evidence for the interaction of KRP4 with CKS1, but not KRP2, in pull-down experiments (Geert de Jaeger personal communication). These data show that CKS1 and KRP1 can interact *in planta*. Whether CKS1 is involved in KRP1 proteolysis needs to be further investigated for

example by measuring the YFP signal strength in the different compartments to check for alterations.

3.5. Conclusion

For all crosses listed in table 6 the localization of KRP1 and of KRP1^{109} remained unchanged. Whether the signal strength in the different cell compartments was altered needs to be tested in a more detailed study. Moreover, it would be interesting to analyze, whether crosses with *Pro$_{GL2}$:YFP:KRP1^{109}* transgenic plants would give the same results as shown above for *Pro$_{GL2}$:KRP1^{109}:YFP* expressing plants, because the N-terminal fusion of YFP to KRP1 interfered with its interaction ability. In this work I could show that KRP1^{109} genetically interacts with CKS1, CYCD3;1 and CDKA;1 but not with the mitotic CDKB1;1 Surprisingly, interaction of KRP1 fused with YFP could be only seen for CYCD3;1. This suggests that the cyclin could be the primary binding partner of KRP1 in the KRP-CDK/cyclin complex and not the CDK. This secenario is supported by the recent finding, that the binding of p27Kip1 to the CDK2/cyclinA complex is a sequential mechanism, which is initiated by the binding to cyclinA (Lacy et al. 2004).

4. Analysis of RBX1a and CSN5A, proteins involved in protein degradation

4.1. RBX1 the central component of the SCF complex

Besides transcriptional control, one important way to modulate the abundance of cell cycle regulators is protein degradation. The ubiquitin-proteasome pathway is involved in the degradation of many plant cell cycle regulators for example the CDK inhibitor KRP2 (Verkest et al., 2005). Ubiquitination of a target protein involves the sequential activity of three enzymes: an ubiquitin-activating enzyme (E1), an ubiquitin-conjugating enzyme (E2) and an ubiquitin-protein ligase (E3). The Skp1-Cullin-F-box complex (SCF) is a well characterized E3 ligase in plants (Hellmann and Estelle, 2002). The core of the SCF complex consists of a member of the cullin family and a RING BOX protein, called RBX, which can bind to the E2 enzyme. In *Arabidopsis* two genes encoding for RBX proteins haven been identified, RBX1a and RBX1b (Gray et al., 2002; Lechner et al., 2002).

It would be interesting to resolve whether the SCF-proteasome dependent pathway also regulates the abundance of the KRP1 protein. To address this I focused on the core component of the SCF the RBX1 protein. Based on available EST sequences 6 ESTs have been found for *RBX1a* and none for *RBX1b* (Gray et al., 2002; Lechner et al., 2002). Therefore misexpression and RNAi experiments were performed with *RBX1a*. Rough analysis of plants carrying the construct Pro_{GL2}*:RBX1a* showed increased trichome branching. This result favors the idea that the SCF-RBX1a complex might be involved in the degradation of an inhibitor of endoreplication and that overexpression of one component of the SCFcomplex is sufficient to enhance the degradation of this inhibitor.

Besides overexpression of RBX1a I also tried to decrease the amount of RBX1a in trichomes by a RNA interference approach. Seven out of 22 primary transformants showed a distinct phenotype. Transgenic seedlings were smaller in comparison to wild type and the length of the hypocotyl was extremely reduced (Fig21A,C). Also the leaf shape was altered rosette leaves were laterally expanded, giving rise to a more round leaf shape in comparison to WT leaves and the length of the petioles was shorter (Fig21A,C). The leaf surface had an irregular appearance and the trichomes seemed to be sunken into it (Fig21C). A similar phenotype has been observed in Pro_{GL2}*:KRP1*^{109} transgenic lines (Fig21B). The rosette leaf trichomes appeared normal with respect to their branch number, however the trichome stalk was much shorter. Detailed analysis including scanning electron microscopy revealed that the trichome neighboring cells were enlarged, similar to the phenotype observed for misexpression of *KRP1*^{109} in trichomes (Fig21D). Previously Gray et al., 2002 and Lechner et al., 2002 reported that *RBX1a* antisense and RBX1a-RNAi *Arabidopsis* plants were somewhat perturbed in their auxin response resulting in a loss of apical dominance. In the present work this phenomenon was also observed in Pro_{GL2}*:RBX1a-RNAi* expressing plants.

The overexpressing and the RNAi lines form the basis for further experiments. They will be used to determine the genetic interaction between *KRPs* and the SCF *RBX1A* or to analyze the protein stability of KRP1, KRP1^{108} and KRP1^{109} in a *RBX1a*-overexpressing or *RBX1a*-depleted background.

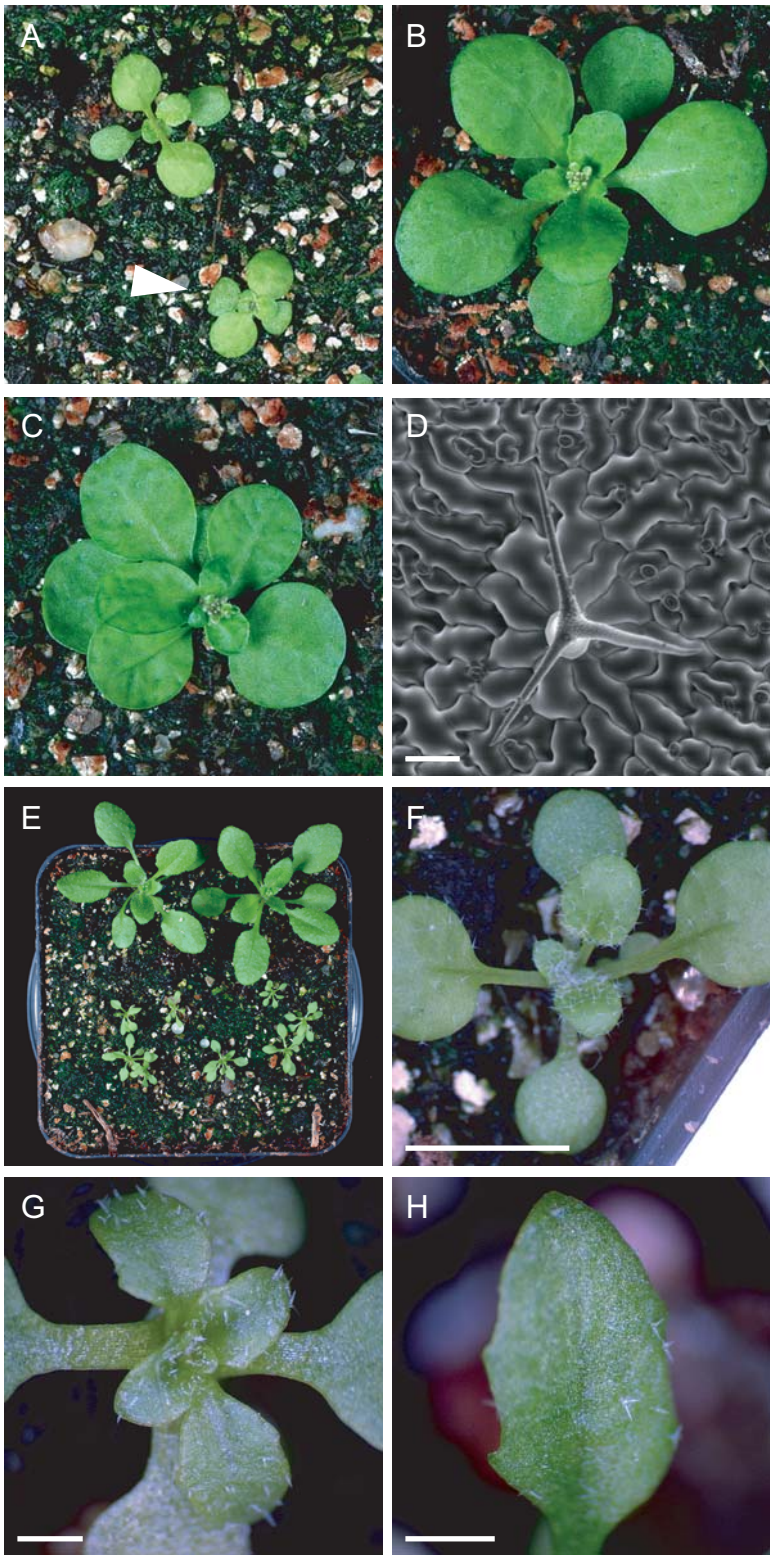

Figure 21 Analysis of *Pro$_{GL2}$:RBX1a-RNAi* misexpressing and *csn5a* mutant plants

4.2. CSN5 a component of the COP9 signalosome

The COP9 signalosome (CSN) is a complex that was first discovered through loss-of-function mutations by which photomorphogenesis was repressed in *Arabidopsis* (Wei et al., 1994; Chamovitz et al., 1996). The CSN seems to be involved in the regulation of protein turnover by E3 ubiquitin ligases and the 26S proteasome and has shown to interact with the cullin and the RBX1 subunits of SCFs (Schwechheimer and Deng, 2001). Interestingly, in mammalian cells it has been shown that CSN5 interacts with the CDK inhibitor $p27^{Kip1}$ causing its translocation from the nucleus to the cytoplasm, where it becomes degraded by the ubiquitin-proteasome pathway (Tomoda et al., 1999; Tomoda et al., 2002). To learn more about the function of the COP9 SIGNALOSOME SUBUNIT 5A I analyzed the phenotype of the *csn5a* mutant phenotype (kindly provided by Claus Schwechheimer). The homozygous *csn5a* mutant plants were severely impaired in their overall growth and rosette leaves had a narrow shape in contrast to wild type plants (Fig21E,F,G,H). Recently, similar phenotypes have been described for a T-DNA insertion line for the CSN5A locus (Gusmaroli et al., 2004). Also trichome development was affected as leaf hairs had a reduced cell-size, fewer branches and a shiny appearance, suggesting a defect in endoreplication (Fig21G,H).

Figure 21 Analysis of *Pro_{GL2}:RBX1a-RNAi* misexpressing and *csn5a* mutant plants

(A) Image of two week old seedlings from *Pro_{GL2}:RBX1a-RNAi* transgenic plant (indicated by arrowhead) and the corresponding wild type, using the same magnification.
(B) Shows a typical three week old *Pro_{GL2}:$KRP1^{109}$* misexpressing seedling.
(C) Shows a three week old *Pro_{GL2}:RBX1a-RNAi* misexpressing seedling.
(D) Scanning electron migrograph of trichome with enlarged socket cells from *Pro_{GL2}:RBX1a-RNAi* misexpressing plant.
(E) Overview over three week old Col wild type (top) and *csn5a* mutant (bottom) seedlings.
(F) Two week old Col wild type seedling
(G) Two week old *csn5a* mutant seedling
(H) Close up of a rosette leaf from *csn5a* showing small trichomes with fewer branches.
Scale bar in (D) 50µm; (F) 5mm; (G) and (H) 500µm

Whether CSN5A is involved in KRP1 regulation has to be investigated. First experiments were initiated to analyze on the one hand the subcellular localization of KRP1, KRP1^{108} and KRP1^{109} in dividing and endoreplicating cells in a *csn5a* mutant background. On the other hand misexpression of *CSN5A* together with *KRP1* in trichomes will be used to analyze whether the KRP phenotype is weaker, indicating that CSN5 is involved in KRP1 proteolysis. Trichome-specific misexpression of *CSN5A* alone under the *GLABRA2* promotor did not result in any morphological changes.

5. The RBR1-E2F pathway in *Arabidopsis*

Schnittger et al. 2003 could demonstrate that the *Arabidopsis* CDK inhibitor KRP1 is involved in the regulation of G1/S transition. Misexpression of *KRP1* in trichomes inhibits endoreplication. It would be interesting to find out whether this block at the G1/S transition could be overcome by triggering entry into S-phase. Good candidates for the regulation of entry into S-phase are the components of the Retinoblastoma-E2F pathway. In the *Arabidopsis* genome, a number of genes involved in this pathway, have been identified. So far one gene encoding for the *Retinoblastoma related* gene (*RBR1*), three genes encoding for *E2Fs* (*E2Fa*, *E2Fb* and *E2Fc*), two genes encoding for their hetero-dimerization partner *DP* (*DPa* and *DPb*) and three genes encoding for *DP-E2F-like* (*DEL1, DEL2* and *DEL3*) proteins have been described (Vandepoele et al., 2002). To learn more about the function of the individual members of the *Arabidopsis* RBR-E2F pathway in an endoreplicating context, trichome specific misexpression lines were generated in this study. For the misexpression approach the *GLABRA2*, *CAPRICE* and *TRIPTYCHON* promotors were used (Pro_{GL2}, Pro_{CPC} and Pro_{TRY}) (Fig4C,D,E). Moreover a knock-out approach was started in which I tried to specifically reduce the transcript levels of *DPa*, *DPb* and *RBR1* in trichome cells.

5.1. Retinoblastoma related RBR1

In the mammalian system the Retinoblastoma tumor suppressor protein (Rb) is a key regulator of the of the G1/S transition. In its non-phosphorylated state Rb binds to the heterodimeric transcription factor E2F-DP thereby masking the transcriptional activation domain rendering it inactive. Upon CDK phosphorylation Rb is released

from the E2F-DP heterodimer and transcription of E2F-DP targets is enabled (Harbour and Dean, 2000).

In plants not much is known about the Retinoblastoma protein and whether the regulatory pathway described above is similar *in planta*. Recently Ebel et al., described a loss of function mutant of *Arabidopsis retinoblastoma related1* (*RBR1)* (2004). The *rbr1* mutant is gametophytic lethal emphasizing the importance of RBR1 in plants. Moreover, the mature unfertilized megagametophyte fails to arrest mitosis and undergoes excessive nuclear proliferation in the embryo sac.

Here I tried to knock-down *RBR1* function by a RNA interference approach. Thereby the complete *RBR1* cDNA in sense and antisense orientation was expressed to produce a double-stranded RNA. Arabidopsis plants were transformed in three independent experiments with the Pro_{GL2}*:RBR1-RNAi* construct but among more than 10000 T1 seeds never any BASTA resistant transformant could be recovered (Tab7). One possible explanation could be that silencing of *RBR1* might be embryo lethal as the *GL2* promotor is active in epidermal cells during early embryo development (Fig4A,B; Fig14D) (Lin and Schiefelbein, 2001; Costa and Dolan, 2003).

Misexpression studies of *RBR1* in trichome cells under control of either the *CPC* or the *TRY* promotor led to trichomes with fewer branches compared to WT. Consistent with the data that the number of trichome branches and DNA content are correlated these results suggest that endoreplication is blocked (Hulskamp et al., 1994). These results are consistent with the data reported from animals that RBR1 is involved in the regulation of the G1/S transition. However, a more detailed analysis of the transgenic lines is needed.

TABLE 7
E2F / DP / RBR1 misexpressing lines

line	background	trichome penotype
Pro$_{CPC}$:E2Fa	L*er*	trichomes with more branches
Pro$_{CPC}$:E2Fa	*gl2*	*gl2*
Pro$_{GL2}$:E2Fa	L*er*	WT
Pro$_{GL2}$:E2Fa	*gl2*	*gl2*
Pro$_{TRY}$:E2Fa	L*er*	trichomes with more branches
Pro$_{TRY}$:E2Fa	*gl2*	*gl2*
Pro$_{CPC}$:E2Fb	L*er*	trichomes with more branches
Pro$_{CPC}$:E2Fb	*gl2*	*gl2*
Pro$_{GL2}$:E2Fb	L*er*	WT
Pro$_{GL2}$:E2Fb	*gl2*	*gl2*
Pro$_{TRY}$:E2Fb	L*er*	WT
Pro$_{TRY}$:E2Fb	*gl2*	*gl2*
Pro$_{GL2}$:E2Fc	L*er*	trichomes with more branches
Pro$_{GL2}$:DPa	L*er*	WT
Pro$_{GL2}$:DPa	*gl2*	*gl2*
Pro$_{GL2}$:DPa-RNAi	L*er*	WT
Pro$_{GL2}$:DPb	L*er*	WT
Pro$_{GL2}$:DPb	*gl2*	*gl2*
Pro$_{GL2}$:DPb-RNAi	L*er*	WT
Pro$_{CPC}$:RBR1	L*er*	trichomes with fewer branches
Pro$_{GL2}$:RBR1	L*er*	WT
Pro$_{TRY}$:RBR1	L*er*	trichomes with fewer branches
Pro$_{GL2}$:RBR1-RNAi	L*er*	no transformants

5.2. E2Fs and DPs

E2Fa and *E2Fb*, together with their interacting partners *DPa* and *DPb*, have been reported to act as positive regulators triggering entry into and progression through S-phase via transcriptional activation of various genes involved in cell cycle machinery, DNA synthesis, replication and repair (De Veylder et al., 2002; Kosugi and Ohashi, 2002c; Menges and Murray, 2002). E2Fc may act as a repressor, because it binds to the same E2F motifs as E2Fa and E2Fb in the promotor region of various genes but

lacks the transcriptional activation domain. The expression of *CDC6* is transcriptionally up-regulated by E2Fa and down-regulated by E2Fc (De Veylder et al., 2002; del Pozo et al., 2002).

In this work *E2Fa, E2Fb* and *E2Fc* were misexpressed in endoreplicating trichome cells. Transgenic lines containing either Pro_{CPC}*:E2Fa,* Pro_{TRY}*:E2Fa,* Pro_{CPC}*:E2Fb* or Pro_{GL2}*:E2Fc* showed an increase in trichome branching (Tab7).

50 out of 90 primary transfomants of Pro_{CPC}*:E2Fa* showed an increase in trichome branching, whereas only 7 out of 80 Pro_{CPC}*:E2Fb* containing T1 plants displayed a similar phenotype. These data suggest that *E2Fa* acts as a more potent transcription factor as *E2Fb*, which is in agreement with the results from Rossignol et al. showing in a transient expression assay a stronger activation with the construct Pro_{35S}*:E2Fa* than with Pro_{35S}*:E2Fb* (2002).

Besides their trichome phenotypes no further morphological alterations could be observed in these transgenic lines in comparison to wild-type. Taken together these data suggest that all three E2Fs were able to enhance endoreplication and seem to function as positive regulators at the G1/S transition.

In contrast to the E2F induced increase in trichome branch number, misexpression of their dimerization partner *DPa* and *DPb* under control of the *GLABRA2* promotor did not result in any obvious changes of trichome branching or of trichome cell size (Tab7). This in agreement with the data reported by de Veylder et al., 2002 and Kosugi and Ohashi, 2003, showing that *DPa* overexpression under control of the CaMV35S promotor in *Arabidopsis* and in tobacco did not alter plant morphology and DNA levels. However, in plants overexpressing both *DPa* and *E2Fa* a synergistic phenotype could be observed with much higher endoreplication levels as plants misexpressing *E2Fa* alone (De Veylder et al., 2002). It still needs to be shown

by crossings of the various *E2F* and *DP* trichome misexpressing lines which specific heterodimers are functional *in planta* and if they act as transcriptional activators or repressors.

The attempts to knock out DP function via post transcriptional gene silencing by misexpressing RNAi variants of *DPa* and *DPb* in trichomes did not result in any morphological changes as compared to wild type (Tab7).

5.3. Rescue of the *glabra2* mutant

Arabidopsis plants with a mutation in the homeobox gene *GLABRA2* display a glabrous leaf phenotype. Closer inspection of these leaves revealed that the *gl2* trichomes were either enlarged abortive epidermal cells that expanded only in the plane of the leaf or developed in unbranched spikes, similar to the trichomes misexpressing *KRP1* (Fig22A,B) (Koornneef, 1990; Rerie et al., 1994). DNA measurements of the outgrowing *gl2* trichomes and the aborted *gl2* trichomes revealed that in both cases endoreplication levels were reduced as compared to wild type (Arp Schnittger, personal communication).

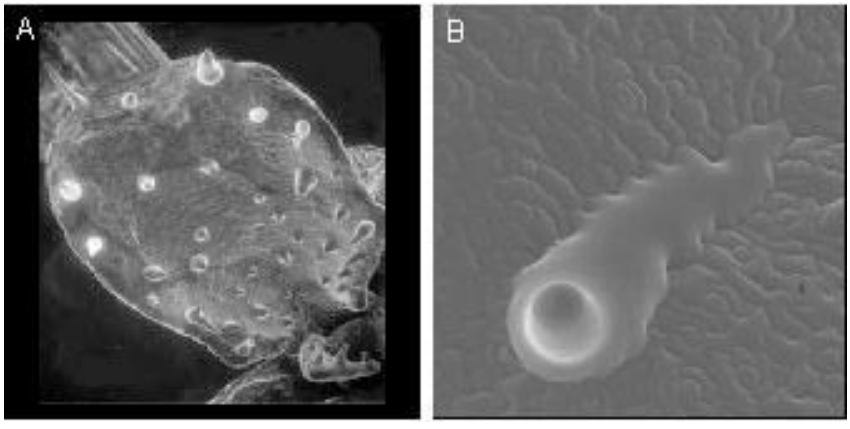

Figure 22 The *glabra2* mutant
(A) and **(B)** Scanning electron micrograhps of *glabra2.* (A) rosette leaf from the *gl2* mutant showing the typical enlarged abortive epidermal cells and the unbranched and small trichomes (picture taken from Szymanski et al., 1998). (B) Close up of such a abortive *gl2* trichome cell.

This brought up the hypothesis that the trichome phenotype of the *glabra2* mutant is caused by a decrease of endoreplication cycles. To test this I misexpressed *E2Fs (E2Fa, E2Fb* and *E2Fc*) and *DPs* (*DPa* and *DPb*) under control of trichome-specific promotors (Pro_{CPC}, Pro_{GL2} and Pro_{TRY}) in the *gl2* mutant background. As mentioned above and based on the correlation of branching and DNA content, not all constructs enhanced endoreplication in the wild-type background (Tab7). In WT plants misexpressing the Pro_{CPC}*:E2Fa,* Pro_{TRY}*:E2Fa,* Pro_{CPC}*:E2Fb* or Pro_{GL2}*:E2Fc* transgene an increase in trichome branching has been observed. Misexpression of these constructs in the *gl2* mutant background resulted in glabrous leaves (Tab7), but whether the endoreplication levels in these trichomes were elevated in comparison to *gl2* mutant trichomes needs to be analyzed. Furthermore misexpression of *E2F* and the respective *DP* in *gl2* trichomes might result in a more pronounced phenotype, since in wild type plants expressing both *E2Fa* and *DPa* the endoreplication enhancement was much stronger (De Veylder et al., 2002).

DISCUSSION

In this work I analyzed how endoreplication is contolled in *Arabidopsis thaliana*. In the first part I studied the regulatory function of RBR1 and E2Fs at G1/S the transition in endoreplicating trichome cells. Preliminary data suggest that RBR1 might act as a negative regulator whereas E2Fa, E2Fb and E2Fc positively affect endorpelication.

In the second part I could show that KRPs are likely to be important regulators of endocycles in plants since the *Arabidopsis* CDK inhibitor KRP1 besides an inhibitory role at the G1/S transition point can block cell division and induce endoreplication. In addition, it was found that KRP1 can act non-cell-autonomously. These findings open a new view on the functions of CDK inhibitors (CKIs) especially with respect to tissue organization and organ growth control in plants. Moreover, the work on KRP1 resulted in the finding that already endoreplicated cells can adopt a certain cell fate, and that endoreplicated cells can re-enter a mitotic cycle.

The RBR-E2F pathway and the regulation of endoreplication

In this work first hints were obtained that the *Arabidopsis* genes encoding for members of the RBR-E2F pathway play a role in the regulation of G1/S transition. Misexpression of the *Arabidopsis* adenovirus E2 promotor binding factor *E2Fa* or *E2Fb* in trichome cells promotes trichome branching. Given the fact that trichome branching correlates with DNA content, these data suggest that E2Fa and E2Fb are able to trigger entry into S-phase, resulting in higher endoreplication levels when misexpressed in trichome cells (Hulskamp et al., 1994). Surprisingly, the misexpression of *E2Fc* in trichomes also resulted in higher branch numbers. This observation stands in contrast to the reported function of E2Fc as a negative regulator.

E2Fc competes with E2Fa and E2Fb for the same E2F promotor binding sites and lacks the transcriptional activation domain (del Pozo et al., 2002; Kosugi and Ohashi, 2002c). However Mariconti et al. could show transcriptional activation of an E2F responsive GUS construct by E2Fc in *Arabidopsis* protoplasts (2002). One possible explanation could be that trichomes are a very sensitive test system for regulators of the G1/S transition suggesting that already a weak transcriptional activation of E2Fc results in a trichome phenotype. However, additional experiments are necessary to understand the function of E2Fc *in planta*.

Misexpression of the *Arabidopsis* E2F dimerization partners *DPa* and *DPb* did not result in any morphological changes, which is in agreement with the data observed by de Veylder et al. for Pro_{35S}*:DPa* transgenic plants (2002). Transgenic plants in which I tried to reduce *DPa* and *DPb* transcript levels by RNA interference did not display a phenotype. But, it remains to be analyzed whether the expression of the *DPs* is reduced *in planta*. It would be interesting to test whether misexpression of *DPs* together with *E2Fs*, could enhance the observed trichome phenotype caused by E2Fs as seen for overexpression of *E2Fa* together with *DPa* (De Veylder et al., 2002). Moreover, in *Arabidopsis* not much is known about the preferences of E2Fs for their dimerization partners.

Misexpression of the Arabidopsis *RBR1* gene led to a decrease in trichome branch number, as one would expect for a negative regulator of the E2F-DP transcription factor. As the E2F misexpression lines are generated one could easily test whether E2Fs are regulated by RBR1 like in animals. To gain more insights in RBR1 regulation by phosphorylation an interesting experiment could be to test whether Pro_{GL2}*:CDKA;1* misexpression can resuce the Pro_{GL2}*:RBR1* trichome phenotype.

However, one has to be careful with the above described results, because these data are only based on morphological observations and need to be confirmed by detailed analyses of the DNA content in these misexpressing lines. It is also worth checking for the transcription levels of E2F downstream targets, such as *CDC6* or *ORC* which have shown to be upregulated in response to overexpression of *E2Fa* together with *DPa* (De Veylder et al., 2002; del Pozo et al., 2002).

CKIs as multiple cell-cycle switches

Based on this study and previous experiments CKIs could have at least three functions in plants. First, KRPs might be important regulators involved in switching from a mitotic to an endoreplicating cell-cycle mode in differentiating cells. As demonstrated by misexpression in trichome-neighboring cells, embryonic epidermis cells, and Pro_{TMM}-positive cells, KRP1 is a very potent inhibitor of entry into mitosis while it allows S-phase to proceed. Such an inhibitory function might be needed in cells determined to switch to an endoreplication cycle but still contain mitotic regulators. For instance in Medicago, mRNA of a mitotic cyclin has been detected in the zone of nitrogen-fixing nodules, in which cells will enter an endoreplication cycle (Cebolla et al., 1999). Consistently, the *KRP1* mRNA was detected in *Arabidopsis* in mature leaves, in which cells often endoreplicate (Ormenese et al., 2004). Lastly, the rescue of *sim* mutant trichomes by *KRP1* expression argues for a function of CKIs in facilitating the switch to an endoreplication cycle. Intriguingly, *SIM* encodes a small protein with limited homology to KRPs (John Larkin, personal communication). Additionally, Verkest et al could demonstrate that KRP2, another member of the KRP family, can block mitosis (2005).

Second, derived from the finding that KRPs can block entry into mitosis I postulate an additional function of KRPs in dividing cells by assisting to establish a G1 phase. Licensing of origins of replication in a G1 phase requires a low CDK activity (Stern and Nurse, 1996). One way to inactivate kinase activity after a preceding mitosis is the APC/C dependent destruction of mitotic cyclins (Peters, 1998; Harper et al., 2002). In addition, it has been shown that in Drosophila a special CDK inhibitor, ROUGHEX (RUX), binds to and inactivates mitotic CDK complexes helping to establish a G1 phase with low CDK activity (Foley et al., 1999; Foley and Sprenger, 2001). *RUX* is an essential gene in Drosophila demonstrating that there is a high demand for this inhibitory activity. Recently, for the human CDK inhibitors $p21^{Cip1}$, $p27^{Kip1}$ and for the RETINOBLASTOMA protein a similar function in controlling mitotic exit by inactivating mitotic CDK activity was found (Chibazakura et al., 2004). A function of KRPs in contributing to a G1 phase could also explain the expression of KRPs in highly proliferating cells, an observation that is so far not understood and appears even contradictory to the previously described function of KRPs as inhibitors of cell proliferation (Breuil-Broyer et al., 2004; Ormenese et al., 2004). Additional hints for a function of KRP1 in or after mitosis come from transcriptional profiling studies of an *Arabidopsis* cell culture that revealed an expression peak of *KRP1* mRNA in late G2/M phase (Menges and Murray, 2002; Menges et al., 2003). Further, genes expressed in late G2 phase and mitosis often contain mitosis-specific-activator (MSA) elements in their promotors, for instance the promotor of *CYCB1;2* shows 5 elements (Ito et al., 1998; Ito, 2000). In the promotor of *KRP1* at least 8 MSA elements can be found supporting an expression during mitosis. However, it remains to be seen how in this scenario KRP1 is prevented from a premature inhibition of a mitotic CDK complex.

Finally, as shown in previous experiments, misexpression of *KRPs* can lead to cells with a reduced DNA content (De Veylder et al., 2001b; Jasinski et al., 2002; Schnittger et al., 2003). Therefore, the third function of KRPs might be to terminate/assist to terminate mitotic as well as endoreplication cycles. First this is supported, by the analysis of *KRP1* transcript over time. In 5-week old *Arabidopsis* leaves, in which presumably all cell-cycle activity has ceased, an increased level of *KRP1* transcript in comparison to *CDKA;1* was found (Wang et al., 1998). Second, further support comes from the analysis of the *KRP1* T-DNA insertion line in which endoreplication levels are increased in trichome cells.

Throwing the switch

What determines which CKI function is executed? Why does an endoreplicating cell undergo an S-phase block whereas a proliferating cell is preferentially blocked at mitosis? It is conceivable that KRP1 could target different CDK complexes or has different affinities to the various CDK/cyclin complexes in endoreplicating trichomes versus mitotic cells. Also, additional components might be present in mitotic and endoreplicating cells, respectively. Misexpression of human $p21^{Cip1}$, for instance, has led to endoreplication only if the RETINOBLASTOMA protein is absent (Niculescu et al., 1998). Also the Drosophila inhibitor RUX was found upon misexpression to block mitosis and convert the 16^{th} embryonic cycle into an endocycles. Earlier embryonic cycles, however, were only converted when in addition cyclin E was absent (Vidwans et al., 2002). Thus, KRP1 could have a cell-type specific function depending on a specific set of cell-cycle regulators.

All previous data, however, were obtained from misexpression studies using strong promotors, either the *GL2* or the *CaMV35S* promotor, precluding any analysis

of CDK function at weaker concentrations. In this study, I looked at KRP1 moving from trichomes into their neighboring cells and the comparison of fluorescence intensities of YFP-tagged KRP proteins between trichomes and their neighboring cells revealed a more than two-fold difference for KRP1^{109}:YFP to YFP: KRP1 between the two cell types. In addition, the *GL2* promotor appears to have weaker expression in young embryos than later in trichome or root development as judged by the strength of the *in situ* hybridization signal and fluorescence intensity of reporter genes (Lin and Schiefelbein, 2001; Costa and Dolan, 2003). Not much is known about the relative strength of the *TMM* promotor but it is presumably weaker than the *CaMV35S* promotor. Thus, it is possible that CDK inhibitors act as concentration dependent switches that block entry into S-phase only at high concentrations. This is substantiated by the finding that a *KRP1*-misexpression like phenotype was found in *sim* mutant plants with high levels of *KRP1* expression whereas at lower expression levels increased endoreplication levels in comparison to the *sim* mutant were found. Recently, similar observations have been reported for weak and strong misexpression of *KRP2* under control of the *CaMV35S* promotor. Low protein concentrations of KRP2 inhibited the mitotic cell cycle, but endoreplication was unaffected. Whereas *Arabidopsis* plants containing high amounts of KRP2 showed reduced endoreplication levels (Verkest et al., 2005). Interestingly, the study of temperature sensitive CDK alleles in yeast has suggested that for entry into mitosis higher levels of CDK activity are required than for entry into S-phase (MacNeill et al., 1991; Ayscough et al., 1992). One deduction from the above is that if CDK inhibitors are involved in establishing endocycles, and thus, are already expressed in endoreplicating cells, e. g. trichomes, the additional expression of KRP1 might then reach a threshold concentration of CDK inhibitor resulting in a block of S-phase entry. This could explain why among the

large number of transgenic plants generated expressing various KRP versions in trichomes one has only found plants with apparently reduced endoreplication levels in trichomes.

Of course, cell-type specific action and concentration dependency of CKIs are not mutually exclusive. Also endocycles induced in trichome-neighboring cells differed from endocycles in wild-type trichomes since in trichomes neither *CYCB1;1* nor *CYCB1;2* promotor activity can be recognized (Schnittger et al., 2002a).

Remarkably, the *CYCB1;1* promotor reporter indicating a G2-phase did not accumulate in endoreplicating trichome-neighboring cells. This reporter carries a destruction box indicating that at least some activity of the APC/C remained even though CDK activity was presumably blocked. In animals and yeast, CDK activity has been found to be necessary for CDC20 (class of APC/C-cofactors) phosphorylation and by that activate the APC/C^{CDC20} (Shteinberg et al., 1999; Kramer et al., 2000). One possibility for *KRP1* misexpressing plants could be that only the affinity to certain substrates or only certain CDKs might be blocked by KRP1 still permitting the activation of APC/C^{CDC20}. One candidate for a CDK that cannot be blocked by KRPs are the plant specific B-type CDKs (Joubes et al., 2000).

Alternatively, also a different APC/C complex could be involved since the CDC20 dependent APC/C is active only in late mitosis (Shteinberg et al., 1999; Kramer et al., 2000). In animals, with the end of mitosis and during a G1 phase of a following cell cycle another APC/C is assembled containing the CDH1cofactor class (Zachariae et al., 1998). Studies from Drosophila have revealed that the APC/C^{CDH1} is also active in the G2 phase and needs to be inactivated prior to mitosis to allow accumulating mitotic cyclins (Grosskortenhaus and Sprenger, 2002). In contrast to CDC20, phosphorylation has been found to inactivate CDH1 (Kotani et al., 1999;

Kramer et al., 2000). Thus, in the case of *KRP1* misexpression another possibility is that blocked CDK activity might result in an active ACP/C^{CDH1}. Yet, it remains to be seen whether plant APC/C is similarly regulated by CDC20 and CDH1 homologs.

Non-cell-autonomous action of CKIs

So far, CKIs have not been found to function in a non-cell-autonomous manner in animals. Besides controlling CKIs within a cell, the non-cell-autonomous action of KRP1 offers a possibility to link decisions on a cellular level with the supracellular division and growth pattern in organs. For instance, it has been found that starting from the leaf tip epidermal cells enter an endocycle (Melaragno et al., 1993). CKIs could help to spread the entry into an endoreplication cycle. In addition, CKIs could be involved in linking developmental programs, e.g. trichomes with trichome-neighboring cells. In contrast to other epidermal cells it was found that the level of endoreplication in trichome-neighboring cells is quite constant around 4-8C. Of course this could be a feature of socket-cell fate. Alternatively, this could also be an indirect effect resulting from a diffusion of CKIs from a centrally located trichome leading to a coordinated entry in and perhaps a coordinated exit from an endoreplication cycle. Analysis of trichome mutants with increased and decreased endoreplication levels might help to answer this question.

The molecular mechanism of the non-cell-autonomous action of KRP1 remains to be analyzed in detail. Transport through plasomodesmata appears to be highly regulated and at least for some nuclear localized proteins a controlled transport mechanism has been found (Gallagher et al., 2004). Conversely, plasmodesmata also allow the passive diffusion of small molecules. The size exclusion limit (SEL) for non-targeted symplastic movement has been estimated to be around 60 kD in young

tobacco leaves and around 40 kD in older tobacco and *Arabidopsis* leaves (Oparka et al., 1999; Crawford and Zambryski, 2000; Itaya et al., 2000). Thus, on the one hand KRP1 is nuclear localized on the other hand KRP1, even fused to YFP, might be small enough (22 kD and 49 kD, respectively) to diffuse between cells whereas a GUS:YFP:KRP1^{109} fusion with 105 kD was retained in trichomes. Yet a third alternative is that not the protein but the mRNA moves between cells (Ruiz-Medrano et al., 1999; Kim et al., 2001), and detailed analyses will be required in future to understand the nature and possible function of the KRP1 non-cell-autonomy.

Regulation of CKIs by their intracellular localization

The finding that KRP1 can move between cells adds another level of complexity to plant development and challenges cell-cycle control on a tissue and organ level. There are at least two possible ways for plants to keep CKIs in check. The first one might be the nuclear localization. Plants misexpressing YFP:KRP1^{108} showed a strong YFP signal in the nucleus, which is in agreement with the recently identified putative NLS of KRP1 harbored in the N-terminus. The second one might be the high instability of the KRP1 proteins. In contrast to *YFP* expressed from the *GL2* promotor full length KRP1 protein could not be detected on western blots. For the N-terminally truncated protein KRP1^{109} a band of the expected size was found. Intriguingly, whereas the full length KRP1 was exclusively found in the nucleus, KRP1^{109} was also located in the cytoplasm. Similar results were recently obtained by Zhou et al. analyzing roots of plants misexpressing *KRP1* from the *CaMV35S* promotor (2003). In animals, p27^{Kip1} abundance and localization is strictly regulated (Sherr and Roberts, 1999; Slingerland and Pagano, 2000). p27^{Kip1} exerts its inhibitory function in the nucleus and in many experimental systems p27^{Kip1} has been found to become degraded in the cytoplasm

(Tomoda et al., 1999; Connor et al., 2003). One likely possibility is that KRP1 becomes degraded in the cytoplasm and that for this degradation a motif in the N-terminus of the protein is required. To test whether proteolysis of KRPs takes place in the cytoplasm KRP1 could be targeted to the cytoplasm, for example by fusing it to a nuclear export signal.

Regulation of CKIs by protein degradation

In animals $p27^{Kip1}$ is recognized by the E3 ligase SCF^{Skp2}, becomes ubiquitinated and then degraded by the 26S proteasome (Carrano et al., 1999; Sutterluty et al., 1999; Tsvetkov et al., 1999). The first hints that the SCF^{Skp2} dependent degradation of CDK inhibitors is also involved in the proteolysis of *Arabidopsis* CKIs came from the misexpression of $KRP1^{109}$ in *Arabidopsis* plants lacking the F-box protein Skp2. The cytoplasmic YFP signal of plants misexpressing Pro_{TMM}*:YFP:*$KRP1^{109}$ in a *skp2-1 skp2-2* double mutant background was stronger in comparison to the misexpression of this construct in wild type (Marquardt, 2005). Interestingly, analysis of the stability of the YFP:$KRP1^{109}$ fusion protein in endoreplicating trichomes by misexpression of Pro_{GL2}*:YFP:*$KRP1^{109}$ in a *skp2-1 skp2-2* double mutant background revealed no changes in the cytoplasmic YFP signal strength. In the trichome-neighboring cells of this line a cytoplasmic signal could be detected, whereas wild-type plants misexpressing Pro_{GL2}*:YFP:*$KRP1^{109}$ showed only a YFP signal in the nucleus (Marquardt, 2005). This indicates that KRP1 is degraded in a Skp2-dependent manner in dividing cells. However, the fact that the YFP:KRP1 fusion protein expressed under control of the *GL2* promotor could not be detected in western blots shows that KRP1 is subjected to degradation also in endoreplicating cells. These findings suggest that KRP1 becomes degraded by a Skp2-independent manner in endoreplicating cells.

This assumption is supported by the phenotypes observed in *Pro$_{GL2}$:RBX1a-RNAi* transgenic plants, which showed similarities to *KRP1* misexpressing plants. The trichome-neighboring cells were enlarged and the rosette leaves were roundish with sunken trichomes, but the trichomes had a wild type appearance with respect to branch number. An exciting experiment would be to analyze the protein stability of KRPs in dividing and endoreplicating cells of plants with reduced RBX1a levels, like in the *Pro$_{GL2}$:RBX1a-RNAi* line.

Mice lacking the CDC KINASE SUBUNIT CKS1 have been shown to accumulate high amount of p27^{Kip1}. Further experiments revealed that CKS1 binds to Skp2, thereby mediating the interaction of Skp2 with p27^{Kip1}and the subsequent ubiquitination of p27^{Kip1} (Spruck et al., 2001). Stabilization of the human CKS1 and Skp2 resulted in enhanced proteolysis of p27^{Kip1} (Bashir et al., 2004). Interestingly, I observed that misexpression of *CKS1* in trichomes could rescue the KRP1 caused trichome phenotype, suggesting that the proteolysis of *Arabidopsis* KRPs might be regulated by a similar SCF$^{Skp2\text{-}CKS1}$ dependent pathway. However, analysis of the stability of the KRP1^{109}:YFP fusion protein in the progeny of the cross of *Pro$_{GL2}$:CKS1* with *Pro$_{GL2}$:KRP1^{109}:YFP* misexpressing plants revealed a strong YFP signal in the cytoplasm and the nucleus. One possible explanation is that the amount of KRP1^{109}:YFP in the crosses with CKS1 is reduced below a certain threshold leading to wild type trichomes. To test this measurements of the YFP intensity of KRP1^{109}:YFP in *Pro$_{GL2}$:CKS1* and wild type background would be needed. Moreover it should be analyzed whether the observed rescue also leads to wild-type DNA levels in the trichomes. Another possibility to explain CKS1 function could be that CKS1 prevents binding of KRP1 to the CDK/cyclin complex. A third possibility is that CKS1 either activates or stabilizes the CDK/cyclin complex. In budding yeast it has

been shown that CKS1 stabilizes and activates the CDK/cyclin (Cdc28/Cln2) complex *in vitro* (Reynard et al., 2000).

Endocycles and terminal differentiation

Endocycles are often regarded as a state of terminal differentiation since the switch to an endocycle is often associated with cell differentiation (Edgar and Orr-Weaver, 2001; Sugimoto-Shirasu and Roberts, 2003). Evident examples for this connection are *Arabidopsis* trichomes (Marks, 1997; Hulskamp et al., 1999), salivary gland cells in Drosophila (Smith and Orr-Weaver, 1991), or human thrombocytes (Zybina and Zybina, 1996).

Here I have shown that endocycles might be much more dynamic and flexible than previously thought. The first observation was that the onset of an endoreplication program still allows cells to adopt, and thus, change their fate. The second observation was that an endoreplicated cell can re-enter a mitotic cycle. Interestingly, already more than 50 years ago it was observed that polyploid plant and animal cells could occasionally reduce their number of chromosomes and return to a diploid chromosome set (Grell, 1946; Huskins, 1948a, b). Here it has been shown that a reduction of DNA content is not limited to tetraploid cells but even highly endoreplicated cells appeared to divide.

What causes these enlarged cells to re-enter mitosis? Three possibilities are conceivable. In animals, it has been observed that binding of $p27^{Kip1}$ can stabilize a CDK4/cyclin D complex (LaBaer et al., 1997; Cheng et al., 1999; Bagui et al., 2000). Correspondingly, KRP1 could conserve a mitotic regulator complex in the trichome-neighboring, cells and after KRP1 is not supplied any longer by the trichome, the mitotic complex is liberated. A mitotic complex stabilized by KRP1 might include

cyclin D as in plants D-type cyclins have been found to have also mitotic activities (Schnittger et al., 2002b; Koroleva et al., 2004). On the other hand a cell-size check point might operate and induce late cell divisions. The endoreplicated trichome-neighboring cells in *KRP1*-misexpressing plants are at least for some time the largest cells found in the epidermis and likely of the entire leaf. Thus, a cell-autonomous control mechanism might be responsible for the onset of cell divisions, and after a certain size might be reached, a new cell division could be initiated.

Finally, also a non-cell-autonomous control mechanism based for instance on stomata index might be responsible. I noticed that new stomata complexes were formed by many cell divisions of trichome-neighboring cells (Fig5E). Stomata density is tightly controlled on the leaf blade (Nadeau and Sack, 2002b; Bergmann, 2004). Stomata can only be generated by cell divisions, and therefore, leaf growth by cell expansion in maturating leaves would lead to a dramatic decrease in stomata density. Interestingly, always a few 2C cells were found in maturing leaf areas in which other cells had undergone a few rounds of endoreplication (Melaragno et al., 1993). These cells have been interpreted as a "reserve" for regenerating cells and also for stomata formation. In the light of my findings, however, these cells might not be set aside but could be generated by divisions of endoreplicated cells.

These different possibilities remain to be tested in future but it already emerges that plant cell-cycle control is much more flexible than anticipated and detailed analysis of division patterns will be needed in future to get a deeper insight into the dynamics of plant cell-cycle control in the context of organ and tissue development.

MATERIAL & METHODS

1.MATERIAL

1.1. Chemicals and antibiotics

All used chemicals and antibiotics of analytical quality have been used from Sigma (Deisenhofen, Germany), Roth (Karlsruhe, Germany), Merck (Darmstadt, Germany) and Duchefa (Haarlem Netherlands).

1.2. Enzymes, primers and kits

Restriction enzymes were used from MBI-fermentas (St.Leon-Rot, Germany) and New England Biolabs (Frankfurt/Main, Germany). Modifying enzymes were used from MBI-fermentas (St.Leon-Rot, Germany), Invitrogen (Karlsruhe, Germany), Roche (Mannheim, Germany), usb (Cleveland, USA), Qbiogene (Heidelberg, Germany), TaKaRa (Otsu, Japan). Primers were generated by Metabion (München, Germany). Kits were supplied from peqlab (Erlangen, Germany), GENOMED (Löhne, Germany), Roche (Mannheim, Germany), QIAGEN (Hilden, Germany) and DYNAL (Oslo, Norway).

1.3. Cloning vectors and constructs

All used cloning vectors and constructs are listed in the appendix.

1.4. Bacterial strains

For standard cloning the *Escherichia coli* strains DH5alpha and XL1blue were used, the DB3;1 strain, which is resistant to the *ccdB* gene, was used for the Gateway Entry, Donor and Destination vectors.

For plant transformation *Agrobacterium tumefaciens* strain GV3101 was used. For all gateway vector based plant transformation GV3101+pMP90RK was used.

1.5. Plant lines

In this study Landsberg *erecta* (L*er),* Columbia (Col), and Wassilewskaja (WS-O) ecotypes were used. All mutants and transgenic lines are listed in the appendix.

2. METHODS

2.1. Plant work

2.1.1. Plant growth conditions

Arabidopsis thaliana plants were grown under long-day conditions (16 h of light, 8 h of darkness) between 18 and 25 ºC under standard greenhouse conditions.

2.1.2. Crossing of plants

At a stage when the flowers were closed and the pollen of the anthers was not ripe the anthers of the acceptor flower were removed completely using very fine forceps. All remaining older and younger flowers were also removed. After two days the stigma of the carpels were pollinated with pollen from the donor plant.

2.1.3. Plant transformation

Plants were transformed according to the "floral dip" method (Clough and Bent, 1998). To gain strong plants, these were allowed to grow at 18°C untill the first flowers appeared at stalks of approximately 10 cm in length. Four days before plant transformation a 5 ml Agrobacteria preculture was incubated for two days at 28°C. This preculture was used to inoculate the final 500 ml culture which was then

incubated again for two days at 28°C. Before transformation 5% sucrose and 0.05% Silwett L-77 were added to the culture. Plants were dipped in this solution for approximately 20 seconds and afterwards covered with a lid. The lid was removed on the following day.

2.1.4. Seed surface sterilization

The surface of the seeds was sterilized by a five min incubation in 95% Ethanol followed by a 10 min incubation in a 20% Klorix solution (containing 0.1% triton X-100). Afterwards the seeds were washed two to three times with 0.01% Triton-X100 solution and than plated under the clean bench on MS-Agar plates (1% Murashige-Skoog salts, 1% sucrose, 0.7% agar, pH5.7).

2.1.5. Selection of transformants

The seeds of transgenic plants carrying in their T-DNA a kanamycin or a hygromycin resistance were selected on MS-Agar plates with 50µg/ml kanamycin or 25 µg/ml hygromycin, respectively. Transgenic plants containing the BASTA resistance were grown on soil for 10 to 15 days. The seedlings were sprayed with a 0.001% BASTA solution, the spraying was repeated after three to seven days.

2.2. Microscopy and cytological methods

2.2.1. Microscopy

Light microscopy was performed with an Axiophot microscope (Zeiss, Heidelberg, Germany) or a Leica DM RA2 (Leica, Wetzlar, Germany) equipped with differential interference contrast (Nomarski) and epifluorescence optics. The DISKUS software package (Carl H. Hilgers-Technisches Büro, Königswinter, Germany; version

4.30.19) was used to quantify the fluorescence intensity of DAPI stained leaves to determine nuclear and cell sizes, and to measure the nuclear size of propidium iodide stained embryos in optical sections. Cryo-scanning electron microscopy was performed as described by Rumbolz et al., 1999. Confocal-laser-scanning microscopy was performed with Leica DM-Irbe (Leica, Wetzlar, Germany) or LSM 510 META (Zeiss, Heidelberg, Germany).

2.2.2. GUS staining

GUS-activity was assayed according to Sessions and Yanofsky, 1999. To allow complete penetration of the X-Gluc-solution plants were vacuum infiltrated in staining buffer (0.2% Triton X-100, 50mM $NaPO_4$ pH 7.2, 2mM potassium-ferrocyanide $K_4Fe(CN)_6*H_2O$, 2mM potassium-ferricyanide $K_3Fe(CN)_6$ containing 2mM X-Gluc) for 15 to 30 minutes and afterwards incubated at 37°C over night. Clearing was

performed in 70% Ethanol at 37°C over night.

2.2.3. Propidium iodide staining

Plant material was incubated for 5 minutes in 100 µg/ml Propidium iodide in H_2O . Afterwards the samples where washed with H_2O, mounted on a slide and analyzed under the microscope with UV excitation.

2.2.4. DAPI staining

To ensure an equal DAPI staining for DNA measurements of socket cells leaves are incubated overnight in 70% Ethanol at RT. Leaves are then vacuum infiltrated for 30 min in a DAPI solution (0.25µg/ml DAPI in H_2O) followed by a wash with H_2O.

For DNA measurements of trichomes, rosette leaves were vacuum infiltrated for 30 min in formaldehyde solution (3.7% formaldehyde in PBST) followed by a 2h incubation at 4ºC. Samples were washed two times for 15 min in PBST. Then leaves were vacuum infiltrated in DAPI solution (0.25µg/ml, 5% DMSO in PBST) for 15 min and incubated overnight in DAPI solution at 4ºC thereafter leaves were washed two times in PBST.

2.2.5. Measurement of DNA content and YFP Intensity

Measurements of DNA content and YFP intensity were performed as described in Weinl et al., 2005.

2.2.6. Fluorescent-Activated Cell Sorting Analysis

FACS Analysis was performed as described in Weinl et al., 2005.

2.3. Molecular-biological methods

2.3.1. RNA isolation, reverse transcription and semiquantitative RT-PCR

Isolation of RNA, DNAse digest, reverse transcription and semiquantitative RT-PCR was performed according to Schnittger et al., 2002; Schnittger et al., 2003 and Weinl et al., 2005. All RT-PCR primers are listed in the table 8.

TABLE 8
RT-PCR primers

gene	S/AS primer	sequence 5'->3'	annealing temp
att-Gateway	**S** attB1	CAA GTT TGT ACA AAA AAG CAG	55
att-Gateway	**AS** attB2	CCA CTT TGT ACA AGA AAG CTG	55
CDKA;1	**AS** cdc2a_511	ATG AGT AAA TGT CCT GAC AGG GAT AC	55
CDKB1;1	**AS** CDKB1;1_560	TCA AGA GGC TTA GGA TTA GGT CC	62
EF1	**S** EF1_UP	ATG CCC CAG GAC ATC GTG ATT TCA T	58
EF1	**AS** EF1_RP	TTG GCG GCA CCC TTA GCT GGA TCA	58
GLABRA2	**S** GL2_UTR_53	GAG GAG AAG AGG GAA GAG ATC ATA A	55
GLABRA2	**AS** GL2_330_AS	TCT TTC TCT TAT TAG TGC CCT TGT	55
GLABRA2	**AS** GL2_685	AGG AAT TAG CCT TGG AAA AAG ACT	55
KRP1	**S** R1/KRP1_617	CTC CGT CGT CGG TGA TAA TG	55
KRP1	**AS** R2/KRP1_1591	AAG ACA CGA CTT TTC TGG GC	55
KRP1	**S** R3/KRP1_1048	GGC GGT TAA AGA ATC GTT AGA T	55
KRP1/KRP1^{109}	**AS** ICK_655_FL	TTT ACC CAT TCG TAA CGT CCT TCT A	60
KRP1^{152}	**AS** ICK_454	CAA CAA CAA TCT AAC GAT TCT TTA ACC	60
YFP	**S** YFP126_S	GCT GAC CCT GAA GTT CAT CTG	55
YFP	**AS** YFP485_AS	TGA TAT AGA CGT TGT GGC TGT TG	55

2.3.2. Genomic DNA preparation

Genomic DNA was isolated by CTAB-preparation (Rogers & Bendich 1988). Plant material (single rosette or cauline leave) was grinded and 200 µl of extraction buffer (2%(w/v) CTAB, 1.4M NaCl, 20mM EDTA, 100mM Tris/HCl pH 8.0, 0.2% b-mercaptoethanol) was added and incubated for 30 minutes at 65°C. After addition of 150 µl Chloroform/Isoamylalcohol (24:1) and careful shaking, the probes were centrifuged for 15 minutes at 4000 rpm. The aqueous phase was transferred into a new tube and mixed with 200 µl isopropanol and centrifuged for 15 min. at 4000 rpm. The pellet was washed with 70% Ethanol and dried, afterwards the pellet was resolved in 20 µl 20mM Tris/HCl pH 8.0.

2.3.3. Plasmid DNA preparation from bacteria

Plasmid preparation was performed using a column pEQ-LAB Plasmid Miniprep KitI (PEQLAB Biotechnology GmbH, Erlangen) according to the manufacturer's protocol.

2.3.4. DNA-manipulation

DNA manipulation and cloning were carried out according to Sambrock et al., 1989 or Ausubel *et a*l., 1994, using standard procedures. All PCR-amplified fragments were sequenced prior to further investigation.

PCR-Primers and constructs were designed using the VectorNTI-suite 7.1 software (Invitrogen, Karlsruhe).

2.3.5. Isolation of T-DNA insertion lines

To isolate T-DNA insertion lines for *KRP1* or *KRP4* of the Csaba Koncz collection a PCR based screen was performed following the protocol of Rios et al., 2002. All screening and T-DNA primers are listed in table 9.

TABLE 9
Screening and T-DNA Primers

primer	sequence 5'->3'	annealing temp
KRP4_S	CCA CAA AGA GCA CTA ATC TTC ACA ACC CTA	68
KRP4_AS	GAG TCC CCC TGT ACC GGA ATT CAT A	68
S1 (KRP1_S)	CGT CAC TGT AAC GGG ACC ACT AAA AC	68
S2 (KRP1_AS)	CTC TAA CTT TAC CCA TTC GTA ACG TCC TTC	68
T1 (left border Fish1)	CTG GGA ATG GCG AAA TCA AGG CAT C	68
T2 (right border Fish2)	CAG TCA TAG CCG AAT AGC CTC TCC A	68
T3 (left border HOOK1)	CTA CAC TGA ATT GGT AGC TCA AA TGT C	68
T4 (right border HOOK4)	TCA GAG CAG CCG ATT GTC TGT TGT G	68
T5 (left border HOOK3)	GTT GAC AGA CTG CCT AGC ATT TGA GTG	68
T6 (right border HOOK2)	TAC TTT CTC GGC AGG AGC AAG GTG A	68

REFERENCES

Albani, D., Mariconti, L., Ricagno, S., Pitto, L., Moroni, C., Helin, K., and Cella, R. (2000). DcE2F, a functional plant E2F-like transcriptional activator from Daucus carota. J Biol Chem **275,** 19258-19267.

Ausubel, F.M. (1994). Current protocols in molecular biology. (New York: John Wiley & Sons, Inc.).

Ayscough, K., Hayles, J., MacNeill, S.A., and Nurse, P. (1992). Cold-sensitive mutants of p34cdc2 that suppress a mitotic catastrophe phenotype in fission yeast. Mol Gen Genet **232,** 344-350.

Bagui, T.K., Jackson, R.J., Agrawal, D., and Pledger, W.J. (2000). Analysis of cyclin D3-cdk4 complexes in fibroblasts expressing and lacking p27(kip1) and p21(cip1). Mol Cell Biol **20,** 8748-8757.

Bashir, T., Dorrello, N.V., Amador, V., Guardavaccaro, D., and Pagano, M. (2004). Control of the SCF(Skp2-Cks1) ubiquitin ligase by the APC/C(Cdh1) ubiquitin ligase. Nature **428,** 190-193.

Bergmann, D.C. (2004). Integrating signals in stomatal development. Curr Opin Plant Biol **7,** 26-32.

Boehm, M., Yoshimoto, T., Crook, M.F., Nallamshetty, S., True, A., Nabel, G.J., and Nabel, E.G. (2002). A growth factor-dependent nuclear kinase phosphorylates p27(Kip1) and regulates cell cycle progression. Embo J **21,** 3390-3401.

Boudolf, V., Barroco, R., Engler Jde, A., Verkest, A., Beeckman, T., Naudts, M., Inze, D., and De Veylder, L. (2004). B1-type cyclin-dependent kinases are essential for the formation of stomatal complexes in Arabidopsis thaliana. Plant Cell **16,** 945-955.

Breuil-Broyer, S., Morel, P., de Almeida-Engler, J., Coustham, V., Negrutiu, I., and Trehin, C. (2004). High-resolution boundary analysis during Arabidopsis thaliana flower development. Plant J **38,** 182-192.

Carrano, A.C., Eytan, E., Hershko, A., and Pagano, M. (1999). SKP2 is required for ubiquitin-mediated degradation of the CDK inhibitor p27. Nat Cell Biol **1,** 193-199.

Cebolla, A., Vinardell, J.M., Kiss, E., Olah, B., Roudier, F., Kondorosi, A., and Kondorosi, E. (1999). The mitotic inhibitor ccs52 is required for endoreduplication and ploidy-dependent cell enlargement in plants. Embo J **18,** 4476-4484.

Chamovitz, D.A., Wei, N., Osterlund, M.T., von Arnim, A.G., Staub, J.M., Matsui, M., and Deng, X.W. (1996). The COP9 complex, a novel multisubunit nuclear regulator involved in light control of a plant developmental switch. Cell **86,** 115-121.

Cheng, M., Olivier, P., Diehl, J.A., Fero, M., Roussel, M.F., Roberts, J.M., and Sherr, C.J. (1999). The p21(Cip1) and p27(Kip1) CDK 'inhibitors' are essential activators of cyclin D-dependent kinases in murine fibroblasts. Embo J **18,** 1571-1583.

Chibazakura, T., McGrew, S.G., Cooper, J.A., Yoshikawa, H., and Roberts, J.M. (2004). Regulation of cyclin-dependent kinase activity during mitotic exit and

maintenance of genome stability by p21, p27, and p107. Proc Natl Acad Sci U S A.

Ciechanover, A. (1998). The ubiquitin-proteasome pathway: on protein death and cell life. Embo J **17,** 7151-7160.

Clough, S.J., and Bent, A.F. (1998). Floral dip: a simplified method for Agrobacterium-mediated transformation of *Arabidopsis thaliana*. Plant J **16,** 735-743.

Colon-Carmona, A., You, R., Haimovitch-Gal, T., and Doerner, P. (1999). Technical advance: spatio-temporal analysis of mitotic activity with a labile cyclin-GUS fusion protein. Plant J **20,** 503-508.

Connor, M.K., Kotchetkov, R., Cariou, S., Resch, A., Lupetti, R., Beniston, R.G., Melchior, F., Hengst, L., and Slingerland, J.M. (2003). CRM1/Ran-mediated nuclear export of p27(Kip1) involves a nuclear export signal and links p27 export and proteolysis. Mol Biol Cell **14,** 201-213.

Costa, S., and Dolan, L. (2003). Epidermal patterning genes are active during embryogenesis in Arabidopsis. Development **130,** 2893-2901.

Crawford, K.M., and Zambryski, P.C. (2000). Subcellular localization determines the availability of non-targeted proteins to plasmodesmatal transport. Curr Biol **10,** 1032-1040.

de Jager, S.M., Menges, M., Bauer, U.M., and Murra, J.A. (2001). Arabidopsis E2F1 binds a sequence present in the promoter of S-phase-regulated gene AtCDC6 and is a member of a multigene family with differential activities. Plant Mol Biol **47,** 555-568.

De Veylder, L., Beemster, G.T., Beeckman, T., and Inze, D. (2001a). CKS1At overexpression in Arabidopsis thaliana inhibits growth by reducing meristem size and inhibiting cell-cycle progression. Plant J **25,** 617-626.

De Veylder, L., Segers, G., Glab, N., Casteels, P., Van Montagu, M., and Inze, D. (1997). The Arabidopsis Cks1At protein binds the cyclin-dependent kinases Cdc2aAt and Cdc2bAt. FEBS Lett **412,** 446-452.

De Veylder, L., Beeckman, T., Beemster, G.T., Krols, L., Terras, F., Landrieu, I., van der Schueren, E., Maes, S., Naudts, M., and Inze, D. (2001b). Functional analysis of cyclin-dependent kinase inhibitors of Arabidopsis. Plant Cell **13,** 1653-1668.

De Veylder, L., Beeckman, T., Beemster, G.T., de Almeida Engler, J., Ormenese, S., Maes, S., Naudts, M., Van Der Schueren, E., Jacqmard, A., Engler, G., and Inze, D. (2002). Control of proliferation, endoreduplication and differentiation by the Arabidopsis E2Fa-DPa transcription factor. Embo J **21,** 1360-1368.

del Pozo, J.C., Boniotti, M.B., and Gutierrez, C. (2002). Arabidopsis E2Fc functions in cell division and is degraded by the ubiquitin-SCF(AtSKP2) pathway in response to light. Plant Cell **14,** 3057-3071.

Ding, B., Itaya, A., and Qi, Y. (2003). Symplasmic protein and RNA traffic: regulatory points and regulatory factors. Curr Opin Plant Biol **6,** 596-602.

Donnelly, P.M., Bonetta, D., Tsukaya, H., Dengler, R.E., and Dengler, N.G. (1999). Cell cycling and cell enlargement in developing leaves of Arabidopsis. Dev Biol **215,** 407-419.

Ebel, C., Mariconti, L., and Gruissem, W. (2004). Plant retinoblastoma homologues control nuclear proliferation in the female gametophyte. Nature **429,** 776-780.

Edgar, B.A., and Orr-Weaver, T.L. (2001). Endoreplication cell cycles: more for less. Cell **105,** 297-306.

Foley, E., and Sprenger, F. (2001). The cyclin-dependent kinase inhibitor Roughex is involved in mitotic exit in Drosophila. Curr Biol **11,** 151-160.

Foley, E., O'Farrell, P.H., and Sprenger, F. (1999). Rux is a cyclin-dependent kinase inhibitor (CKI) specific for mitotic cyclin-Cdk complexes. Curr Biol **9,** 1392-1402.

Gagne, J.M., Downes, B.P., Shiu, S.H., Durski, A.M., and Vierstra, R.D. (2002). The F-box subunit of the SCF E3 complex is encoded by a diverse superfamily of genes in Arabidopsis. Proc Natl Acad Sci U S A **99,** 11519-11524.

Gallagher, K.L., Paquette, A.J., Nakajima, K., and Benfey, P.N. (2004). Mechanisms regulating SHORT-ROOT intercellular movement. Curr Biol **14,** 1847-1851.

Ganoth, D., Bornstein, G., Ko, T.K., Larsen, B., Tyers, M., Pagano, M., and Hershko, A. (2001). The cell-cycle regulatory protein Cks1 is required for SCF(Skp2)-mediated ubiquitinylation of p27. Nat Cell Biol **3,** 321-324.

Geisler, M.D., Nadeau, J.A., and Sack, F.D. (2000). Oriented asymmetric divisions that generate the stomatal spacing pattern in Arabidopsis are disrupted by the *too many mouths* mutation. Plant Cell **12,** 2075-2086.

Gray, W.M., Hellmann, H., Dharmasiri, S., and Estelle, M. (2002). Role of the Arabidopsis RING-H2 protein RBX1 in RUB modification and SCF function. Plant Cell **14,** 2137-2144.

Grell, M. (1946). Cytological studies in culex I: Somatic reduction divisions. Genetics **31,** 60-76.

Grosskortenhaus, R., and Sprenger, F. (2002). Rca1 inhibits APC-Cdh1(Fzr) and is required to prevent cyclin degradation in G2. Dev Cell **2,** 29-40.

Gusmaroli, G., Feng, S., and Deng, X.W. (2004). The Arabidopsis CSN5A and CSN5B subunits are present in distinct COP9 signalosome complexes, and mutations in their JAMM domains exhibit differential dominant negative effects on development. Plant Cell **16,** 2984-3001.

Harbour, J.W., and Dean, D.C. (2000). The Rb/E2F pathway: expanding roles and emerging paradigms. Genes Dev **14,** 2393-2409.

Harper, J.W., Burton, J.L., and Solomon, M.J. (2002). The anaphase-promoting complex: it's not just for mitosis any more. Genes Dev **16,** 2179-2206.

Haseloff, J., Siemering, K.R., Prasher, D.C., and Hodge, S. (1997). Removal of a cryptic intron and subcellular localization of green fluorescent protein are required to mark transgenic *Arabidopsis* plants brightly. Proc. Natl. Avad. Sci. USA **94,** 2122-2127.

Hayles, J., Beach, D., Durkacz, B., and Nurse, P. (1986). The fission yeast cell cycle control gene cdc2: isolation of a sequence suc1 that suppresses cdc2 mutant function. Mol Gen Genet **202,** 291-293.

Hellmann, H., and Estelle, M. (2002). Plant development: regulation by protein degradation. Science **297,** 793-797.

Hemerly, A., Engler, J., Bergounioux, C., Van Montagu, M., Engler, G., Inze, D., and Ferreira, P. (1995). Dominant negative mutants of the Cdc2 kinase uncouple cell division from iterative plant development. Embo J **14,** 3925-3936.

Holm, M., Ma, L.G., Qu, L.J., and Deng, X.W. (2002). Two interacting bZIP proteins are direct targets of COP1-mediated control of light-dependent gene expression in Arabidopsis. Genes Dev **16,** 1247-1259.

Hulskamp, M., Misra, S., and Jurgens, G. (1994). Genetic dissection of trichome cell development in Arabidopsis. Cell **76,** 555-566.

Hulskamp, M., Schnittger, A., and Folkers, U. (1999). Pattern formation and cell differentiation: trichomes in Arabidopsis as a genetic model system. Int Rev Cytol **186,** 147-178.

Huskins, C.L. (1948a). Chromosome multiplication and reduction in somatic tissues. Nature **161,** 80-83.

Huskins, C.L. (1948b). Segregation and reduction in somatic tissues. Journal of Heredity **39,** 311-325.

Itaya, A., Liang, G., Woo, Y.-M., Nelson, R.S., and Ding, B. (2000). Nonspecific intercellular protein trafficking probed by green-fluorescent protein in plants. Protoplasma **213,** 165-175.

Ito, M. (2000). Factors controlling cyclin B expression. Plant Mol Biol **43,** 677-690.

Ito, M., Iwase, M., Kodama, H., Lavisse, P., Komamine, A., Nishihama, R., Machida, Y., and Watanabe, A. (1998). A novel cis-acting element in promoters of plant B-type cyclin genes activates M phase-specific transcription. Plant Cell **10,** 331-341.

Jacqmard, A., De Veylder, L., Segers, G., de Almeida Engler, J., Bernier, G., Van Montagu, M., and Inze, D. (1999). Expression of CKS1At in Arabidopsis thaliana indicates a role for the protein in both the mitotic and the endoreduplication cycle. Planta **207,** 496-504.

Jakoby, M., and Schnittger, A. (2004). Cell cycle and differentiation. Curr Opin Plant Biol **7,** 661-669.

Jasinski, S., Riou-Khamlichi, C., Roche, O., Perennes, C., Bergounioux, C., and Glab, N. (2002). The CDK inhibitor NtKIS1a is involved in plant development, endoreduplication and restores normal development of cyclin D3;1-overexpressing plants. J Cell Sci **115,** 973-982.

Joubes, J., Chevalier, C., Dudits, D., Heberle-Bors, E., Inze, D., Umeda, M., and Renaudi, J.P. (2000). CDK-related protein kinases in plants. Plant Mol Biol **43,** 607-620.

Kamura, T., Hara, T., Matsumoto, M., Ishida, N., Okumura, F., Hatakeyama, S., Yoshida, M., Nakayama, K., and Nakayama, K.I. (2004). Cytoplasmic ubiquitin ligase KPC regulates proteolysis of p27(Kip1) at G1 phase. Nat Cell Biol **6,** 1229-1235.

Kawakami, T., Chiba, T., Suzuki, T., Iwai, K., Yamanaka, K., Minato, N., Suzuki, H., Shimbara, N., Hidaka, Y., Osaka, F., Omata, M., and Tanaka, K. (2001). NEDD8 recruits E2-ubiquitin to SCF E3 ligase. Embo J **20,** 4003-4012.

Kim, M., Canio, W., Kessler, S., and Sinha, N. (2001). Developmental changes due to long-distance movement of a homeobox fusion transcript in tomato. Science **293,** 287-289.

Kirik, V., Bouyer, D., Schöbinger, U., Bechtold, N., Herzog, M., Bonneville, J.-M., and Hülskamp, M. (2001). *CPR5* is involved in cell proliferation and cell death control and encodes a novel transmembrane protein. Curr Biol **11,** 1891-1895.

Kondorosi, E., and Kondorosi, A. (2004). Endoreduplication and activation of the anaphase-promoting complex during symbiotic cell development. FEBS Lett **567,** 152-157.

Kondorosi, E., Roudier, F., and Gendreau, E. (2000). Plant cell-size control: growing by ploidy? Curr Opin Plant Biol **3,** 488-492.

Koornneef, M. (1990). Mutations affecting the testa colour in *Arabidopsis*. Arab. Inf. Serv. **27,** 1-4.

Koroleva, O.A., Tomlinson, M., Parinyapong, P., Sakvarelidze, L., Leader, D., Shaw, P., and Doonan, J.H. (2004). CycD1, a Putative G1 Cyclin from Antirrhinum majus, Accelerates the Cell Cycle in Cultured Tobacco BY-2 Cells by Enhancing Both G1/S Entry and Progression through S and G2 Phases. Plant Cell **16,** 2364-2379.

Kosugi, S., and Ohashi, Y. (2002a). E2Ls, E2F-like repressors of arabidopsis that bind to E2F-sites in a monomeric form. J Biol Chem.

Kosugi, S., and Ohashi, Y. (2002b). E2F sites that can interact with E2F proteins cloned from rice are required for meristematic tissue-specific expression of rice and tobacco proliferating cell nuclear antigen promoters. Plant J **29,** 45-59.

Kosugi, S., and Ohashi, Y. (2002c). Interaction of the Arabidopsis E2F and DP proteins confers their concomitant nuclear translocation and transactivation. Plant Physiol **128,** 833-843.

Kosugi, S., and Ohashi, Y. (2003). Constitutive E2F expression in tobacco plants exhibits altered cell cycle control and morphological change in a cell type-specific manner. Plant Physiol **132,** 2012-2022.

Kotani, S., Tanaka, H., Yasuda, H., and Todokoro, K. (1999). Regulation of APC activity by phosphorylation and regulatory factors. J Cell Biol **146,** 791-800.

Kowles RV, P.R. (1985). DNA amplification patterns in maize endosperm nuclei during kernel development. Proceedings of the National Academy of Sciences, USA **82,** 7010-7014.

Kramer, E.R., Scheuringer, N., Podtelejnikov, A.V., Mann, M., and Peters, J.M. (2000). Mitotic regulation of the APC activator proteins CDC20 and CDH1. Mol Biol Cell **11,** 1555-1569.

LaBaer, J., Garrett, M.D., Stevenson, L.F., Slingerland, J.M., Sandhu, C., Chou, H.S., Fattaey, A., and Harlow, E. (1997). New functional activities for the p21 family of CDK inhibitors. Genes Dev **11,** 847-862.

Lacy ER, F.I., Lewis WS, Otieno S, Xiao L, Weiss S, Hengst L, Kriwacki RW. (2004). p27 binds cyclin-CDK complexes through a sequential mechanism involving binding-induced protein folding. Nature Structural & Molecular Biology **11,** 358-364.

Landrieu, I., Hassan, S., Sauty, M., Dewitte, F., Wieruszeski, J.M., Inze, D., De Veylder, L., and Lippens, G. (2004a). Characterization of the Arabidopsis thaliana Arath;CDC25 dual-specificity tyrosine phosphatase. Biochem Biophys Res Commun **322,** 734-739.

Landrieu, I., da Costa, M., De Veylder, L., Dewitte, F., Vandepoele, K., Hassan, S., Wieruszeski, J.M., Corellou, F., Faure, J.D., Van Montagu, M., Inze, D., and Lippens, G. (2004b). A small CDC25 dual-specificity tyrosine-phosphatase isoform in Arabidopsis thaliana. Proc Natl Acad Sci U S A **101,** 13380-13385.

Larkin, J., Brown, M., and Schiefelbein, J. (2003). HOW DO CELLS KNOW WHAT THEY WANT TO BE WHEN THEY GROW UP? Lessons from Epidermal Patterning in Arabidopsis. Annual Review of Plant Biology **54,** 403-430.

Larkin, J., Young, N., Prigge, M., and Marks, M. (1996). The control of trichome spacing and number in *Arabidopsis*. Development **122,** 997-1005.

Lechner, E., Xie, D., Grava, S., Pigaglio, E., Planchais, S., Murray, J.A., Parmentier, Y., Mutterer, J., Dubreucq, B., Shen, W.H., and Genschik, P. (2002). The AtRbx1 protein is part of plant SCF complexes, and its down-

regulation causes severe growth and developmental defects. J Biol Chem **277,** 50069-50080.

Leiva-Neto, J.T., Grafi, G., Sabelli, P.A., Dante, R.A., Woo, Y.M., Maddock, S., Gordon-Kamm, W.J., and Larkins, B.A. (2004). A dominant negative mutant of cyclin-dependent kinase A reduces endoreduplication but not cell size or gene expression in maize endosperm. Plant Cell **16,** 1854-1869.

Lin, Y., and Schiefelbein, J. (2001). Embryonic control of epidermal cell patterning in the root and hypocotyl of Arabidopsis. Development **128,** 3697-3705.

MacNeill, S.A., Creanor, J., and Nurse, P. (1991). Isolation, characterisation and molecular cloning of new mutant alleles of the fission yeast p34cdc2+ protein kinase gene: identification of temperature-sensitive G2-arresting alleles. Mol Gen Genet **229,** 109-118.

Magyar, Z., Atanassova, A., De Veylder, L., Rombauts, S., and Inze, D. (2000). Characterization of two distinct DP-related genes from Arabidopsis thaliana. FEBS Lett **486,** 79-87.

Mariconti, L., Pellegrini, B., Cantoni, R., Stevens, R., Bergounioux, C., Cella, R., and Albani, D. (2002). The E2F family of transcription factors from Arabidopsis thaliana: Novel and conserved components of the pRB/E2F pathway in plants. J Biol Chem.

Marks, M.D. (1997). Molecular Genetic Analysis of Trichome Development in *Arabidopsis*. Annu. Rev. Plant Physiol. Plant Mol. Biol. **48,** 137-163.

Marquardt, S. (2005). Regulation des CDK-Inhibitors KRP1 in Arabidopsis. In Lehrstuhl für Botanik III (Köln: Universität Köln).

Melaragno, J.E., Mehrotra, B., and Coleman, A.W. (1993). Relationship between endopolyploidy and cell size in epidermal tissue of Arabidopsis. Plant Cell **5,** 1661-1668.

Menges, M., and Murray, J.A. (2002). Synchronous Arabidopsis suspension cultures for analysis of cell-cycle gene activity. Plant J **30,** 203-212.

Menges, M., Hennig, L., Gruissem, W., and Murray, J.A. (2003). Genome-wide gene expression in an Arabidopsis cell suspension. Plant Mol Biol **53,** 423-442.

Molhoj, M., Jorgensen, B., Ulvskov, P., and Borkhardt, B. (2001). Two Arabidopsis thaliana genes, KOR2 and KOR3, which encode membrane-anchored endo-1,4-beta-D-glucanases, are differentially expressed in developing leaf trichomes and their support cells. Plant Mol Biol **46,** 263-275.

Montagnoli, A., Fiore, F., Eytan, E., Carrano, A.C., Draetta, G.F., Hershko, A., and Pagano, M. (1999). Ubiquitination of p27 is regulated by Cdk-dependent phosphorylation and trimeric complex formation. Genes Dev **13,** 1181-1189.

Nadeau, J.A., and Sack, F.D. (2002a). Control of stomatal distribution on the *Arabidopsis* leaf surface. Science **296,** 1697-1700.

Nadeau, J.A., and Sack, F.D. (2002b). Stomatal development in Arabidopsis. In The Arabidopsis book, C.R. Somerville and E.M. Meyerowitz, eds (American Society Plant Biologists.

Nagl, W. (1976). Zellkern und Zellzyklen : Molekularbiologie, Organisation und Entwicklungsphysiologie der Desoxyribonucleinsaeure und des Chromatins. (Stuttgart: Ulmer).

Niculescu, A.B., 3rd, Chen, X., Smeets, M., Hengst, L., Prives, C., and Reed, S.I. (1998). Effects of p21(Cip1/Waf1) at both the G1/S and the G2/M cell cycle transitions: pRb is a critical determinant in blocking DNA replication and in preventing endoreduplication. Mol Cell Biol **18,** 629-643.

Olashaw, N., Bagui, T.K., and Pledger, W.J. (2004). Cell Cycle Control: A Complex Issue. Cell Cycle **3,** 263-264.

Oparka, K.J. (2004). Getting the message across: how do plant cells exchange macromolecular complexes? Trends Plant Sci **9,** 33-41.

Oparka, K.J., Roberts, A.G., Boevink, P., Santa Cruz, S., Roberts, I., Pradel, K.S., Imlau, A., Kotlizky, G., Sauer, N., and Epel, B. (1999). Simple, but not branched, plasmodesmata allow the nonspecific trafficking of proteins in developing tobacco leaves. Cell **97,** 743-754.

Ormenese, S., de Almeida Engler, J., De Groodt, R., De Veylder, L., Inze, D., and Jacqmard, A. (2004). Analysis of the spatial expression pattern of seven Kip related proteins (KRPs) in the shoot apex of Arabidopsis thaliana. Ann Bot (Lond) **93,** 575-580.

Osterlund, M.T., Wei, N., and Deng, X.W. (2000). The roles of photoreceptor systems and the COP1-targeted destabilization of HY5 in light control of Arabidopsis seedling development. Plant Physiol **124,** 1520-1524.

Pagano, M., Tam, S.W., Theodoras, A.M., Beer-Romero, P., Del Sal, G., Chau, V., Yew, P.R., Draetta, G.F., and Rolfe, M. (1995). Role of the ubiquitin-proteasome pathway in regulating abundance of the cyclin-dependent kinase inhibitor p27. Science **269,** 682-685.

Park, J.A., Ahn, J.W., Kim, Y.K., Kim, S.J., Kim, J.K., Kim, W.T., and Pai, H.S. (2005). Retinoblastoma protein regulates cell proliferation, differentiation, and endoreduplication in plants. Plant J **42,** 153-163.

Patra, D., Wang, S.X., Kumagai, A., and Dunphy, W.G. (1999). The xenopus Suc1/Cks protein promotes the phosphorylation of G(2)/M regulators. J Biol Chem **274,** 36839-36842.

Pavletich, N.P. (1999). Mechanisms of cyclin-dependent kinase regulation: structures of Cdks, their cyclin activators, and Cip and INK4 inhibitors. J Mol Biol **287,** 821-828.

Payne, C.T., Zhang, F., and Lloyd, A.M. (2000). *GL3* encodes a bHLH protein that regulates trichome development in Arabidopsis through interaction with *GL1* and *TTG1*. Genetics **156,** 1349-1362.

Peng, Z., Serino, G., and Deng, X.W. (2001a). Molecular characterization of subunit 6 of the COP9 signalosome and its role in multifaceted developmental processes in Arabidopsis. Plant Cell **13,** 2393-2407.

Peng, Z., Serino, G., and Deng, X.W. (2001b). A role of Arabidopsis COP9 signalosome in multifaceted developmental processes revealed by the characterization of its subunit 3. Development **128,** 4277-4288.

Peters, J.M. (1998). SCF and APC: the Yin and Yang of cell cycle regulated proteolysis. Curr Opin Cell Biol **10,** 759-768.

Ramirez-Parra, E., Frundt, C., and Gutierrez, C. (2003). A genome-wide identification of E2F-regulated genes in Arabidopsis. Plant J **33,** 801-811.

Ramirez-Parra, E., Xie, Q., Boniotti, M.B., and Gutierrez, C. (1999). The cloning of plant E2F, a retinoblastoma-binding protein, reveals unique and conserved features with animal G(1)/S regulators. Nucleic Acids Res **27,** 3527-3533.

Rerie, W.G., Feldmann, K.A., and Marks, M.D. (1994). The *GLABRA2* gene encodes a homeodomain protein required for normal trichome development in *Arabidopsis*. Genes Dev. **8,** 1388-1399.

Reynard, G.J., Reynolds, W., Verma, R., and Deshaies, R.J. (2000). Cks1 is required for G(1) cyclin-cyclin-dependent kinase activity in budding yeast. Mol Cell Biol **20,** 5858-5864.

Rios, G., Lossow, A., Hertel, B., Breuer, F., Schaefer, S., Broich, M., Kleinow, T., Jasik, J., Winter, J., Ferrando, A., Farras, R., Panicot, M., Henriques, R., Mariaux, J.B., Oberschall, A., Molnar, G., Berendzen, K., Shukla, V., Lafos, M., Koncz, Z., Redei, G.P., Schell, J., and Koncz, C. (2002). Rapid identification of Arabidopsis insertion mutants by non-radioactive detection of T-DNA tagged genes. Plant J **32,** 243-253.

Riou-Khamlichi, C., Huntley, R., Jacqmard, A., and Murray, J.A. (1999). Cytokinin activation of Arabidopsis cell division through a D-type cyclin. Science **283,** 1541-1544.

Riou-Khamlichi, C., Menges, M., Healy, J.M., and Murray, J.A. (2000). Sugar control of the plant cell cycle: differential regulation of Arabidopsis D-type cyclin gene expression. Mol Cell Biol **20,** 4513-4521.

Rossignol, P., Stevens, R., Perennes, C., Jasinski, S., Cella, R., Tremousaygue, D., and Bergounioux, C. (2002). AtE2F-a and AtDP-a, members of the E2F family of transcription factors, induce Arabidopsis leaf cells to re-enter S phase. Mol Genet Genomics **266,** 995-1003.

Ruiz-Medrano, R., Xoconostle-Cazares, B., and Lucas, W.J. (1999). Phloem long-distance transport of CmNACP mRNA: implications for supracellular regulation in plants. Development **126,** 4405-4419.

Rumbolz, J., Kassemeyer, H.-H., Steinmetz, V., Deising, H.B., Mendgen, K., Mathys, D., Wirtz, S., and Guggenheim, R. (1999). Differentiation of infection structures of the powdery mildew fungus Uncinula necator and adhesion to the host cuticle. Canadian Journal of Botany **78,** 409-421.

Sambrook, J., Fritsch, E., and Maniatis, T. (1989). Molecular cloning: a laboratory manual. (Cold Spring Harbor, New York: Cold Spring Harbor Laboratory Press).

Schellmann, S., Schnittger, A., Kirik, V., Wada, T., Okada, K., Beermann, A., Thumfahrt, J., Jurgens, G., and Hulskamp, M. (2002). TRIPTYCHON and CAPRICE mediate lateral inhibition during trichome and root hair patterning in Arabidopsis. Embo J **21,** 5036-5046.

Schnittger, A., and Hulskamp, M. (2002). Trichome morphogenesis: a cell-cycle perspective. Philos Trans R Soc Lond B Biol Sci **357,** 823-826.

Schnittger, A., Schobinger, U., Stierhof, Y.D., and Hulskamp, M. (2002a). Ectopic B-type cyclin expression induces mitotic cycles in endoreduplicating Arabidopsis trichomes. Curr Biol **12,** 415-420.

Schnittger, A., Weinl, C., Bouyer, D., Schobinger, U., and Hulskamp, M. (2003). Misexpression of the cyclin-dependent kinase inhibitor ICK1/KRP1 in single-celled Arabidopsis trichomes reduces endoreduplication and cell size and induces cell death. Plant Cell **15,** 303-315.

Schnittger, A., Schobinger, U., Bouyer, D., Weinl, C., Stierhof, Y.D., and Hulskamp, M. (2002b). Ectopic D-type cyclin expression induces not only DNA replication but also cell division in Arabidopsis trichomes. Proc Natl Acad Sci U S A **99,** 6410-6415.

Schwechheimer, C., and Deng, X.W. (2001). COP9 signalosome revisited: a novel mediator of protein degradation. Trends Cell Biol **11,** 420-426.

Sekine, M., Ito, M., Uemukai, K., Maeda, Y., Nakagami, H., and Shinmyo, A. (1999). Isolation and characterization of the E2F-like gene in plants. FEBS Lett **460,** 117-122.

Sessions, A., Weigel, D., and Yanofsky, M.F. (1999). The Arabidopsis thaliana MERISTEM LAYER 1 promoter specifies epidermal expression in meristems and young primordia. Plant J **20,** 259-263.

Sheaff, R.J., Groudine, M., Gordon, M., Roberts, J.M., and Clurman, B.E. (1997). Cyclin E-CDK2 is a regulator of p27Kip1. Genes Dev **11,** 1464-1478.

Sherr, C.J., and Roberts, J.M. (1999). CDK inhibitors: positive and negative regulators of G1-phase progression. Genes Dev **13,** 1501-1512.

Shimotohno, A., Umeda-Hara, C., Bisova, K., Uchimiya, H., and Umeda, M. (2004). The plant-specific kinase CDKF;1 is involved in activating phosphorylation of cyclin-dependent kinase-activating kinases in Arabidopsis. Plant Cell **16,** 2954-2966.

Shin, I., Rotty, J., Wu, F.Y., and Arteaga, C.L. (2005). Phosphorylation of p27Kip1 at Thr-157 interferes with its association with importin alpha during G1 and prevents nuclear re-entry. J Biol Chem **280,** 6055-6063.

Shteinberg, M., Protopopov, Y., Listovsky, T., Brandeis, M., and Hershko, A. (1999). Phosphorylation of the cyclosome is required for its stimulation by Fizzy/cdc20. Biochem Biophys Res Commun **260,** 193-198.

Siemering, K.R., Golbik, R., Sever, R., and Haseloff, J. (1996). Mutations that suppress the thermosensitivity of green fluorescent protein. Curr Biol **6,** 1653-1663.

Slingerland, J., and Pagano, M. (2000). Regulation of the cdk inhibitor p27 and its deregulation in cancer. J Cell Physiol **183,** 10-17.

Smith, A.V., and Orr-Weaver, T.L. (1991). The regulation of the cell cycle during Drosophila embryogenesis: the transition to polyteny. Development **112,** 997-1008.

Spruck, C., Strohmaier, H., Watson, M., Smith, A.P., Ryan, A., Krek, T.W., and Reed, S.I. (2001). A CDK-independent function of mammalian Cks1: targeting of SCF(Skp2) to the CDK inhibitor p27Kip1. Mol Cell **7,** 639-650.

Stern, B., and Nurse, P. (1996). A quantitative model for the cdc2 control of S phase and mitosis in fission yeast. Trends Genet **12,** 345-350.

Sugimoto-Shirasu, K., and Roberts, K. (2003). "Big it up": endoreduplication and cell-size control in plants. Curr Opin Plant Biol **6,** 544-553.

Sutterluty, H., Chatelain, E., Marti, A., Wirbelauer, C., Senften, M., Muller, U., and Krek, W. (1999). p45SKP2 promotes p27Kip1 degradation and induces S phase in quiescent cells. Nat Cell Biol **1,** 207-214.

Szymanski, D.B., Jilk, R.A., Pollock, S.M., and Marks, M.D. (1998). Control of GL2 expression in Arabidopsis leaves and trichomes. Development **125,** 1161-1171.

Tomoda, K., Kubota, Y., and Kato, J. (1999). Degradation of the cyclin-dependent-kinase inhibitor p27Kip1 is instigated by Jab1. Nature **398,** 160-165.

Tomoda, K., Kubota, Y., Arata, Y., Mori, S., Maeda, M., Tanaka, T., Yoshida, M., Yoneda-Kato, N., and Kato, J.Y. (2002). The cytoplasmic shuttling and subsequent degradation of p27Kip1 mediated by Jab1/CSN5 and the COP9 signalosome complex. J Biol Chem **277,** 2302-2310.

Tsvetkov, L.M., Yeh, K.H., Lee, S.J., Sun, H., and Zhang, H. (1999). p27(Kip1) ubiquitination and degradation is regulated by the SCF(Skp2) complex through phosphorylated Thr187 in p27. Curr Biol **9,** 661-664.

Vandepoele, K., Raes, J., De Veylder, L., Rouze, P., Rombauts, S., and Inze, D. (2002). Genome-wide analysis of core cell cycle genes in Arabidopsis. Plant Cell **14,** 903-916.

Verkest, A., Manes, C.L., Vercruysse, S., Maes, S., Van Der Schueren, E., Beeckman, T., Genschik, P., Kuiper, M., Inze, D., and De Veylder, L. (2005). The Cyclin-Dependent Kinase Inhibitor KRP2 Controls the Onset of the Endoreduplication Cycle during Arabidopsis Leaf Development through Inhibition of Mitotic CDKA;1 Kinase Complexes. Plant Cell.

Vidwans, S.J., DiGregorio, P.J., Shermoen, A.W., Foat, B., Iwasa, J., Yakubovich, N., and O'Farrell, P.H. (2002). Sister chromatids fail to separate during an induced endoreplication cycle in Drosophila embryos. Curr Biol **12,** 829-833.

Vlach, J., Hennecke, S., and Amati, B. (1997). Phosphorylation-dependent degradation of the cyclin-dependent kinase inhibitor p27. Embo J **16,** 5334-5344.

Vlieghe, K., Boudolf, V., Beemster, G.T., Maes, S., Magyar, Z., Atanassova, A., de Almeida Engler, J., De Groodt, R., Inze, D., and De Veylder, L. (2005). The DP-E2F-like gene DEL1 controls the endocycle in Arabidopsis thaliana. Curr Biol **15,** 59-63.

Vroemen, C.W., Mordhorst, A.P., Albrecht, C., Kwaaitaal, M.A., and de Vries, S.C. (2003). The CUP-SHAPED COTYLEDON3 gene is required for boundary and shoot meristem formation in Arabidopsis. Plant Cell **15,** 1563-1577.

Walker, J.D., Oppenheimer, D.G., Concienne, J., and Larkin, J.C. (2000). SIAMESE, a gene controlling the endoreduplication cell cycle in Arabidopsis thaliana trichomes. Development **127,** 3931-3940.

Wang, C., Hou, X., Mohapatra, S., Ma, Y., Cress, W.D., Pledger, W.J., and Chen, J. (2005). Activation of p27Kip1 Expression by E2F1. A negative feedback mechanism. J Biol Chem **280,** 12339-12343.

Wang G, K.H., Sun Y, Zhang X, Zhang W, Altman N, DePamphilis CW, Ma H. (2004). Genome-wide analysis of the cyclin family in Arabidopsis and comparative phylogenetic analysis of plant cyclin-like proteins. Plant Physiol **135,** 1084-1099.

Wang, H., Fowke, L.C., and Crosby, W.L. (1997). A plant cyclin-dependent kinase inhibitor gene. Nature **386,** 451-452.

Wang, H., Zhou, Y., Gilmer, S., Whitwill, S., and Fowke, L.C. (2000). Expression of the plant cyclin-dependent kinase inhibitor ICK1 affects cell division, plant growth and morphology. Plant J **24,** 613-623.

Wang, H., Qi, Q., Schorr, P., Cutler, A.J., Crosby, W.L., and Fowke, L.C. (1998). ICK1, a cyclin-dependent protein kinase inhibitor from Arabidopsis thaliana interacts with both Cdc2a and CycD3, and its expression is induced by abscisic acid. Plant J **15,** 501-510.

Wei, N., Chamovitz, D.A., and Deng, X.W. (1994). Arabidopsis COP9 is a component of a novel signaling complex mediating light control of development. Cell **78,** 117-124.

Weinberg, R.A. (1995). The retinoblastoma protein and cell cycle control. Cell **81,** 323-330.

Weingartner, M., Binarova, P., Drykova, D., Schweighofer, A., David, J.P., Heberle-Bors, E., Doonan, J., and Bogre, L. (2001). Dynamic recruitment of Cdc2 to specific microtubule structures during mitosis. Plant Cell **13,** 1929-1943.

Wu, K., Chen, A., and Pan, Z.Q. (2000). Conjugation of Nedd8 to CUL1 enhances the ability of the ROC1-CUL1 complex to promote ubiquitin polymerization. J Biol Chem **275,** 32317-32324.

Zachariae, W., Schwab, M., Nasmyth, K., and Seufert, W. (1998). Control of cyclin ubiquitination by CDK-regulated binding of Hct1 to the anaphase promoting complex. Science **282,** 1721-1724.

Zhou, Y., Fowke, L.C., and Wang, H. (2002). Plant CDK inhibitors: studies of interactions with cell cycle regulators in the yeast two-hybrid system and functional comparison in transgenic Arabidopsis plants. Plant Cell Rep **20,** 967-975.

Zhou, Y., Li, G., Brandizzi, F., Fowke, L.C., and Wang, H. (2003). The plant cyclin-dependent kinase inhibitor ICK1 has distinct functional domains for in vivo kinase inhibition, protein instability and nuclear localization. Plant J **35,** 476-489.

Zybina, E.V., and Zybina, T.G. (1996). Polytene chromosomes in mammalian cells. Int Rev Cytol **165,** 53-119.

#	construct	cloning / source	resistance
CK1	AtCycB1;2	trunc Cyclin B1;2 cDNA (mit 5'u.3'UTR) kloniert via Linker in pKS (EcoRI+XhoI) **Arp Schnittger**	Amp
CK2	AtCycD3;1	Cyclin D3;1 cDNA kloniert in pKS (NotI) **Arp Schnittger**	Amp
CK3	Atcdc2a-A	cdc2a cDNA (mit 170 bp 5' u. 290 bp 3' UTR) in pGEM-7Zf(-) (EcoRI) **Arp Schnittger**	Amp
CK4	Atcdc2a-D	cdc2a cDNA in pKS (EcoRV) **Daniel Bouyer**	Amp
CK5	pBinpGL2	2.2 kb GL2-Promotor in pBI101 **Arp Schnittger**	Kan
CK6	AJH1 = CSN5A	Ara.JAB Homolog 1cDNA in pKS (EcoRI) von **Claus Schwechheimer**	Amp
CK7	Red1-C1	pDsRed1-C1 **Clontech**	Kan
CK8	Red1-N1	pDsRed1-N1 **Clontech**	Kan
CK9	EYFP	pEYFP-N1 von Clontech subkloniert in pKS (XhoI+NotI) **Jaideep Mathur**	Amp
CK10	BY1	144bp PCR-Fragment in pGEM-T (template CK1; Primer B1-RFP_U u. B1-RFP_L)	Amp
CK11	BY2	CK10 (AgeI+XhoI) in CK9 (AgeI+XhoI+Cip)	Amp
CK12	BY3	CK1 (1.3kb NotI-T4+XhoI-partial)in CK11 (Acc65I-T4+XhoI+Cip)	Amp
CK13	BY4 / **pGL2:trunc-CycB1;2-YFP**	CK12 (2kb BamHI+SacI-partial) in CK5 (BamHI+SacI+Cip)	Kan
CK14	BY5	CK13 in Agros	Rif+Kan+Genta
CK15	YB1	EYFP (Bsp1407I+NotI) MunI via Linker eingeführt u. Stop eliminiert	Amp
CK16	YB2	300 bp PCR-Fragment in pKS (EcoRV) (temp CK1; Primer YFP-B1;2_U u. YFP-B1;2_L)	Amp
CK17	YB3	CK16 (0.3 kb Mva1296I+BamHI) in CK1 (Mva1296I+BamHI+Cip)	Amp
CK18	YB4	CK17 (1.4 kb Acc65I-T4+MunI) in CK15 (NotI-T4+MunI+Cip)	Amp
CK19	YB5 / **pGL2::YFP-CycB1;2**	CK18 (ca. 2kb BamHI+SacI-partial) in CK5 (BamHI+SacI+Cip)	Kan
CK20	YB6	CK19 in Agros	Rif+Kan+Genta
CK21	CR1	PCR-Fragment in pGEM-T (template CK3; Primer cdc-RFP_U u.cdc-RFP_L	Amp
CK22	CR2	CK21 (70 bp BamHI+AgeI) in CK8 (BamHI+AgeI+Cip)	Kan
CK23	CR3	CK3 (0.9 kb BamHI) in CK22 (BamHI+Cip)	Kan
CK24	CR4	CK23 (NotI) SacI via Linker (Oligo: SacI-1 u. SacI-2) eingeführt	Kan
CK25	CR5/ **pGL2::cdc2a-RFP**	CK24 (1.8 kb SacI+BamHI-partial) in CK5 (BamHI+SacI+Cip)	Kann
CK26	CR6	CK25 in Agros	Rif+Kan+Genta
CK27	AJH1-A	CK6 (BamHI-T4-religiert) BamHI eliminiert	Amp
CK28	AJH1-B	CK27 (HindIII+SalI) BamHI via Linker (Oligo: BamHI-IIa u. BamHI-IIb) eingeführt	Amp
CK29	AJH1-C/ **pGL2::CSN5A**	CK28 (1.4 kb BamHI+SacI) in CK5 (BamHI+SacI+Cip)	Kann
CK30	AJH1-D	CK29 in Agros	Rif+Kan+Genta
CK31	AtDPa	AtDPa cDNA (AJ294531) (=pDP1b) **Dirk Inze**	Amp

CK32	AtDPb	AtDPb cDNA **Dirk Inze**	Amp
CK33	AtE2Fb	AtE2Fb cDNA (AJ294533) (=pGBT-E2F3) **Dirk Inze**	Amp
CK34	AtE2Fa	AtE2Fa cDNA (AJ294534) (=pBinE2F5) **Dirk Inze**	Kan
CK35	pJawohl8RNAi	binärer RNAi Destination-Vektor im GATEWAY-System mit 35S-Promotor u. pA35S **Bekir Ülker**	Chloramp./Amp
CK36	p35SGW-Myc	binärer Myc-tag Destination Vektor im GATEWAY-System mit 35S-Promotor u.pA35S **Franziska Turck**	Chloramp./Amp
CK37	pBender	binärer Destination-Vektor im GATEWAY-System mit 35S-Promotor u. Nos-Terminator **Marc Jacoby**	Amp
CK38	pENTR4	Entry-Vektor im GATEWAY-System INVITROGEN	Kan
CK39	pDONR201	Donor-Vektor im GATEWAY-System INVITROGEN	Kan
CK40	pDONR207	Donor-Vektor im GATEWAY-System INVITROGEN	Genta
CK41	pENTR1A	Entry-Vektor im GATEWAY-System INVITROGEN	Kan
CK42	pAM-PAT-GW	binärer Destination-Vektor im GATEWAY-System mit 35S-Promotor u. pA35S **Bekir Ülker**	Chloramp./Amp
CK43	pENTR1A ohne ccdB	CK41(EcoRI) ccdB-Gen raus+religiert **Arp Schnittger**	Kan
CK44	pENTR1A	CK41(DraI+Acc65-Klenow+religiert) pENTR1A ohne DraI,XmnI,SalI,BamHI,KpnI	Kan
CK45	pART30+SdaI	pART30 von Arp Schnittger (NotI+XbaI) via Linker SdaI rein	Amp
CK46	**5'ICK1::GUS-CDB**	CK45 (SdaI+SalI) in MT79 von Michael Lenhard (SdaI+SalI+Cip) (=ICK-G1)	Kan
CK47	ICK-G1	CK46 in Agros	Rif+Kan+Genta
CK48	**5'ICK1::GUS-CDB-3'ICK1**	CK45 (SdaI+SalI) in pART 39 von Arp Schnittger (SdaI+SalI+Cip) (I=CK-G2)	Kan
CK49	ICK-G2	CK48 in Agros	Rif+Kan+Genta
CK50	pHannibal	RNAi-Vektor **Wesley et al PJ 2001**	Amp
CK51	pKannibal	RNAi-Vektor **Wesley et al PJ 2001**	Kan
CK52	pGL2 in pUC18	GL2-Promotor (2.2 kb in pUC18) **Daniel Bouyer**	Amp
CK53	**pGL2::YFP** in pBI101	CK9 (0.7kb BamHI+SacI) in CK5 (BamHI+SacI+SAP)	Kann
CK54	GL2::YFP	CK53 in Agros	Rif+Kan+Genta
CK55	Red-N-SacI	CK8 (NotI) SacI via Linker eingeführt (Oligos: SacI-1 u. SacI-2)	Kan
CK56	**pGL2::RFP** in pBI101	CK55 (0.7kb BamHI+SacI) in CK5 (BamHI+SacI+SAP)	Kann
CK57	pGL2::RFP	Ck56 in Agros	Rif+Kan+Genta
CK58	AtML1-Promotor (=pART5)	AtML1-Promotor (3.4 kb HindIII-Fragment) **Arp Schnittger**	Kan
CK59	pUC19	pUC19	Amp
CK60	pKS	pBlueskript II KS- STRATAGENE	Amp
CK61	pKS-AscI	CK60 (HindIII) AscI via Linker eingeführt	Amp
CK62	pGL2 in pKS	CK52 (2.3kb HindIII+BamHI) in CK60 (HindIII+BamHI+SAP)	Amp
CK63	AtE2Fb in pUC19-II	CK33 (EcoRI+BamHI+T4) in CK59 (SmaI+SAP)	Amp
CK64	AtE2Fb in pUC19-I	CK33 (EcoRI+BamHI+T4) in CK59 (SmaI+SAP)	Amp

CK65	AtE2Fb in pKS	CK33 (EcoRI+BamHI+T4) in pKS(SmaI+SAP)	Amp
CK66	AtE2Fa in pUC19-I	CK34 (BamHI+NcoI+T4) in CK59 (SmaI+SAP)	Amp
CK67	AtE2Fa in pUC19-II	CK34 (BamHI+NcoI+T4) in CK59 (SmaI+SAP)	Amp
CK68	**pGL2::E2Fb** in pBI101	CK63 (BamHI+SacI) in CK5 (BamHI+SacI+SAP)	Kan
CK69	pGL2::E2Fb in	CK68 in Agros	Rif+Kan+Genta
CK70	**pGL2::anti-E2Fb** in pBI101	CK64 (BamHI+SacI) in CK5 (BamHI+SacI+SAP)	Kan
CK71	pGL2::anti-E2Fb	CK70 in Agros	Rif+Kan+Genta
CK72	**pGL2::E2Fa** in pBI101	CK66 (BamHI+SacI) in CK5 (BamHI+SacI+SAP)	Kann
CK73	pGL2::E2Fa	CK72 in Agros	Rif+Kan+Genta
CK74	**pGL2::antiE2Fa** in pBI101	CK67 (BamHI+SacI) in CK5 (BamHI+SacI+SAP)	Kan
CK75	pGL2::antiE2Fa	CK74 in Agros	Rif+Kan+Genta
CK76	pGL2 in pUC18 +AscI	CK52 (HindIII) AscI via Linker eingeführt	Amp
CK77	pGL2 in pUC18+AscI+XhoI	CK76 (BamHI+Acc65I) XhoI via Linker eingeführt	Amp
CK78	AtCycB1;1 (=pCYC1At)	AtCycB1;1 cDNA in pGEM-T **Arp Schnittger**	Amp
CK79	AtICK1 (=AtKRP1)	AtICK1 cDNA **Arp Schnittger**	
CK80	AtGL2	AtGL2 cDNA	
CK81	anti-cdc2a in pENTR1A	CK3 (EcoRI) in CK41(EcoRI+SAP) antisense Orientierung von cdc2a	Kan
CK82	pGL2 in pKS + EcoRI	CK62 (XhoI+Acc65I) EcoRI via Linker eingeführt	Amp
CK83	B1;1 in pENTR1A	CK78 (SalI+BamHI) in CK43 (SalI+BamHI+SAP)	Kan
CK84	B1;2 in pENTR1A	CK1 (BamHI+Acc65I) in CK43 (BamHI+Acc65I+SAP)	Kan
CK85	pGL2-JawohI8RNAi	CK77(AscI+XhoI) in CK35 (AscI+XhoI+SAP)	Chloramp./Amp
CK86	pGL2-pAM-PAT-GW	CK77(AscI+XhoI) in CK42 (AscI+XhoI+SAP)	Chloramp./Amp
CK87	**pGL2::(anti)cdc2a-RNAi**	**KLON FALSCH weiterarbeiten mit KLON CK226** CK81 via LR Reaktion in CK85	Amp
CK88	**pGL2::CycB1;2-RNAi**	CK84 via LR-Reaktion in CK85	Amp
CK89	**pGL2::CycB1;1-RNAi**	CK83 via LR-Reaktion in CK85	Amp
CK90	binärer Vektor für pHannibal	binärer Vektor für pHannibal und pKannibal **Weley et al PJ 2001**	
CK91	anti-cdc2a in pENTR1A	**KLON VERLOREN** CK3 (EcoRI) in CK44(EcoRI+SAP) antisense Orientierung von cdc2a	Kan
CK92	pGEJAE-3D1	cdc2a-Antikörperfragment **Geert de Jaeger**	Amp
CK93	pGEJAE-3D2	cdc2a-Antikörperfragment **Geert de Jaeger**	Amp
CK94	pGEJAE-3D10	cdc2a-Antikörperfragment **Geert de Jaeger**	Amp
CK95	pGEJAE-3D25	cdc2a-Antikörperfragment **Geert de Jaeger**	Amp
CK96	pGEJAE-4D21	cdc2a-Antikörperfragment **Geert de Jaeger**	Amp
CK97	pGEJAE-4D47	cdc2a-Antikörperfragment **Geert de Jaeger**	Amp

CK98	pG4ER	scFV-G4... **Geert de Jaeger**	Amp
CK99	pWUS-BD-35S-(-60)Mini	4xWUS-BD-35S-(-60)Mini-Promotor::GUS-NLS in pKS von **Michael Lenhard**	Amp
CK100	ICK1-YFP in pGEMT	Fusion mit PCR Methode (siehe Primer-Liste u. Laborbuch S. I-138f, II-44 und Uli S III-92) 1293 bp in pGEMT	Amp
CK101	ICK1_108-YFP in pGEMT	Fusion mit PCR Methode (siehe Primer-Liste u. Laborbuch S. I-138f, II-44 und Uli S III-92) 1044 bp in pGEMT	Amp
CK102	ICK1_109-YFP in pGEMT	Fusion mit PCR Methode (siehe Primer-Liste u. Laborbuch S. I-138f, II-44 und Uli S III-92) 972 bp in pGEMT	Amp
CK103	YFP-ICK1 in pGEMT	Fusion mit PCR Methode (siehe Primer-Liste u. Laborbuch S. I-138f, II-44 und Uli S III-92) 1293 bp in pGEMT	Amp
CK104	YFP-ICK1_108 in pGEMT	Fusion mit PCR Methode (siehe Primer-Liste u. Laborbuch S. I-138f, II-44 und Uli S III-92) 1044 bp in pGEMT	Amp
CK105	YFP-ICK1_109 in pGEMT	Fusion mit PCR Methode (siehe Primer-Liste u. Laborbuch S. I-138f, II-44 und Uli S III-92) 969 bp in pGEMT	Amp
CK106	GL2::anti-cdc2a-RNAi	CK87 in Agros	Carb/Rif/Kann
CK107	GL2::CycB1;1-RNAi	CK89 in Agros	Carb/Rif/Kann
CK108	GL2::CycB1;2-RNAi	CK88 in Agros	Carb/Rif/Kann
CK109	pWUS-BD in pGEMT	trichomspezifischer Promotor (CK99 via PCR mit Primer WUS_DB_S+WUS_DB_AS ampl. u. seq.) in pGEMT	Amp
CK110	pWUS-BD-Jawohl8-RNAi	CK109 (AscI+XhoI) in CK 35 (AscI+XhoI+SAP)	Chloramp./Amp
CK111	pWUS-BD-pAM-PAT-GW	CK109 (AscI+XhoI) in CK 42 (AscI+XhoI+SAP)	Chloramp./Amp
CK112	AtKRP4	AtKRP4 cDNA in pGEMT **Dirk Inze**	Amp
CK113	AtWEE1	AtWEE1 cDNA in pDONR 207 **Dirk Inze**	Genta
CK114	AtRBR1	AtRBR1 cDNA in pCAMBIA (=pCATRBR3473-S) **Wilhelm Gruissem**	Kan
CK115	AtRBR1-RNAi	AtRBR1 RNAi Konstrukt in pCAMBIA (=PCARi-323) **Wilhelm Gruissem**	Kan
CK116	pKS+BstEII	pKS (ApaI+XhoI) und BstEII via Linker (Oligo:BstEII_1+ BstEII_2) eingeführt	Amp
CK117	AtRBR1 in pKS	CK114 (ApaI+BstEII) in CK116 (ApaI+BstEII+SAP)	Amp
CK118	AtRBR1 in pENTR1A	CK117 (Acc65I+XhoI) in CK41 (Acc65I+XhoI+SAP)	Kan
CK119	ICK1 cDNA = pART29	ICK1 cDNA in pKS =pART29 **Arp Schnittger**	Amp
CK120	ICK1-108_ I in pGEMT	ICK1-108 I in pGEMT (PCR mit Hifi temp. ICK1 Primer ICK_108_S u. AS)	Amp
CK121	ICK1-108_ II in pGEMT	ICK1-108 II in pGEMT (PCR mit Hifi temp. ICK1 Primer ICK_108_S (BamHI)u. AS (SacI))	Amp
CK123	CK119 EcoRI+EcoO109I relig.	CK119 (EcoRI+EcoO109I+blunt+relig.)	Amp
CK124	ICK1 in pENTR1A	CK123 (Acc65I+NotI) in CK41 (Acc65I+NotI+SAP)	Kan
CK125	AtKRP4 in pENTR1A	CK112 (BamHI) in CK43 (BamHI+SAP)	Kan
CK126	KRP-cons in pDONR201	141 bp KRP-cons-Frag. via BP in pDONR201 (PCR mit Hifi-Pol template CK112 u. Primer KRP-RNAiS+AS)	Kan
CK127	**pGL2::AtWEE1**	CK113 via LR Reaktion in CK86	Amp
CK128	**pGL2::AtWEE1-RNAi**	CK113 via LR Reaktion in CK85	Amp
CK129	GL2::B1;2-RNAi	CK88 in Agros	Carb/Rif/Kann
CK130	pGL2::CycB1;1-RNAi	CK89 in Agros	Carb/Rif/Kann
CK131	antiKRP4 in pENTR1A	CK112 (BamHI) in CK43 (BamHI+SAP)	Kan

CK132	**pGL2::KRP4**	CK125 via LR Reaktion in pGL2-pAM-PAT (CK86)	Amp
CK133	**pGL2::KRP4-RNAi**	CK125 via LR Reaktion in pGL2-JawohI8-RNAi (CK85)	Amp
CK134	**pGL2::AtRBR1**	CK118 via LR-Reaktion in pGL2-pAM-PAT (CK86)	Amp
CK135	**pGL2::AtRBR1-RNAi**	CK118 via LR-Reaktion in pGL2-JawohI8-RNAi (CK85)	Amp
CK136	**AtKRP4::GUS**	pGSV4.KRP4GUS **Dirk Inze**	Strep50+Spec50
CK137	AtDEL1	DP-E2F-Like1 cDNA in ...**CROP DESIGN**	
CK138	AtDEL3	DP-E2F-Like2 cDNA in ... **CROP DESIGN**	
CK139	**pGL2::KRP1-RNAi**	CK124 via LR Reaktion in CK85	Amp
CK140	**pGL2::KRP1**	CK124 via LR Reaktion in CK86	Amp
CK141	pGL2::AtWEE1	CK127 in Agros	Carb/Rif/Kann
CK142	pGL2::AtWEE1-RNAi	CK128 in Agros	Carb/Rif/Kann
CK143	pGL2::KRP4	CK132 in Agros	Carb/Rif/Kann
CK144	pGL2::KRP4-RNAi	CK133 in Agros	Carb/Rif/Kann
CK145	pGL2::KRP1-RNAi	CK139 in Agros	Carb/Rif/Kann
CK146	KRP-cons in pGEM-T	141 bp KRP-cons-Frag. in pGEM-T (PCR mit Hifi-Pol template CK112 u. Primer KRP-RNAiS+AS)	Amp
CK147	**pGL2::KRPcons-RNAi**	CK126 via LR in pGL2-JawohI8-RNAi (CK85)	Amp /Carb+Rif+Kann
CK148	pGL2::KRP1	CK140 in Agros	Carb/Rif/Kann
CK149	AtE2F3 in pENTR1A	CK63 (BamHI+Acc65I) in pENTR1A-ccdB (BamHI+Acc65I+SAP)	Kan
CK150	**pGL2::AtE2F3-RNAi**	CK149 via LR-Reaktion in pGL2-JawohI8-RNAi (CK85)	Amp /Carb+Rif+Kann
CK151	AtE2F5 in pENTR1A	CK66 (BamHI+Acc65I) in pENTR1A-ccdB (BamHI+Acc65I+SAP)	Kan
CK152	**pGL2::AtE2F5-RNAi**	CK 151 via LR-Reaktion in pGL2-JawohI8-RNAi (CK85)	Amp /Carb+Rif+Kann
CK153	AtDPa in pENTR1A	CK31 (EcoRI) in pENTR1A (EcoRI+SAP)	Kan
CK154	**pGL2::AtDPa-RNAi**	CK153 via LR-Reaktion in pGL2-JawohI8-RNAi (CK85)	Amp /Carb+Rif+Kann
CK155	AtDPb in pENTR1A	CK32 (EcoRI) in pENTR1A (EcoRI+SAP)	Kan
CK156	**pGL2::AtDPb-RNAi**	CK155 via LR-Reaktion in pGL2-JawohI8-RNAi (CK85)	Amp /Carb+Rif+Kann
CK157	antiDPb in pENTR1A	CK32 (EcoRI) in pENTR1A (EcoRI+SAP)	Kan
CK158	pGL2::DPa	GL2::DPa in Agros **Ulrike Schöbinger**	Rif+Kan+Genta
CK159	pGL2::anti-DPa	GL2::anti-DPa in Agros **Ulrike Schöbinger**	Rif+Kan+Genta
CK160	pGL2::DPb	GL2::DPb in Agros **Ulrike Schöbinger**	Rif+Kan+Genta
CK161	pGL2::anti-DPb	GL2::anti-DPb in Agros **Ulrike Schöbinger**	Rif+Kan+Genta
CK162	**p35S::Histon2B-YFP**	35S::Histon-2B-YFP **Fred Berger**	Kann
CK163	p35S::Histon2B-YFP	35S::Histon-2B-YFP in Agros	Rif+Kan+Genta
CK164	**pGL2::DPa**	DPa (CK31) (BcuI+Cfr42I gebluntet) in pBinGL2 (CK5) (SmaI+Ecl136II+SAP) **Ulrike Schöbinger**	Kan

CK165	**pGL2::anti-DPa**	DPa (CK31) (BcuI+Cfr42I gebluntet) in pBinGL2 (CK5) (SmaI+Ecl136II+SAP) **Ulrike Schöbinger**	Kan
CK166	**pGL2::DPb**	DPb (CK32) (EcoRI gebluntet) in pBinGL2 (CK5) (SmaI+Ecl136II+SAP) **Ulrike Schöbinger**	Kann
CK167	**pGL2::anti-DPb**	DPb (CK32) (EcoRI gebluntet) in pBinGL2 (CK5) (SmaI+Ecl136II+SAP) **Ulrike Schöbinger**	Kann
CK168	N-KRP1-RNAi in pDONR201	ca.200bp PCR Fragment (KRP1_RNAi_S+KRP1_RNAi_AS) temp.CK124 in pDONR201 via BP Reaktion	Kan
CK169	N-KRP4-RNAi in pDONR201	ca.223bp PCR Fragment (KRP4_RNAi_S+AS) temp.CK112 in pDONR201 via BP Reaktion	Kan
CK170	pGEJAE-3D1-Stop in pENTR1A	**CK92 ( ) in pENTR1A ( ) ohne Stop Xiaoguo Zhang**	Kan
CK171	pGEJAE-3D2-Stop in pENTR1A	**CK93 ( ) in pENTR1A ( ) ohne Stop Xiaoguo Zhang**	Kan
CK172	pGEJAE-3D10-Stop in pENTR1A	**CK94 ( ) in pENTR1A ( ) ohne Stop Xiaoguo Zhang**	Kan
CK173	pGEJAE-3D25-Stop in pENTR1A	**CK95 ( ) in pENTR1A ( ) ohne Stop Xiaoguo Zhang**	Kan
CK174	pGEJAE-4D21-Stop in pENTR1A	**CK96 ( ) in pENTR1A ( ) ohne Stop Xiaoguo Zhang**	Kan
CK175	pGEJAE-4D47-Stop in pENTR1A	**CK97 ( ) in pENTR1A ( ) ohne Stop Xiaoguo Zhang**	Kan
CK176	pG4ER-Stop in pENTR1A	**CK98 ( ) in pENTR1A ( ) ohne Stop Xiaoguo Zhang**	Kan
CK177	**pGL2::pGEJAE-3D1-Stop**	CK170 via LR Reaktion in CK86 (pGL2-pAM-PAT) STOP fehlt geeignet für Fusionen **Xiaoguo Zhang**	Amp /Carb+Rif+Kann
CK178	**pGL2::pGEJAE-3D2-Stop**	CK171 via LR Reaktion in CK86 (pGL2-pAM-PAT) STOP fehlt geeignet für Fusionen **Xiaoguo Zhang**	Amp /Carb+Rif+Kann
CK179	**pGL2::pGEJAE-3D10-Stop**	CK172 via LR Reaktion in CK86 (pGL2-pAM-PAT) STOP fehlt geeignet für Fusionen **Xiaoguo Zhang**	Amp /Carb+Rif+Kann
CK180	**pGL2::pGEJAE-3D25-Stop**	CK173 via LR Reaktion in CK86 (pGL2-pAM-PAT) STOP fehlt geeignet für Fusionen **Xiaoguo Zhang**	Amp /Carb+Rif+Kann
CK181	**pGL2::pGEJAE-4D21-Stop**	CK174 via LR Reaktion in CK86 (pGL2-pAM-PAT) STOP fehlt geeignet für Fusionen **Xiaoguo Zhang**	Amp /Carb+Rif+Kann
CK182	**pGL2::pGEJAE-4D47-Stop**	CK175 via LR Reaktion in CK86 (pGL2-pAM-PAT) STOP fehlt geeignet für Fusionen **Xiaoguo Zhang**	Amp /Carb+Rif+Kann
CK183	**pGL2::pG4ER-Stop**	CK176 via LR Reaktion in CK86 (pGL2-pAM-PAT) STOP fehlt geeignet für Fusionen **Xiaoguo Zhang**	Amp /Carb+Rif+Kann
CK184	pGEJAE-3D1-MYC in pENTR1A	**CK92 ( ) in pENTR1A ( ) Xiaoguo Zhang**	Kan
CK185	pGEJAE-3D2-MYC in pENTR1A	**CK93 ( ) in pENTR1A ( ) Xiaoguo Zhang**	Kan
CK186	pGEJAE-3D10-MYC in pENTR1A	**CK94 ( ) in pENTR1A ( ) Xiaoguo Zhang**	Kan
CK187	pGEJAE-3D25-MYC in pENTR1A	**CK95 ( ) in pENTR1A ( ) Xiaoguo Zhang**	Kan
CK188	pGEJAE-4D21-MYC in pENTR1A	**CK96 ( ) in pENTR1A ( ) Xiaoguo Zhang**	Kan
CK189	pGEJAE-4D47-MYC in pENTR1A	**CK97 ( ) in pENTR1A ( ) Xiaoguo Zhang**	Kan
CK190	pG4ER-MYC in pENTR1A	**CK98 ( ) in pENTR1A ( ) Xiaoguo Zhang**	Kan
CK191	**pGL2::pGEJAE-3D1-MYC**	**CK184 via LR Reaktion in CK86 Xiaoguo Zhang**	Amp /Carb+Rif+Kann
CK192	**pGL2::pGEJAE-3D2-MYC**	**CK185 via LR Reaktion in CK86 Xiaoguo Zhang**	Amp /Carb+Rif+Kann
CK193	**pGL2::pGEJAE-3D10-MYC**	**CK186 via LR Reaktion in CK86 Xiaoguo Zhang**	Amp /Carb+Rif+Kann
CK194	**pGL2::pGEJAE-3D25-MYC**	**CK187 via LR Reaktion in CK86 Xiaoguo Zhang**	Amp /Carb+Rif+Kann
CK195	**pGL2::pGEJAE-4D21-MYC**	**CK188 via LR Reaktion in CK86 Xiaoguo Zhang**	Amp /Carb+Rif+Kann
CK196	**pGL2::pGEJAE-4D47-MYC**	**CK189 via LR Reaktion in CK86 Xiaoguo Zhang**	Amp /Carb+Rif+Kann
CK197	**pGL2::pG4ER-MYC**	**CK190 via LR Reaktion in CK86 Xiaoguo Zhang**	Amp /Carb+Rif+Kann

CK198	**pGL2::N-KRP1-RNAi**	CK168 via LR Reaktion in CK85	Amp /Carb+Rif+Kann
CK199	**pGL2::N-KRP4-RNAi**	CK169 via LR Reaktion in CK85	Amp /Carb+Rif+Kann
CK200	KRP1_109 in pDONR201	PCR-Frag. via BP in pDONR201 (template CK79; Primer ICK1_109-S und ICK1_109-AS, Hifi-Polymerase)	Kan
CK201	**pGL2::DPa**	CK153 via LR-Reaktion in pGL2-pAM-PAT (CK86)	Amp /Carb+Rif+Kann
CK202	**pGL2::DPb**	CK155 via LR-Reaktion in pGL2-pAM-PAT (CK86)	Amp /Carb+Rif+Kann
CK203	**pGL2::E2Fb**	CK149 via LR-Reaktion in pGL2-pAM-PAT (CK86)	Amp /Carb+Rif+Kann
CK204	**pGL2::E2Fa**	CK151 via LR-Reaktion in pGL2-pAM-PAT (CK86)	Amp /Carb+Rif+Kann
CK205	pENTR1A-ccdB +SacI	pENTR1A-ccdB (CK43) (BamHI+Acc65I) und SacI-Linker (SacI_U+SacI_L) eingeführt	Kan
CK206	KRP1-YFP in pENTR1A	CK100 (BamHI+SacI) in CK205 (BamHI+SacI+SAP)	Kan
CK207	KRP1_108-YFP in pENTR1A	CK101 (BamHI+SacI) in CK205 (BamHI+SacI+SAP)	Kan
CK208	KRP1_109-YFP in pENTR1A	CK102 (BamHI+SacI) in CK205 (BamHI+SacI+SAP)	Kan
CK209	YFP-KRP1 in pENTR1A	CK103 (BamHI+SacI) in CK205 (BamHI+SacI+SAP)	Kan
CK210	YFP-KRP1_108 in pENTR1A	CK104 (BamHI+SacI) in CK205 (BamHI+SacI+SAP)	Kan
CK211	YFP-KRP1_109 in pENTR1A	CK105 (BamHI+SacI) in CK205 (BamHI+SacI+SAP)	Kan
CK212	cdc2a in pENTR1A	CK3 (XhoI+SacI) in CK205 (SalI+SacI+SAP)	Kan
CK213	**pGL2:KRP1_109**	CK200 via LR Reaktion in CK86 (pGL2-pAM-PAT)	Amp /Carb+Rif+Kann
CK214	**pWUS-BD::KRP1_109**	CK200 via LR Reaktion in CK111 (pWUS-BD::pAM-PAT)	Amp /Carb+Rif+Kann
CK215	**pWUS-BD::E2Fb**	CK149 via LR-Reaktion in pWUS-BD-pAM-PAT (CK111)	Amp /Carb+Rif+Kann
CK216	**pWUS-BD::E2Fa**	CK151 via LR-Reaktion in pWUS-BD-pAM-PAT (CK111)	Amp /Carb+Rif+Kann
CK217	AtCycD4	AtCycD4 cDNA **Arp Schnittger**	
CK218	AtCKS	AtCKS cDNA in pGEM **Arp Schnittger**	Amp
CK219	**pGL2::KRP1-YFP**	CK206 via LR Reaktion in CK86 (pGL2-pAM-PAT)	Amp /Carb+Rif+Kann
CK220	**pGL2::KRP1_108-YFP**	CK207 via LR Reaktion in CK86 (pGL2-pAM-PAT)	Amp /Carb+Rif+Kann
CK221	**pGL2::KRP1_109-YFP**	CK208 via LR Reaktion in CK86 (pGL2-pAM-PAT)	Amp /Carb+Rif+Kann
CK222	**pGL2::YFP-KRP1**	CK209 via LR Reaktion in CK86 (pGL2-pAM-PAT)	Amp /Carb+Rif+Kann
CK223	**pGL2::YFP-KRP1_108**	CK210 via LR Reaktion in CK86 (pGL2-pAM-PAT)	Amp /Carb+Rif+Kann
CK224	**pGL2::YFP-KRP1_109**	CK211 via LR Reaktion in CK86 (pGL2-pAM-PAT)	Amp /Carb+Rif+Kann
CK225	cdc2a in pDONR201	PCR-Frag. via BP in pDONR201 (template CK3; Primer GRR-S und GRRR-AS, Pfu-Polymerase) PRAKTIKUM	Kan
CK226	**pGL2::cdc2a-RNAi**	CK225 old (mit 2 Seq. Fehlern, deshalb noch mal neues CK225 mit Pfu gemacht) via LR Reaktion in CK85	Amp /Carb+Rif+Kann
CK227	**pGL2::CycB1;2**	CK84 via LR-Reaktion in CK86	Amp /Carb+Rif+Kann
CK228	GUS in pENTR1A	GUS cDNA in pENTR von **Bekir Uelker...**	Kan
CK229	pTMM-pAM-PAT-GW	TMM-Promotor in pAM-PAT-GW (via AscI und XhoI) **Xiaoguo Zhang**	Chloramp./Amp
CK230	**pGL2::GUS**	CK228 via LR Reaktion in CK86	Amp /Carb+Rif+Kann

CK231	**pWUS-BD::GUS**	CK228 via LR Reaktion in CK111	Amp /Carb+Rif+Kann
CK232	**pTMM::GUS**	CK228 via LR Reaktion in CK229	Amp /Carb+Rif+Kann
CK233	**pGL2::KRP1 ohne attL1-site**	CK140 Acc65I+XhoI/partial+ T4 religiert	Amp /Carb+Rif+Kann
CK234	**pGL2::CycB1;2 ohne attL1-site**	CK227 PstI+XhoI/partial+ T4 religiert	Amp /Carb+Rif+Kann
CK235	cdc2a in pDONR201	PCR-Frag. via BP in pDONR201 (template CK3; Primer GRR-S und GRRR-AS, Pfu-Polymerase)	Kan
CK236	**pGL2::AtDEL3**	**Xiaoguo Zhang**	Amp /Carb+Rif+Kann
CK237	pART30+AscI	pART30 (2.6kb 5'genomisch von KRP1) von Arp Schnittger (NotI+BamHI) via Linker AscI rein	Amp
CK238	pKRP1-pAM-PAT	CK 237 (AscI+SalI) in pGL2-pAM-PAT (AscI+XhoI+SAP)	Amp
CK239	HA-mKRP2 (N186A)	pRep42 HA-KRP2 N186A **Lieven de Veylder**	Amp
CK240	HA-mKRP2 (D188A)	pRep42 HA-KRP2 D188A **Lieven de Veylder**	Amp
CK241	HA-mKRP2 (N186A/D188A))	pRep42 HA-KRP2 N186A+D188A **Lieven de Veylder**	Amp
CK242	KRP-interactor 1	At5g03660 (unknown protein) BC004 in pDONR201 **Lieven de Veylder**	Kan
CK243	KRP-interactor 2	At2g28520 (putative vacuolar proton ATPase subunit) BC23 in pDONR201 **Lieven de Veylder**	Kan
CK244	KRP-interactor 3	At4g19700 (ring-finger protein) BC78 in pDONR201 **Lieven de Veylder**	Kan
CK245	KRP-interactor 4	At5g01370 (unknown protein) BC112 in pDONR201 **Lieven de Veylder**	Kan
CK246	pCPC-pAM-PAT	pCPC in pAM-PAT (AscI+XhoI) **Martina Pesch**	Chloramp./Amp
CK247	pTRY-pAM-PAT	pTRY in pAM-PAT (AscI+XhoI) **Martina Pesch**	Chloramp./Amp
CK248	**pCPC::CycB1;2**	CK84 via LR in CK246	Amp /Carb+Rif+Kann
CK249	**pCPC::KRP1**	CK124 via LR in CK246	Amp /Carb+Rif+Kann
CK250	**pCPC::KRP4**	CK125 via LR in CK246	Amp /Carb+Rif+Kann
CK251	**pTRY::CycB1;2**	CK84 via LR in CK247	Amp /Carb+Rif+Kann
CK252	**pTRY::KRP1**	CK124 via LR in CK247	Amp /Carb+Rif+Kann
CK253	**pTRY::KRP4**	CK125 via LR in CK247	Amp /Carb+Rif+Kann
CK254	pKRP1-pLEELA	CK237 (AscI+SalI) in pLEELA (AscI+XhoI+SAP) CK262	Chloramp./Amp
CK255	KRP1_108 in pENTR1A	CK121 (BamHI+SacI) in CK205 (BamHI+SacI+SAP)	Kan
CK256	pUAS-pAM-PAT	UAS mit MinimalPromotor via AscI+XhoI in pAM-PAT **Martina Pesch**	Chloramp./Amp
CK257	pUAS-JawohI-RNAi	UAS mit MinimalPromotor via AscI+XhoI in pJawohI-RNAi **Martina Pesch**	Chloramp./Amp
CK258	**pUAS::KRP1**	CK124 via LR Reaktion in CK256	Amp /Carb+Rif+Kann
CK259	**pUAS::KRP1_109**	CK200 via LR Reaktion in CK256	Amp /Carb+Rif+Kann
CK260	**pUAS::RBR1**	CK118 via LR Reaktion in CK256	Amp /Carb+Rif+Kann
CK261	**pUAS::RBR1-RNAi**	CK118 via LR Reaktion in CK257	Amp /Carb+Rif+Kann
CK262	pLeeL a	binäre Destination-Vektor im GATEWAY-System mit 2x35S-Promotor +Intron u. pA35S **Marc Jakoby**	Chloramp./Amp
CK263	**p2x35S::KRP1_109**	CK200 via LR Reaktion in CK262	Amp /Carb+Rif+Kann

CK264	**pCPC::E2Fb**	CK149 via LR Reation in CK 246	Amp /Carb+Rif+Kann
CK265	**pTRY::E2Fb**	CK149 via LR Reation in CK 247	Amp /Carb+Rif+Kann
CK266	**pCPC::E2Fa**	CK151 via LR Reation in CK 246	Amp /Carb+Rif+Kann
CK267	**pTRY::E2Fa**	CK151 via LR Reation in CK 247	Amp /Carb+Rif+Kann
CK268	**pCPC::RBR1**	CK118 via LR Reation in CK 246	Amp /Carb+Rif+Kann
CK269	**pTRY::RBR1**	CK118 via LR Reation in CK 247	Amp /Carb+Rif+Kann
CK270	**p2x35S::RBR1**	CK118 via LR Reation in CK 262	Amp /Carb+Rif+Kann
CK271	pGL2-LeeLa	CK77 (AscI+XhoI) in CK262 (AscI+XhoI+SAP) **Stefan** (Klon PL1)	Chloramp./Amp
CK272	**pGL2::E2Fb-LeeLa**	CK149 via LR-Reaktion in CK271	Amp /Carb+Rif+Kann
CK273	**pGL2::E2Fa-LeeLa**	CK151 via LR-Reaktion in CK271	Amp /Carb+Rif+Kann
CK274	AtE2Fc in pDONR221	E2Fc cDNA in DONR221 von **Lieven de Veylder**	Kan
CK275	HA-AtKRP2-fl	pREP42 HA-N-KRP2-FL **Lieven de Veylder**	Amp
CK276	HA-KRP2-1_110	pREP42 HA-N-KRP2-1_110 **Lieven de Veylder**	Amp
CK277	HA-KRP2-110_190	pREP42 HA-N-KRP2-110_190 **Lieven de Veylder**	Amp
CK278	HA-KRP2-110_209	pREP42 HA-N-KRP2-110_209 **Lieven de Veylder**	Amp
CK279	HA-KRP2-170_209	pREP42 HA-N-KRP2-170_209 **Lieven de Veylder**	Amp
CK280	**p35S::mGFP5-ER**	p35S::mGFP5-ER in binären Vektor(welcher?) **Daniel Bouyer** (wer hats gemacht??)	Kan
CK281	**pGL2::KRP-Interactor_1**	CK242 via LR Reaktion in CK86	Amp /Carb+Rif+Kann
CK282	**pGL2::KRP-Interactor_2**	CK243 via LR Reaktion in CK86	Amp /Carb+Rif+Kann
CK283	**pGL2::KRP-Interactor_3**	CK244 via LR Reaktion in CK86	Amp /Carb+Rif+Kann
CK284	**pGL2::KRP-Interactor_4**	CK245 via LR Reaktion in CK86	Amp /Carb+Rif+Kann
CK285	**pGL2::E2Fc**	CK274 via LR Reaktion in CK86	Amp /Carb+Rif+Kann
CK286	**pGL2::GUS LeeLa**	CK228 via LR Reaktion in CK271	Amp /Carb+Rif+Kann
CK287	**pGL2::CycB1;2 LeeLa**	CK84 via LR Reaktion in CK271	Amp /Carb+Rif+Kann
CK288	**pGL2::KRP1 LeeLa**	CK124 via LR Reaktion in CK271	Amp /Carb+Rif+Kann
CK289	human p21	HA-tagged Hsp21 cDNA in pCruz **Ludger Hengst**	Kan
CK290	human p27	HA-tagged Hsp27 cDNA in pCruz **Ludger Hengst**	Kan
CK291	**pCPC::E2Fc**	CK274 via LR Reaktion in CK246	Amp /Carb+Rif+Kann
CK292	**pTRY::E2Fc**	CK274 via LR Reaktion in CK247	Amp /Carb+Rif+Kann
CK293	**pCPC::KRP1_109**	CK200 via LR Reaktion in CK246	Amp /Carb+Rif+Kann
CK294	**pTRY::KRP1_109**	CK200 via LR Reaktion in CK247	Amp /Carb+Rif+Kann
CK295	AJH1 in pDONR201	PCR-Frag. via BP in pDONR201 (template CK6; Primer AJH1-S undAJH1-AS, hifi-Polymerase)	kan
CK296	**pTMM::KRP1_109**	CK200 via LR Reaktion in pTMM-pAM-PAT	Amp /Carb+Rif+Kann

CK297	KRP1_152 in pDONR		
CK298	**pUAS::KRP1_152**	CK297 via LR Reaktion in CK256	
CK299	E2Fb in pDONR201	E2Fb cDNA via PCR (Primer E2F3_S+E2F3_AS, template CK33, hifi) u. via BP Reaktion in pDONR201	Kan
CK300	**pGL2::PCR-E2Fb**	CK299 via LR Reaktion in CK86	Amp /Carb+Rif+Kann
CK301	E2Fa in pDONR201	E2Fa cDNA via PCR (Primer E2F5_S+E2F5_AS, template CK34) u. via BP Reaktion in pDONR201	Kan
CK302	**pGL2::PCR-E2Fa**	CK301 via LR Reaktion in CK86	Amp /Carb+Rif+Kann
CK303	KRP1 in pDONR	KRP1 cDNA via PCR (P1 ICK-Myc_S+Myc-ICK_AS, templat CK119, hifi) und BP Reaktion in pDONR201	Kan
CK304	**pGL2::KRP1-PCR-pAM-PAT**	CK303 via LR Reaktion in pGL2-pAM-PAT CK86	Amp /Carb+Rif+Kann
CK305	KRP1_108 in pDONR	KRP1_108 via PCR (Primer ICK-Myc_S + Myc-ICK_108_AS, templat CK119, hifi) und BP in pDONR201	Kan
CK306	**pGL2::KRP1_108-pAM-PAT**	CK305 via LR Reaktion in pGL2-pAM-PAT CK86	Amp /Carb+Rif+Kann
CK307	**pTMM::KRP1_109-YFP**	CK208 via LR Reaktion in pTMM-pAM-PAT	Amp /Carb+Rif+Kann
CK308	**pTMM::YFP-KRP1_109**	CK211 via LR Reaktion in pTMM-pAM-PAT	Amp /Carb+Rif+Kann
CK309	YFP in pDONR	YFP cDNA in pDONR201 (Primer YFP_S +YFP_AS template CK9, hifi)	Kan
CK310	**pTMM::YFP**	CK309 via LR Reaktion in pTMM-pAM-PAT	Amp /Carb+Rif+Kann
CK311	**pGL2::AJH1**	CK295 via LR Reaktion in pGL2-pAM-PAT (CK86)	Amp /Carb+Rif+Kann
CK312	**pGL2:KRP1_109 BIN**	**Daniel Bouyer**	Amp /Carb+Rif+Kann
CK313	**p2x35S:YFP:KRP1 LeeLa**	CK209 via LR Reaktion in pLeeLa CK262	Amp /Carb+Rif+Kann
CK314	**p2x35S:KRP1_109:YFP LeeLa**	CK208 via LR Reaktion in pLeeLa CK262	Amp /Carb+Rif+Kann
CK315	**p2x35S:YFP:KRP1_109 LeeLa**	CK211 via LR Reaktion in pLeeLa CK262	Amp /Carb+Rif+Kann
CK316	**KRP1 für Y-2-Hybrid**	KRP1 (in-frame) in pDONR (**Stefan Pusch**) via LR in pB42D-GWY (**Marc Jakoby**) für Y-2-Hybrid	Amp
CK317	**KRP1_109 für Y-2-Hybrid**	KRP1_109 (in-frame) in pDONR (**Stefan Pusch**) via LR in pB42D-GWY (**Marc Jakoby**) für Y-2-Hybrid	Amp
CK318	**pTMM:YFP:KRP1**	CK209 via LR in pTMM-pAM-PAT CK229 siehe CK337	
CK319	**pXCSG-3xHA**	p2x35S-C-terminal 3xHA-tag Gateway von **Laurent Noel** (LN139) AG Parker	Chloramp./Amp
CK320	**pXCSG-6xmyc**	p2x35S-C-terminal 6xmyc-tag Gateway von **Laurent Noel** (LN172) AG Parker	Chloramp./Amp
CK321	**pJ2B-3xHA**	p2x35S-N-terminal 3xHA-tag Gateway von **Nieves Medina-Escobar** (NME48) AG Parker	Chloramp./Amp
CK322	**pJ2B-6xmyc**	p2x35S-N-terminal 6xmyc-tag Gateway von **Nieves Medina-Escobar** (NME48) AG Parker	Chloramp./Amp
CK323	**p35S:CycB1;2:CFP**	CK351 via LR in CK329	Amp
CK324	**p35S:CDKA;1:CFP**	CK333 (CDKA;1 von Stefan)via LR in CK330 pEXSG-YFP	Amp
CK325	**p35S:CDKA;1:YFP**	CK333 (CDKA;1 von Stefan)via LR in CK330 pEXSG-YFP	Amp
CK326	**p35S:CKS1:CFP**	CKS1 in pEXSG-CFP **Stefan Pusch** (ST92) wird nicht klappen da CKS noch Stop hat	Amp
CK327	**p35S:CFP:CKS1**	CK336 via LR in CK331 CKS1 in pENSG-CFP	Amp
CK328	**p35S:YFP:CKS1**	CKS1 in pENSG-YFP **Stefan Pusch** (ST94)	Amp
CK329	**pEXSG-CFP**	**Marcel Wiemer** AG Parker	Amp/Chloramph.

CK330	**pEXSG-YFP**	**Marcel Wiemer** AG Parker	Amp/Chloramph.
CK331	**pENSG-CFP**	**Marcel Wiemer** AG Parker	Amp/Chloramph.
CK332	**pENSG-YFP**	**Marcel Wiemer** AG Parker	Amp/Chloramph.
CK333	CDKA;1-ohne stop in pDONR201	**Stefan Pusch** (ST30), sequenziert und ok, stille Mutation Nt180 05.10.04	Kana
CK334	KRP1-ohne stop in pDONR201	**Stefan Pusch** (ST31) sequneziert und ok 05.10.04	Kana
CK335	KRP1_109-ohne stop in pDONR201	**Stefan Pusch** (ST32) sequenziert und ok 05.10.04	Kana
CK336	CKS1-mit stop in pDONR201	**Stefan Pusch** (ST34) hat laut sequenzierung doch noch sein stop!!!!!!! Ansonsten ok 05.10.04	Kana
CK337	**pTMM:YFP:KRP1**	CK209 via LR in pTMM-pAM-PAT CK229	Amp /Carb+Rif+Kann
CK338	**p2x35S:3xHA:KRP1**	CK334 via LR in CK321	Amp /Carb+Rif+Kann
CK339	**p2x35S:6xMyc:KRP1**	CK334 via LR in CK322	Amp /Carb+Rif+Kann
CK340	**p2x35S:3xHA:KRP1_109**	CK335 via LR in CK321	Amp /Carb+Rif+Kann
CK341	**p2x35S:6xMyc:KRP1_109**	CK335 via LR in CK322	Amp /Carb+Rif+Kann
CK342	**p2x35S:3xHA:CDKA;1**	CK333 via LR in CK321	Amp /Carb+Rif+Kann
CK343	**p2x35S:6xMyc:CDKA;1**	CK333 via LR in CK322	Amp /Carb+Rif+Kann
CK344	**p2x35S:CDKA;1:3xHA**	CK333 via LR in CK319	Amp /Carb+Rif+Kann
CK345	**p2x35S:CDKA;1:6xMyc**	CK333 via LR in CK320	Amp /Carb+Rif+Kann
CK346	**p2x35S:3xHA:CKS1**	CK336 via LR in CK321	Amp /Carb+Rif+Kann
CK347	**p2x35S:6xMyc:CKS1**	CK336 via LR in CK322	Amp /Carb+Rif+Kann
CK348	**p2x35S:CKS1:3xHA**	CK336 via LR in CK319 nicht möglich mit CK336 da stop noch in CKS1	Amp /Carb+Rif+Kann
CK349	**p2x35S:CKS1:6xMyc**	CK336 via LR in CK320 nicht möglich mit CK336 da stop noch in CKS1	Amp /Carb+Rif+Kann
CK350	pGEM-T	pGEM-T cloning vector PROMEGA	Amp
CK351	CycB1;2 ohne stop in pDONR	PCR via BP in pDONR201; template CK1 Primer (J604+CW15) Hifi Polymerase sequenziert CK351A alles ok	Kana
CK352	truncCycB1;2 ohne stop in pDONR	PCR via BP in pDONR201; template CK1 Primer (CW16+CW15)Hifi Polymerase sequenziert CK352B alles ok	Kana
CK353	**p2x35S:CycB1;2:3xHA**	CK351 via LR in CK319	Amp /Carb+Rif+Kann
CK354	**p2x35S:CycB1;2:6xMyc**	CK351 via LR in CK320	Amp /Carb+Rif+Kann
CK355	**p2x35S:truncCycB1;2:3xHA**	CK352 via LR in CK319	Amp /Carb+Rif+Kann
CK356	**p2x35S:truncCycB1;2:6xMyc**	CK352 via LR in CK320	Amp /Carb+Rif+Kann
CK357	pDONR201	pDONR201 **Invitrogen**	Kana
CK358	GUS:YFP:KRP1_109 in pDONR201	GUS:YFP:KRP1_109 in pDONR201 **Moritz Nowack** (MN17)	Kana
CK359	**pTMM:GUS:YFP:KRP1_109**		Amp /Carb+Rif+Kann
CK360	**pTMM:KRP1_108:YFP**	CK207 via LR Reaktion in CK229	Amp /Carb+Rif+Kann
CK361	**pTMM:YFP:KRP1_108**	CK210 via LR Reaktion in CK229	Amp /Carb+Rif+Kann
CK362	**p2x35S:KRP1_108:YFP LeeLa**	CK207 via LR Reaktion in CK262	Amp /Carb+Rif+Kann

CK363	**p2x35S:YFP:KRP1_108 LeeLa**	CK210 via LR Reaktion in CK262	Amp /Carb+Rif+Kann
CK364	**p35S:CFP:CDKA;1**	CK333 (CDKA;1 von Stefan)via LR in CK331 pENSG-YFP	Amp
CK365	**p35S:YFP:CDKA;1**	CK333 (CDKA;1 von Stefan) via LR in CK332 pENSG-CFP	Amp
CK366	**p35S:CycB1;2:YFP**	CK351 via LR in CK330	Amp
CK367	**p35S:truncCycB1;2:CFP**	CK352 via LR in CK329	Amp
CK368	**p35S:truncCycB1;2:YFP**	CK352 via LR in CK330	Amp
CK369	**pGL2:GUS:YFP:KRP1_109**	MN17 via LR in pGL2:pAM-PAT **Moritz Nowack** (MN21)	Amp /Carb+Rif+Kann
CK370	**p35S:KRP1-RNAi_Exon3A**	template KRP1, Primer Ex3a_S+ EX3a_AS in pDONR via LR in pJawohl8RNAi **Oliver Hofmann**	Amp /Carb+Rif+Kann
CK371	**p35S:KRP1-RNAi_Exon3B**	nicht geklappt	Amp /Carb+Rif+Kann
CK372	**p35S:KRP7-RNAi_Exon4A**	template KRP7, Primer Ex4a_S+ EX4a_AS in pDONR via LR in pJawohl8RNAi **Oliver Hofmann**	Amp /Carb+Rif+Kann
CK373	**p35S:KRP7-RNAi_Exon4B**	template KRP7, Primer Ex4b_S+ EX4b_AS in pDONR via LR in pJawohl8RNAi **Oliver Hofmann**	Amp /Carb+Rif+Kann

WT, mutants, gifts					
		ecotype	**resistance**		**source**
Wildtyp Landsberg *erecta*		L*er*	none		
Wildtyp Columbia		Col	none		
Wildtyp Wassilewskaja		WS-0	none		
gl2-/- 362		Col	BASTA		Giorgio Morelli
gl2-/- 4AA		Col	Kan		Giorgio Morelli
Poethig #232		Col	Kan		Scott Poethig
Poethig #254		Col	Kan		Scott Poethig
Poethig #1801		Col	Kan		Scott Poethig
cpc try		WS-0x L*er*	Hygro		Schellmann et al., 2002
sim		Col	none		Walker et al., 2000
glabra3-1		L*er*	none		Payne et al., 2000
ajh1+/-		Col	Kan		Claus Schwechheimer
cpr5		WS-0	Kan+BASTA		Kirik et al., 2001
krp1		Col	Hygro		Csaba Koncz T-DNA Collection
ProGL2:KRP1		L*er*	Kan		Schnittger et al. 2003
ProGL2:KRP1_109		L*er*	Kan		Schnittger et al. 2003
ProGL2:CDKA;1		L*er*	Kan		Schnittger et al. 2003
ProGL2:CDKA;1-AF		L*er*	Kan		Arp Schnittger
ProGL2:CDKB1;1		L*er*	Kan		Schnittger et al. 2003
ProGL2:CycD3;1		L*er*	Kan		Schnittger et al. 2002b
ProGL2:truncCycB1;2		L*er*	Kan		Schnittger et al. 2002a
ProGL2:CKS1		Ler	Kan		Arp Schnittger
ProGL2:GUS		L*er*	Kan		Arp Schnittger
ProGL2:GFP5-ER		L*er*	Kan		Arp Schnittger
ProGL2:nls:GFP:GUS		L*er*	Kan		Arp Schnittger
ProCycB1;2:GUS:DB		L*er*	Kan		Schnittger et al. 2002a
ProGL2:GUS:YFP:KRP1_109		L*er*	BASTA		Moritz Nowack
ProGL2:NLS:YFP:KRP1_109		L*er*	BASTA		Moritz Nowack
ProCPC:GUS		L*er*	BASTA		Martina Pesch

ProTRY:GUS		L*er*	BASTA		Martina Pesch
ProTMM:GFP5-ER		Col	BASTA		Oliver Hofmann
Transgenic lines					
Construct	**#**	**ecotype**	**resistance**	**number of T1 plants**	**phenotype**
pGL2::truncAtCycB1;2-YFP	CK13	L*er*	Kan	>20	like pGL2:trunc-CycB1;2 multicellular and Clusters
pGL2::YFP-AtCycB1;2	CK19	L*er*	Kan	>20	no phenotype
pGL2::Atcdc2a-RFP	CK25	L*er*	Kan	not selected	
pGL2::AtCSN5A	CK29	L*er*	Kan	>100	no phenotype, 1 line increased trichome numberl
rev 3 gen.KRP1::GUS-DB	CK46	L*er*	Kan	3	line A and C GUS positive
rev 3 gen.KRP1::GUS-DB	CK46	L*er*	Kan	>30	not analyzed
rev 3 gen.KRP1::GUS-DB:rev 5'gen	CK48	L*er*	Kan	2	line D GUS positive
rev 3 gen.KRP1::GUS-DB:rev 5'gen	CK48	L*er*	Kan	>30	not analyzed
pGL2::YFP	CK53	L*er*	Kan	>20	YFP positive
pGL2::RFP	CK56	L*er*	Kan	>20	RFP positive
pGL2::AtE2Fb	CK68	L*er*	Kan	8	no phenotype
pGL2::AtE2Fb	CK68	Col	Kan	not selected	
pGL2.:AtE2Fb	CK68	*gl2* 362	Kan	18	*gl2*
pGL2::anti-AtE2Fb	CK70	L*er*	Kan	not selected	
pGL2::AtE2Fa	CK72	L*er*	Kan	1	no phenotype
pGL2::AtE2Fa	CK72	Col	Kan	not selected	
pGL2.:AtE2Fa	CK72	*gl2* 362	Kan	14	*gl2*
pGL2::anti-AtE2Fa	CK74	L*er*	Kan	not selected	
pGL2::anti-Atcdc2a-RNAi	CK87/106	L*er*	BASTA	18	no phenotype
pGL2::AtCycB1;2-RNAi	CK88/129	L*er*	BASTA	>45	no phenotype
pGL2::AtCycB1;1-RNAi	CK89/130	L*er*	BASTA	32	20 lines more 4-branched trichomes
pGL2::AtWEE1	CK127/141	L*er*	BASTA	65	no phenotype
pGL2::AtWEE1-RNAi	CK128/142	L*er*	BASTA	30	no phenotype
pGL2::AtKRP4	CK132/143	L*er*	BASTA	>90	10 strong lines with 2-branched and unbranched trichomes
pGL2::AtKRP4-RNAi	CK133/144	L*er*	BASTA	27	not analyzed
pGL2::AtRBR1	CK134	L*er*	BASTA	>30	WT
pGL2::AtRBR1-RNAi	CK135	L*er*	BASTA	no transformants	

pKRP4::GUS	CK136	L*er*	Kan ??	not selected	
pGL2::AtKRP1-RNAi	CK139/145	L*er*	BASTA	15	no phenotype
pGL2::KRP1	CK140/148	L*er*	BASTA	>70	no phenotype
pGL2::AtKRP-cons-RNAi	CK147	L*er*	BASTA	25	no phenotype
pGL2::AtE2F3-RNAi	CK150	L*er*	BASTA	not selected	
pGL2::AtE2F5-RNAi	CK152	L*er*	BASTA	not selected	
pGL2::AtDPa-RNAi	CK154	L*er*	BASTA	4	no phenotype
pGL2::AtDPb-RNAi	Ck156	L*er*	BASTA	3	no phenotype
p35S::Histon2B-YFP	CK162	L*er*	Kan		construct and seeds from Fred Berger
pGL2::AtDPa	CK164/158	L*er*	Kan	13	no phenotype
pGL2::AtDPa	CK164/158	Col	Kan	not selected	
pGL2::AtDPa	CK164/158	*gl2* 362	Kan	2	*gl2*
pGL2::anti-AtDPa	CK165/159	Ler	Kan	not selected	
pGL2::AtDPb	CK166/160	Ler	Kan	1	no phenotype
pGL2::AtDPb	CK166/160	Col	Kan	not selected	
pGL2::AtDPb	CK166/160	*gl2* 362	Kan	25	*gl2*
pGL2::anti-AtDPb	CK167/161	L*er*	Kan	not selected	
pGL2::pGEJAE-3D1-Stop	CK177	L*er*	BASTA	>80	no phenotype
pGL2::pGEJAE-3D2-Stop	CK178	L*er*	BASTA	>80	no phenotype
pGL2::pGEJAE-3D10-Stop	CK179	L*er*	BASTA	>80	no phenotype
pGL2::pGEJAE-3D25-Stop	CK180	L*er*	BASTA	>80	no phenotype
pGL2::pGEJAE-4D21-Stop	CK181	L*er*	BASTA	>80	no phenotype
pGL2::pGEJAE-4D47-Stop	CK182	L*er*	BASTA	>80	no phenotype
pGL2::pG4ER-Stop	CK183	L*er*	BASTA	>80	no phenotype
pGL2::pGEJAE-3D1-MYC	CK191	L*er*	BASTA	14	no phenotype
pGL2::pGEJAE-3D2-MYC	CK192	L*er*	BASTA	23	no phenotype
pGL2::pGEJAE-3D10-MYC	CK193	L*er*	BASTA	20	no phenotype
pGL2::pGEJAE-3D25-MYC	CK194	L*er*	BASTA	>20	no phenotype
pGL2::pGEJAE-4D21-MYC	CK195	L*er*	BASTA	not selected	
pGL2::pGEJAE-4D47-MYC	CK196	L*er*	BASTA	25	no phenotype
pGL2::pG4ER-MYC	CK197	L*er*	BASTA	>20	no phenotype
pGL2::N-AtKRP1-RNAi	CK198	L*er*	BASTA	12	no phenotype
pGL2::N-AtKRP4-RNAi	CK199	L*er*	BASTA	12	no phenotype

pGL2::AtDPa	CK201	L*er*	BASTA	>20	no phenotype
pGL2::AtDPa	CK201	Col	BASTA	not transformed	
pGL2::AtDPa	CK201	*gl2* 4AA	BASTA	66	*gl2*
pGL2::AtDPb	CK202	L*er*	BASTA	>20	no phenotype
pGL2::AtDPb	CK202	Col	BASTA	not transformed	
pGL2::AtDPb	CK202	*gl2* 4AA	BASTA	not selected	
pGL2::AtE2Fb	CK203	L*er*	BASTA	>20	no phenotype
pGL2::AtE2Fb	CK203	Col	BASTA	not transformed	
pGL2::AtE2Fb	CK203	*gl2* 4AA	BASTA	7	II-107, 3x*gl2*, 2xWT, 1x more trichome clusters, 1x clusters and multicellular
pGL2::AtE2Fa	CK204	L*er*	BASTA	>20	no phenotype
pGL2::AtE2Fa	CK204	Col	BASTA	not transformed	
pGL2::AtE2Fa	CK204	*gl2* 4AA	BASTA	14	*gl2*
pGL2::AtKRP1_109	CK213	L*er*	BASTA	23	3x weak, 1x strong KRP1-phenotype
pGL2::AtKRP1_109	CK213	Poethig 232	BASTA	not selected	
pGL2::AtKRP1_109	CK213	*cpc try*	BASTA	9	8x typ cpc, 1x WT
pGL2::AtKRP1_109	CK213	Col	BASTA	Marc Jakoby	
pGL2::AtKRP1_109	CK213	*sim*	BASTA	>51	5x KRP-strong, 9x KRP-weak, 29x sim-weak, 7xsim-mediuml, 1x sim-strong
pWUS-BD::AtKRP1_109	CK214	L*er*	BASTA	not selected	
pWUS-BD::AtE2F3	CK215	L*er*	BASTA	not selected	
pWUS-BD::AtE2F5	CK216	L*er*	BASTA	not selected	
pGL2::AtKRP1-YFP	CK219	L*er*	BASTA	60	no phenotype
pGL2::AtKRP1-YFP	CK219	Col	BASTA	not transformed	
pGL2::AtKRP1_108-YFP	CK220	L*er*	BASTA	38	no phenotype
pGL2::AtKRP1_108-YFP	CK220	Col	BASTA	Marc Jakoby	
pGL2::AtKRP1_109-YFP	CK221	L*er*	BASTA	83	13x weak, 14x medium, 7x strong KRP1 phenotype
pGL2::AtKRP_109-YFP	CK221	*cpc try*	BASTA	2	1x more trichome branches. 1x normal
pGL2::AtKRP_109-YFP	CK221	Col	BASTA	Marc Jakoby	
pGL2::AtKRP_109-YFP	CK221	*sim*	BASTA	24	5xKRP-weak, 16x sim-weak, 1xsim-medium, 2x sim-strong
pGL2::YFP-AtKRP1	CK222	L*er*	BASTA	77	11x weak, 6x medium, 4x strong KRP1-phenotype
pGL2::YFP-AtKRP1	CK222	*cpc try*	BASTA	not transformed	
pGL2::YFP-AtKRP1	CK222	Col	BASTA	Marc Jakoby	
pGL2::YFP-AtKRP1	CK222	*sim*	BASTA	14	1xKRP-weak, 3xsim-weak, 6xsim-medium, 4xsim-strong
pGL2::YFP-AtKRP1	CK222	*ajh1+/-*	BASTA+Kana	not selected	

pGL2::YFP-AtKRP1_108	CK223	L*er*	BASTA	15	no phenotype
pGL2::YFP-AtKRP1_108	CK223	*ajh1+/-*	BASTA+Kana	not selected	
pGL2::YFP-AtKRP1_109	CK224	L*er*	BASTA	89	19x weak, 14x medium, 8x strong KRP1-phenotype
pGL2::YFP-AtKRP1_109	CK224	*cpc try*	BASTA	no transformants	
pGL2::YFP-AtKRP1_109	CK224	Col	BASTA	Marc Jakoby	
pGL2::YFP-AtKRP1_109	CK224	*sim*	BASTA	27	12xKRP, 11x sim-weak, 3x sim-medium, 2x sim-strong
pGL2::YFP-AtKRP1_109	CK224	*ajh1+/-*	BASTA+Kana	not selected	
pGL2::Atcdc2a-RNAi	CK226	L*er*	BASTA	not selected	
pGL2::AtCycB1;2	CK227	L*er*	BASTA	8	seeds for Farshad
pGL2::GUS	CK230	L*er*	BASTA	>12	seeds for Farshad
pWUS-BD::GUS	CK231	L*er*	BASTA	>19	not analyzed
pTMM::GUS	CK232	L*er*	BASTA		seeds for Oliver
pGL2::AtDEL3	CK236	L*er*	BASTA	>100 /// >70	1/3 häufig 4-verzweigt /// 18 Linien häufiger 2-verzweigt
pGL2::CycD3;2	Xiaoguo	L*er*	BASTA	>80	no phenotype
pGL2::CycD3;3	Xiaoguo	L*er*	BASTA	12	no phenotype
pGL2::RBX1-RNAi	Xiaoguo	L*er*	BASTA	22	II-86-87 weak-medium and strong phenotype see B8 SEM pictures
pGL2::RBX1	Xiaoguo	L*er*	BASTA	65	10 lines with more 4-branched trichomes
pGL2::Bax-Inhibitor-RNAi	Xiaoguo	L*er*	BASTA	30	8 lines with moe 4-branched trichomes
pGL2::ANT-RNAi	Xiaoguo	L*er*	BASTA	34	2 lines with 4-and 5-branched trichomes
pWUS::cdc2aDN	Xiaoguo	L*er*	BASTA	13	no phenotype
pWUS::KRP4	Xiaoguo	L*er*	BASTA	>20	no phenotype
pWUS::KRP1	Xiaoguo	L*er*	BASTA	14	no phenotype
pWUS::KRP4-RNAi	Xiaoguo	L*er*	BASTA	45	no phenotype
pWUS::APC11-RNAi	Xiaoguo	L*er*	BASTA	34	no phenotype
pWUS::CycB1;2	Xiaoguo	L*er*	BASTA	8	1 line with 5-branched trichomes
pWUS::E2Fb	Xiaoguo	L*er*	BASTA	22	no phenotype
pWUS::DEL1	Xiaoguo	L*er*	BASTA	>100	3 lines with more 2-branched trichomes
pWUS::DEL1-RNAi	Xiaoguo	L*er*	BASTA	42	no phenotype
pWUS::ANT-RNAi	Xiaoguo	L*er*	BASTA	23	no phenotype
pWUS::DEL3	Xiaoguo	L*er*	BASTA	46	not analyzed
pWUS::ANT	Xiaoguo	L*er*	BASTA	17	not analyzed
pWUS::RBX1	Xiaoguo	L*er*	BASTA	27	6 lines with more 4-branched trichomes 1x 5-branched trichomes
pWUS::APC11	Xiaoguo	L*er*	BASTA	63	no phenotype

pWUS::DEL3-RNAi	Xiaoguo	L*er*	BASTA	35	not analyzed
pPRP3::RBXII-RNAi	Xiaoguo	L*er*	BASTA	2	not analyzed
pPRP3::KRP4-RNAi	Xiaoguo	L*er*	BASTA	2	not analyzed
pPRP3::DEL1-RNAi	Xiaoguo	L*er*	BASTA	4	not analyzed
pPRP3::CycB1;2	Xiaoguo	L*er*	BASTA	24	not analyzed
pPRP3::RBXI	Xiaoguo	L*er*	BASTA	7	not analyzed
pPRP3::ANT-RNAi	Xiaoguo	L*er*	BASTA	23	not analyzed
pPRP3::KRP4	Xiaoguo	L*er*	BASTA	23	not analyzed
pPRP3::APC11	Xiaoguo	L*er*	BASTA	21	not analyzed
pPRP3::E2Fb	Xiaoguo	L*er*	BASTA	12	not analyzed
pPRP3::ANT	Xiaoguo	L*er*	BASTA	18	not analyzed
pPRP3::cdc2aDN	Xiaoguo	L*er*	BASTA	27	not analyzed
pPRP3::DEL1	Xiaoguo	L*er*	BASTA	27	not analyzed
pPRP::RBXI-RNAi	Xiaoguo	L*er*	BASTA	3	not analyzed
pPPR3::DEL3	Xiaoguo	L*er*	BASTA	27	not analyzed
pCPC::CycB1;2	CK248	L*er*	BASTA	not transformed	
pCPC::KRP1	CK249	L*er*	BASTA	not transformed	
pCPC::KRP4	CK250	L*er*	BASTA	not transformed	
pTRY::CycB1;2	CK251	L*er*	BASTA	not transformed	
pTRY::KRP1	CK252	L*er*	BASTA	not transformed	
pTRY::KRP4	CK253	L*er*	BASTA	not transformed	
35S-UAS::KRP1	CK258	Poethig 232	BASTA	>70	not analyzed
35S-UAS::KRP1	CK258	Col	BASTA	not selected	
35S-UAS::KRP1_109	CK259	Poethig 232	BASTA	>60	26 GFP positive, WT with Bino
35S-UAS::KRP1_109	CK259	Col	BASTA	not selected	
35S-UAS::RBR	CK260	Poethig 232	BASTA	>30	7 GFP positive, WT with Bino
35S-UAS::RBR	CK260	Col	BASTA	not selected	
35S-UAS::KRP1	CK258	Poethig 254	BASTA	>100	>90% GFP positive
35S-UAS::KRP1_109	CK259	Poethig 254	BASTA	>100	>90% GFP positive
35S-UAS::RBR	CK260	Poethig 254	BASTA	>50	>90% GFP positive
35S-UAS::KRP1	CK258	Poethig 1801	BASTA	not selected	
35S-UAS::KRP1_109	CK259	Poethig 1801	BASTA	not selected	
35S-UAS::RBR	CK260	Poethig 1801	BASTA	not selected	

p2x35S::KRP1_109	CK263	L*er*	BASTA	not selected	
p2x35S::KRP1_109	CK263	Poethig 232	BASTA	not selected	
p2x35S::KRP1_109	CK263	Poethig 254	BASTA	not selected	
p2x35S::KRP1_109	CK263	Poethig 1801	BASTA	not selected	
pCPC::E2Fb	CK264	L*er*	BASTA	>80	7 lines with slight increase in 4-branched trichomes
pCPC::E2Fb	CK264	*gl2* 4AA	BASTA	>150	*gl2*
pTRY::E2Fb	CK265	L*er*	BASTA	>50	no phenotype
pTRY::E2Fb	CK265	*gl2* 4AA	BASTA	>150	*gl2*
pCPC::E2Fa	CK266	L*er*	BASTA	90	50 lines with 4-and 5-branched trichomes; 2 ines with less branched trichomes
pCPC::E2Fa	CK266	*gl2* 4AA	BASTA	>150	*gl2*
pTRY::E2Fa	CK267	L*er*	BASTA	>50	16 lines with 4-branched trichomes, 1 line multicellular
pTRY::E2Fa	CK267	*gl2* 4AA	BASTA	>150	*gl2*
pCPC::RBR1	CK268	L*er*	BASTA	10	II-141 6 lines more 2-branched trichomes no unbranched
pTRY::RBR1	CK269	L*er*	BASTA	5	II-141 2 lines more 2-branched trichomes no unbranched
p2x35S::RBR1	CK270	L*er*	BASTA	not transformed	
pGL2::E2Fb-LeeLa	CK272	L*er*	BASTA	56	14 lines with more 2-branched trichomes
pGL2::E2Fb-LeeLa	CK272	*gl2* 4AA	BASTA	>150	*gl2*
pGL2::E2Fa-LeeLa	CK273	L*er*	BASTA	38	no phenotype
pGL2::E2Fa-LeeLa	CK273	*gl2* 4AA	BASTA	>150	*gl2*
pGL2::KRP-Interactor_1	CK281	L*er*	BASTA	5	WT
pGL2::KRP-Interactor_2	CK282	L*er*	BASTA	not transformed	
pGL2::KRP-Interactor_3	CK283	L*er*	BASTA	>50	no phenotype
pGL2::KRP-Interactor_4	CK284	L*er*	BASTA	not transformed	
pGL2::E2Fc	CK285	L*er*	BASTA	>80	more 4-branched trichomes
pGL2::GUS LeeLa	CK286	L*er*	BASTA	not selected	
pGL2::CycB1;2 LeeLa	CK287	L*er*	BASTA		seeds for Farshad
pGL2::KRP1 LeeLa	CK288	L*er*	BASTA	14	1 line wih slightly less branched trichomes
pCPC::E2Fc	CK291	L*er*	BASTA	not transformed	
pTRY::E2Fc	CK292	L*er*	BASTA	not transformed	
pCPC::KRP1_109	CK293	L*er*	BASTA	27	12 lines with KRP phenotype
pTRY::KRP1_109	CK294	L*er*	BASTA	19	15 lines with KRP phenotype
pTMM::KRP1_109	CK296	L*er*	BASTA	58	#1-6 round leaves and smaller plants
pGL2::PCR-E2Fb	CK300	L*er*	BASTA	not transformed	

pGL2::PCR-E2Fa	CK302	L*er*	BASTA	not transformed	
pGL2::KRP1-PCR-pAM-PAT	CK304	L*er*	BASTA	not transformed	
pGL2::KRP1_108-pAM-PAT	CK306	L*er*	BASTA	not transformed	
pTMM::KRP1_109-YFP	CK307	L*er*	BASTA	>30	
pTMM::KRP1_109-YFP	CK307	Col	BASTA	not selected	
pTMM::YFP-KRP1_109	CK308	L*er*	BASTA	10	
pTMM::YFP-KRP1_109	CK308	Col	BASTA	>100	63 lines with phenotypes weak-medium-strong (#101-#140)
pTMM::YFP-KRP1_109	CK308	*ajh1+/-*	BASTA+Kana	not selected	
pGL2::AJH1	CK311	L*er*	BASTA	not transformed	
pGL2:KRP1_109 BIN von Arp	CK312	L*er*	KAN	not transformed	
pGL2:KRP1_109 BI von Arp	CK312	*try-cpc*	KAN	not transformed	
pGL2:ICK1 von Arp		*sim*	KAN	40	11x KRP-strong, 22x KRP-weak, 7x sim-weak
pGL2:CKS1 von Arp		*sim*	KAN	not selected	
p2x35S:YFP:KRP1 LeeLa	CK313		BASTA	not transformed	
p2x35S:KRP1_109:YFP LeeLa	CK314		BASTA	not transformed	
p2x35S:YFP:KRP1_109 LeeLa	CK315		BASTA	not transformed	
p35S:CycB1;2:CFP	CK323		BASTA	not transformed	
p35S:CDKA;1:CFP	CK324		BASTA	not transformed	
p35S:CDKA;1:YFP	CK325		BASTA	not transformed	
p35S:CFP:CKS1	CK327		BASTA	not transformed	
p35S:YFP:CKS1	CK328		BASTA	not transformed	
pTMM:YFP:KRP1	CK337	L*er*	BASTA	no transformants	
pTMM:YFP:KRP1	CK337	Col	BASTA	>100	enlarged epidermal cells
pTMM:YFP:KRP1	CK337	*ajh1+/-*	BASTA+Kana	not selected	
p2x35S:3xHA:KRP1	CK338		BASTA	Agro-Infil. in tobacco	
p2x35S:6xMyc:KRP1	CK339		BASTA	Agro-Infil. in tobacco	
p2x35S:3xHA:KRP1_109	CK340		BASTA	Agro-Infil. in tobacco	
p2x35S:6xMyc:KRP1_109	CK341		BASTA	Agro-Infil. in tobacco	
p2x35S:3xHA:CDKA;1	CK342		BASTA	Agro-Infil. in tobacco	
p2x35S:6xMyc:CDKA;1	CK343		BASTA	Agro-Infil. in tobacco	
p2x35S:CDKA;1:3xHA	CK344		BASTA	Agro-Infil. in tobacco	
p2x35S:CDKA;1:6xMyc	CK345		BASTA	Agro-Infil. in tobacco	
p2x35S:3xHA:CKS1	CK346		BASTA	Agro-Infil. in tobacco	

p2x35S:6xMyc:CKS1	CK347		BASTA	Agro-Infil. in tobacco	
p2x35S:CycB1;2:3xHA	CK353		BASTA	Agro-Infil. in tobacco	
p2x35S:CycB1;2:6xMyc	CK354		BASTA	Agro-Infil. in tobacco	
p2x35S:truncCycB1;2:3xHA	CK355		BASTA	Agro-Infil. in tobacco	
p2x35S:truncCycB1;2:6xMyc	CK356		BASTA	Agro-Infil. in tobacco	
pTMM:KRP1_108:YFP	CK360	L*er*	BASTA	not selected	
pTMM:KRP1_108:YFP	CK360	Col	BASTA	not selected	
pTMM:YFP:KRP1_108	CK361	Ler	BASTA	20	not analyzed
pTMM:YFP:KRP1_108	CK361	Col	BASTA	>100	no phenotype, 4 lines tested for YFP all positive
pTMM:YFP:KRP1_108	CK361	*ajh1+/-*	BASTA+Kana	not selected	
p2x35S:KRP1_108:YFP LeeLa	CK362		BASTA	not transformed	
p2x35S:YFP:KRP1_108 LeeLa	CK363		BASTA	not transformed	
p35S:CFP:CDKA;1	CK364		BASTA	not transformed	
p35S:YFP:CDKA;1	CK365		BASTA	not transformed	
p35S:CycB1;2:YFP	CK366		BASTA	not transformed	
p35S:truncCycB1;2:CFP	CK367		BASTA	not transformed	
p35S:truncCycB1;2:YFP	CK368		BASTA	not transformed	
Oliver Hofmann constructs					
35S:KRP1-RNAi_Exon3A	CK370	L*er*	BASTA	>50	no phenotype
35S:KRP1-RNAi_Exon3A	CK370	Col	BASTA	>51	no phenotype
35S:KRP7-RNAi_Exon4B	CK373	L*er*	BASTA	>52	no phenotype
35S:KRP7-RNAi_Exon4B	CK373	Col	BASTA	>53	no phenotype
35S:KRP7-RNAi_Exon4A	CK372	L*er*	BASTA	>54	no phenotype
35S:KRP7-RNAi_Exon4A	CK372	Col	BASTA	>55	no phenotype

Erklärung

Ich versichere, daß ich die von mir vorgelegte Dissertation selbständig angefertigt, die benutzten Quellen und Hilfsmittel vollständig angegeben und die Stellen der Arbeit – einschließlich Tabellen, Karten und Abbildungen -, die anderen Werken im Wortlaut oder dem Sinn nach entnommen sind, in jedem Einzelfall als Entlehnung kenntlich gemacht habe; daß diese Dissertation noch keiner anderen Fakultät oder Universität zur Prüfung vorgelegen hat; daß sie – abgesehen von unten angegebenen Teilpublikationen – noch nicht veröffentlicht worden ist sowie, daß ich eine solche Veröffentlichung vor Abschluß des Promotionsverfahrens nicht vornehmen werde. Die von mir vorgelegte Dissertation ist von Prof. Dr. Martin Hülskamp betreut worden.

Christina Weinl

Ectopic D-type cyclin expression induces not only DNA replication but also cell division in Arabidopsis trichomes
Schnittger A, Schöbinger U, Bouyer D, Weinl C, Stierhof YD, Hülskamp M
Proc Natl Acad Sci U S A. 2001, **99**: 6410-6415

Misexpression of the cyclin-dependent kinase inhibitor ICK1/KRP1 in single-celled *Arabidopsis* trichomes reduces endoreduplication and cell size and induces cell death.
Schnittger A, Weinl C, Bouyer D, Schöbinger U, Hülskamp M
Plant Cell 2003, **15**: 303-315

Novel functions of plant cyclin-dependent kinase inhibitors - ICK1/KRP1 can act non-cell-autonomously and inhibit entry into mitosis
Weinl C, Marquardt S, Kuijt SJH, Nowack MK, Jakoby MJ, Hülskamp M, Schnittger A
Plant Cell 2005, **17**:1704-1722